Halide Transfer Reactions of Arsenic, Antimony and Bismuth

Helen Collins

Thesis Submitted for the Degree of Doctor of Philosophy

University of Warwick,
Department of Chemistry.

June 1991

To Mum and Dad

-for making this possible

Contents

List of Tables

List of Figures

Acknowledgements

I would especially like to thank Dr Gerald Willey for the continual support and encouragement that he has provided throughout this work.

My appreciation is also extended to the following:

Dr M. G. B. Drew and A. W. Johans at the University of Reading for the crystal structure determination.

Dr O. W. Howarth, Dr J. Lall and J. Hastings for the high-field NMR spectra.

Technical staff at the University of Warwick.

The SERC for funding this work.

My thanks also go to Dr S. Rawle for proof reading and to Dr A. F. Hill for providing typing facilities.

Finally I wish to thank my friends and colleagues for their support during the last three years.

Declaration - All of the work described in this thesis is original and was, except where otherwise indicated, carried out by the author.

Helen Collins
(June 1991)

Some of the work described in this thesis has been published in the following references.

Halide Abstraction Reactions of Sb(V) Chloride: Synthesis and Characterisation of Hexachloroantimonate Salts of M(II) M = Zn, Mg; M(III) M = Cr; M(IV) M = Ti, Sn and Related $Cp_2M(IV)$ M = Ti, Zr and Hf.

Paul N. Billinger, Preet P. K. Claire, Helen Collins and Gerald R. Willey, *Inorganica Chimica Acta.*, 1988, **149**, 63.

Halide Transfer Reactions Involving Bismuth(III) Chloride: Synthesis and Identification of the Ternary Complexes $BiCl_3.SbCl_5$ 4MeCN (I), $2MgCl_2.4BiCl_3.12MeCN$ (II) and $3MgCl_2.4BiCl_3.18MeCN$ (III). X-ray Structural Characterisation of (II) as the Tetranuclear Bismuth(III) Complex $[Mg(MeCN)_6]_2[Bi_4Cl_{16}]$ and Comments on its Structural Relationships with Other Complex Chloro-Bismuth(III) Anions.

Helen Collins, Michael G. B. Drew and Gerald R. Willey, *J. Chem. Soc., Dalton Transactions*, 1991, 961.

Abbreviations

Bipy	Bipyridyl
DMO	N, N' -Dimethyloxamide
DEDTO	N, N' -Diethyldithiooxamide
en	Ethylenediamine
TMEDA	N, N', N', N' -Tetramethylethylenediamine
TPP	Tetraphenylporphinato
MeCN	Acetonitrile
DMF	N, N' -Dimethylformamide
DMSO	Dimethylsulphoxide
THF	Tetrahydrofuran
EtOAc	Ethylacetate
Et	Ethyl
Ph	Phenyl
Me	Methyl
PPh_3	Triphenylphosphine
dppe	1, 2 -bis(diphenylphosphino)ethane
dmpe	1, 2,-bis(dimethylphosphino)ethane
N_2	nitrogen
Cl_2	chlorine
mol	mole
p.p.m.	parts per million
R.T.	room temperature
h	hour
m.p.	melting point
I.R.	infra-red
vs	very strong
s	strong
m	medium
w	weak
vw	very weak
sh	sharp
br	broad
U.V.	ultra-violet
(sh)	shoulder
N.M.R.	nuclear magnetic resonance
m	multiplet
s	singlet
S.C.E.	standard calomel electrode
E^o	standard electrode potential
Λ_e	equivalent conductivity
Λ_m	molar conductivity
Λ_o	molar conductivity at infinite dilution

Summary

The study of Group 15 (As, Sb, Bi) halide exchange reactions.

The Lewis acidity of $SbCl_5$ was displayed using various metal halides. Treatment of the metal halides MCl_n (n=2, M=Mg, Sn; n=3, M=Sc, Y, La, Ti, In; n=4, M=Ti, Sn) with $SbCl_5$ in MeCN provided antimonate(V) salts of the type $[MCl_{n-1}L_{7-n}][SbCl_6]$ characterised by ^{121}Sb nmr, electronic and infra-red spectroscopy and accompanying microanalytical data. Depending upon the stoichiometry of the reactants used the antimonate salts have been formulated as $[MCl_{n-x}L_{6-(n-x)}]^{x+}[SbCl_6]_x^-$ (where n=2, 3, 4; x=1, 2, 3). The formation of mono-, di- and tricationic metal species has been effected by single and multiple halide abstraction, the resultant formation of 1:1, 1:2 and 1:3 electrolytes in MeCN has been confirmed by conductivity studies.

The Lewis acidity and basicity of $BiCl_3$ was illustrated by treatment of MCl_n (n=2, M=Mg; n=5, M=Sb respectively) with $BiCl_3$ in MeCN. Reaction with n=2, M=Mg gave bismuthate(III) salts of the type $\{Mg(MeCN)_6\}_m[Bi_4Cl_{12+2m}]^{2m-}$, m=2, 3, depending upon the stoichiometry of the reactants used. The crystal structure of the product m=2 in MeCN resulted in the hexa-coordinated magnesium $[Mg(MeCN)_6]^{2+}$ dication and the novel tetranuclear bismuth(III) chloro anion $[Bi_4Cl_{16}]^{4-}$, which contains three different types of chlorine atoms; ten terminal, four μ^2 and two μ^3. Where m=3 gave a tetranuclear anion $[Bi_4Cl_{18}]^{6-}$. Further variation of the stoichiometry of the $MgCl_2/BiCl_3$ system did not give any other products. Conductivity measurements confirm the products as 2:1 and 3:1 electrolytes in DMF. However reaction of $BiCl_3$ with n=3, m=Ti, V, Cr, Fe; n=4, M=Ti, Sn led to the neutral $[MCl_3L_3]$ and $[MCl_4L_2]$ adducts.

The limited Lewis acidity of $SbCl_3$ towards MCl_n was displayed by reaction of MCl_n (n=3, M=Ti, Fe, In, Bi; n=4, M=Ti, Sn) with $SbCl_3$ in MeCN which gave the neutral MCl_nL_x (L=MeCN, x=2, 3) adducts. Reaction with n=5, M=Sb provided $SbCl_3.SbCl_5.4MeCN$.

The oxidation of As(III) to As(V) using chlorine and reaction with MCl_n (n=4, M=Ti, Sn, n=2, M=Zn) gave the MCl_nL_x adducts. Reaction with n=2, M=Mg and Me_4NCl gave $[Mg(MeCN)_6][AsCl_6]$ and $[Me_4N][AsCl_6]$.

$[TiCl_3(MeCN)_3][SbCl_6]$ and $[TiCl_2(MeCN)_4][SbCl_6]_2$ have been shown to behave as reactive centres for ligand and/or chloride exchange reactions with neutral, L' and anionic, L'' ligands (L'=PPh_3; L''=Cl^-, Br^-). Reaction with L'=PPh_3 gave $[TiCl_3(PPh_3)][SbCl_6]$ and with L''=Cl^- gave $TiCl_4L_2$.

Reaction of $TiCl_4$ with $MgCl_2$ in MeCN gave the ternary complex $MgCl_2.TiCl_4.6MeCN$.

CHAPTER 1

1.1.Some Group Trends

Amongst the elements of the Periodic Table, those of Group 15, the Pnictides, namely nitrogen, phosphorus, arsenic, antimony and bismuth, show an extremely diverse range of physical and chemical properties.

There is a distinct trend from non-metallic to metallic properties with increasing atomic number. Arsenic and antimony behave as metalloids, while bismuth is a typical B metal, like tin or lead. [1]

Phosphorus and nitrogen form covalent compounds; arsenic, antimony and bismuth exhibit increasing tendencies towards cationic behaviour. [2] There is a steady decrease in the strength of covalent bonds in the order P > As > Sb > Bi, which is well illustrated by the instability of BiH_3. [3]

Except in its valence shell electronic configuration, nitrogen bears very little resemblance to the other elements of the group. The ground state electronic configuration, s^2p^3 dictates the two main valence states of the group, three and five. These result from the loss or use of the three outer shell *p* electrons and the five outer shell *s* and *p* electrons respectively.

Group 15 compounds display a wide variety of donor/acceptor properties. Trivalent ER_3 compounds (where E=P, As, Sb, Bi and R=alkyl, aryl, alkoxy, aryloxy, halide, hydrogen) vary enormously in their donor/acceptor abilities, depending, on R. Pentavalent EX_5 compounds; where X=halogen invariably behave as acceptor molecules.

1.2.Trivalent Group 15 Compounds as Ligands

NR_3 compounds can function as simple donors by virtue of the lone pair on the central atom. Nitrogen has no other available orbitals, but other ER_3 compounds (E=P, As, Sb, Bi; R=alkyl, aryl, alkoxy, aryloxy, halide, hydrogen) have empty *d* orbitals of fairly low energy. [4] When the acceptor atom has partially or fully filled orbitals of similar symmetry and energy to these empty *d* orbitals, back donation of electron density may occur. This results in overall multiple bond character; in particular, $d\pi$-$d\pi$ bonding crucially affects the stability of transition metal complexes with EX_3 compounds. Mono-, bi- and multidentate ligands and macrocyclic phosphines, arsines, stibines and bismuthines have been reported in the literature. [2,5,6,7] Rather more unusual Group 15 ligands such as arsenobenzene have been recently reported. [8,9,10] Transition metals do not bond directly to the arsenic atom of arsenobenzene, but to a delocalized π bonded system analogous to metallocenes and η-allyl complexes. In addition ligands containing pnictide-element [11] and pnictide-pnictide multiple bonds, can form cluster compounds. [12]

1.2.1.Bonding of Tertiary Group 15 Ligands

Pnictide-transition metal bonds are essentially covalent. The simplest model comprises donation of the lone pair of the pnictide atom (which behaves as a Lewis base), to a suitably available empty orbital on the metal, thus generating a donor covalent bond.

This simple picture involves only σ type bonding, but π bonding and steric effects, modify the ligand's contribution to

the M-E bond. In an octahedral transition metal complex the e_g orbitals participate in σ bonding with the six ligands, leaving the t_{2g} orbitals as non-bonding orbitals directed between the six M-E bonds. When ligand coordination occurs the pyramidal (approximately p^3) bonding of the ligand changes towards tetrahedral sp^3. (This increase in s character has important steric implications). The σ bond can thus be viewed as forming between a d^2sp^3 hybrid metal orbital and an sp^3 hybrid phosphorus orbital.

The Lewis basicities (σ donor ability) of ER_3 ligands vary dramatically with R. [13] (R=alkyl, aryl, alkoxy, aryloxy, halide, hydrogen). This is reflected in pK_a values (Table 5.2, $pK_a(H_2O)$ is a measure of Bronsted basicity (proton affinity), which differs from Lewis basicity, but there is a close correlation). The basicity of some common phosphine ligands decrease in the order $PBu_3^t > P(OR)_3 > PR_3 \sim PPh_3 > PF_3 > P(OPh)_3$. Electron-releasing substituents increase the electron availability on phosphorus thus increasing basicity. Bulky substituents expand the R-P-R angle, which increases the p character of the lone pair and subsequently the basicity. The basicity of the pnictides decreases in the order P > As > Sb > Bi, according to enthalpy [14] and photoelectron spectroscopy data. [15]

Pnictide ligands can also accept π electron density, resulting in transition metal backbonding. The extents of σ donation and back-bonding depend upon the substituents attached to phosphorus, and the synergistic relationship between them is the cause of some dispute. [16] Pi backbonding was originally thought to involve a transfer of charge to empty

d orbitals on the pnictide atom. The symmetry of the d_{π}-d_{π} orbitals involved in such bonding is illustrated in Figure 1.1.

Figure 1.1: M-P Back-bonding Using Phosphorus d-orbitals

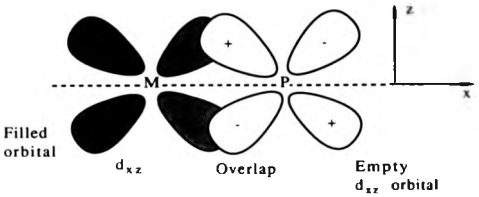

Recent quantum mechanical calculations imply that the EX_3 acceptor orbitals are *p* orbitals on E [17] and E-X σ* orbitals,[18] with a rebuttal of the dπ orbitals. Such ideas find support in the electron transmission spectroscopy measurements of Giordan *et al* .[19] On the basis of bond length calculations Orpen and Connelly [20] have suggested that the LUMO's of PX_3, PR_3 etc have σ* nature which incorporate some *3d* character from phosphorus. There is now a general consensus that M-P π "backbonding" involves the P-X antibonding σ* orbitals rather than the *3d* orbitals of phosphorus.

CO stretching frequencies and ^{13}C chemical shifts of $LNi(CO)_3$ and $LCr(CO)_5$ (L=pnictide ligand) [21] indicate that π acceptor ability decreases in the following order: NO > RCN ≈ PF_3 > PCl_3 > $PCl_2(OR)$ > PCl_2R > PBr_2R > $PCl(OR)_2$ > $PClR_2$ > $P(OR)_3$ > PR_3

(π acid series). [22] The π acidity of As and Sb ligands follows that of the corresponding P ligands. It was previously thought that the greater π acidity of PF_3 and PCl_3 was due to the electronegativity of the substituents lowering the energy of the phosphorus d-orbitals, thus increasing their availability for π bonding. According to Marynick *et al.* [18] the highly polar P-F bonds give rise to low lying σ^* orbitals of similar symmetry to the metal *d* orbitals. In addition the σ bond is highly polarised towards F, so the σ^* orbital necessarily polarises towards P, increasing σ^*-metal $d\pi$ orbital overlap. By contrast the most basic phosphines, PBu_3 and PCy_3 are best described as σ and π donors, [16] with very limited π acceptor ability.

Steric factors play a subtle role in the chemistry of transition metal-pnictide ligand complexes. Steric requirements of phosphine ligands are expressed by Tolman's Cone Angle, θ. The cone just encloses the Van der Waals surface of all ligand atoms over all rotational orientations about an M-P bond of length 2.28Å. The cone angles of ER_3 ligands have been measured or calculated using X-ray data and molecular models. The bulkiness of phosphine ligands modifies the solubility [24] and rates of reaction of complexes [25] and, most importantly, the coordination numbers and geometries that complexes can adopt.

<u>To summarize the bonding of ER_3 ligands</u> :[26]

σ donor ability decreases in the order P > As > Sb > Bi.

π acceptor ability increases in the order P < As < Sb < Bi.

Steric effects due to the donor atom increase in the order P < As < Sb < Bi.

Steric effects of the substituents on the donor atom decrease in the order P > As > Sb.

1.3. GROUP 15 HALIDES

1.3.1. Trihalides

All twelve trihalides are known, they exhibit considerable diversity in their chemical and physical properties, and in their structures (Table 1.1). [2,3,5]

Table 1.1: Physical Properties of Group 15 Trihalides [3]

Halide	Physical state at 25°C	M.p(°C)	B.p(°C)
AsF_3	Liquid	-6.0	62.8
$AsCl_3$	Liquid	-16.2	130.2
$AsBr_3$	Solid	+13.2	221
AsI_3	Solid	140.4	400
SbF_3	Solid	290	345
$SbCl_3$	Deliquescent solid	73.4	223
$SbBr_3$	Deliquescent solid	96.0	288
SbI_3	Solid	170.5	401
BiF_3	Solid	649	900
$BiCl_3$	Deliquescent solid	233.5	441
$BiBr_3$	Deliquescent solid	219.0	462
BiI_3	Solid	408.6	542 (extrap)

Melting points and boiling points reflect the different structures and bonding modes adopted by the trihalides, hence AsF_3, $AsCl_3$, $AsBr_3$, $SbCl_3$ and $SbBr_3$ are volatile molecular species, while the other trihalides interact significantly in the solid state.

The trihalides have low conductivities (Table 1.2), hence the degree of auto-ionization is negligible: [3]

$$2EX_3 \rightleftharpoons EX_2^+ + EX_4^-$$

Table 1.2: Conductivities of Trihalides

Halide	Conductivity (S cm^{-1})
$AsCl_3$/20°C	1.4×10^{-7}
$SbCl_3$/75°C	1.4×10^{-6}

Above its melting point $SbCl_3$ is a molecular liquid similar to water in its physical properties. Liquid $SbCl_3$ has low conductivity and viscosity, but a high dielectric constant, (33.2 at 75°C). [27] Both it and $AsCl_3$ are therefore suitable for use as nonaqueous solvents for inorganic solutes. [28, 29] They have liquid ranges of 150°C and are good media for chloride ion transfer reactions. Both have such low electrical conductivities that they have been suggested as solvents for nmr spectroscopy. [30]

1.3.2.Structural Properties

The principle valence orbitals of EX_3 undergo approximate sp^3 hybridization; the XEX angles fall short of the tetrahedral angle (109°) due to lone pair-bond pair repulsions (Table 1.3). [31]

Table 1.3 shows that weak secondary contacts are a common feature of the crystal structures of the Group 15 halides. [49] Thus while the lone pair and the primary E-X bonds describe a polyhedron whose shape can be predicted from VSEPR theories, [50] the secondary contacts cap the faces or bridge the edges of this polyhedron. More detailed discussion of the stereochemistry of the Group 15 trihalide complexes appears later in this chapter.

In the vapour phase AsF_3 [51], $AsCl_3$ [52], $AsBr_3$ [53], AsI_3 [54], $SbCl_3$ [55], $SbBr_3$ [56] and $BiCl_3$ [57] are essentially pyramidal monomers (Figure 1.2). The XAsX angles increase from 96.2° (X=F) [51] to 100.2° (X=I). [54]

Figure 1.2: Pyramidal Shape of Group 15 Trihalides EX_3

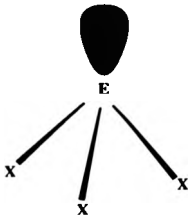

Table 1.3
Bond Lengths, Contact Lengths [a] and Bond Angles of Group 15 Trihalides

Halide	E-X Length(Å)	E···X Length(Å)	Angle XEX°	Ref
NCl_3(s)	1.71(2)-1.78(1)	<3.19(2)	105.1(9)-109.6(13)	32
PCl_3(s)	2.019, 2.034(2)	3.892(2)(x2), 3.657(2), 3.874(1)(x2)	100.04, 100.19(7)	33, 34, 35
AsF_3(s)	1.699(12), 1.700(11), 1.721(10)	2.886(12), 2.990(10), 3.052(11), 3.184(12), 3.099(12)	92.9, 93.3, 95.5(5)	36
$AsCl_3$(s)	2.162, 2.169, 2.171(2)	3.692, 3.727, 3.773(3), 3.865, 3.968(2)	97.3, 97.5, 98.3(1)	33, 37
α$AsBr_3$(s)	2.345(15)	3.738, 3.717, 3.863	97.3, 97.5, 98.2(5)	38
AsI_3(s)	2.591(1)	3.467(2)	99.67(5)	39
SbF_3(s)	1.90, 1.94(2)	2.60(2), 2.60(2), 2.63(3)	85.7(8), 89.0(8)	40
$SbCl_3$(s)	2.340(2), 2.368(x2)	3.736(1)(x2), 3.609(2), 3.457(1)(x2)	90.98, 95.7(5)(x2)	41, 42
$SbBr_3$(s)	2.50(5)	3.79	95	36
SbI_3(s)	2.686	3.32(1)	95.8(3)	43
BiF_3(s)	2.23, 2.31, 2.34(1)(x2)	2.40(1)(x2), 2.50(1)(x2)	135.1(3), 100.5(1), 72.9-88.8	44, 45
$BiCl_3$(s)	2.468(4), 2.513, 2.517	3.224(3), 3.398(8), 3.450(9), 3.216(9), 3.256(9)	84.45, 93.2, 94.9(3)	46
α$BiBr_3$(s)	2.660, 2.692, 2.636(4)	3.246, 3.306, 3.699	88.2, 90.1, 96.3(1)	47
β$BiBr_3$(s)	2.82(x6)(>158° C)	3.397, 4.106	90	47
BiI_3	3.07		90.0	43

[a] contact lengths describe the intermolecular and interionic contacts shorter than Van der Waals distances, but significantly longer than conventional single bonds. They can be defined as secondary bonds. [48]

In most of the crystal structures of the Group 15 trichlorides and tribromides discrete EX_3 molecules are the primary structural units.

An early crystal structure determination of antimony trichloride [58] illustrates its pyramidal shape. Discrete $SbCl_3$ molecules are located on mirror planes, with three pyramidally directed single Sb-Cl bonds of average length 2.36(3)Å (two at 2.37Å and one at 2.35Å). The average XEX angle is 95.2°. The lone pair occupies the fourth distorted tetrahedral position, exerting a substantial steric control over the shape of the molecule. A redetermination by Lipka [41] reveals the same triangular pyramidal shape (with mirror symmetry), but the coordination polyhedra differ in their intermolecular contacts. There are three covalent Sb-Cl bonds, two of 2.368(1)Å, the third of length 2.340(2)Å, and five intermolecular Sb···Cl contacts, all significantly shorter than the Van der Waals radii of 4.0Å (Table 1.3). These secondary bonds increase the coordination number of the antimony atom to eight, yielding a bicapped trigonal prism (Figure 1.3). Presumably the lone pair occupies an orbital below the pyramidal $SbCl_3$ unit within the trigonal prism, which causes the observed lengthening of the contacts to the trigonal base.

Figure 1.3: Bicapped Trigonal Prismatic Structure of $SbCl_3$ [41]

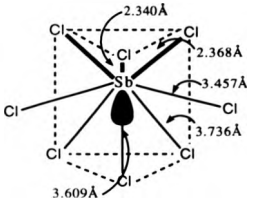

The coordination of the Sb atom is best described as [3+2+3]. One trigonal base of the bicapped trigonal prism is formed by three covalently bonded Cl atoms, the other by the three most distant Cl atoms. The remaining two secondary Sb-Cl bonds are trans to the two shortest intermolecular contacts, All interactions, including the two longest Sb···Cl contacts involve the same crystallographically independent Cl atom. In the resulting three-dimensional network the Cl atoms adopt distorted hexagonal close-packing. The [3+2+3] coordination of the Sb atom is unique to the $SbCl_3$ structure. In $SbCl_3$ complexes the intermolecular contacts usually complete octahedral, [59] ψ-octahedral or pentagonal bipyramidal [60] coordination of the Sb atom. $SbCl_3$ is similar in structure to $BiCl_3$ [46] which has five nearest neighbours in addition to the three pyramidally directed Bi-Cl bonds. The eightfold coordination of a bicapped trigonal prism around the metal seems to be a common feature of Group 15 trihalides and can also be seen in the structures of $SbBr_3$ [36] and PBr_3. [61]

The closely related coordination polyhedron of a tricapped trigonal prism is found in $AsCl_3$,[33] $AsBr_3$[38] and PCl_3.[33,34,35] All edges and faces of the EX_3A tetrahedron (A=lone pair) are involved in secondary bonding interactions, the overall geometry being $EX_3Y_3Y'_3A$ (X=primary bonds, Y=face-capping and Y'=edge-bridging secondary bonds). This tricapped trigonal prism of ligands is distorted by the lone pair, which caps a triangular face of the trigonal prism (Figure 1.4).

Figure 1.4: Tricapped Trigonal Prism in PCl_3.[33]

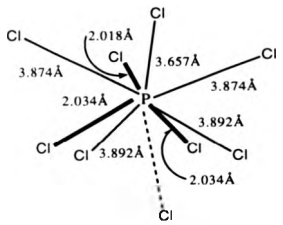

The structure of NCl_3[32] differs from the above trigonal prismatic structures; the chlorine atoms build up distorted octahedra, tetrahedra and trigonal prisms around the nitrogen atom.

In some Group 15 trihalides the stereochemical activity of the lone pair A influences the geometry of both the primary and secondary bonds while in others it has no effect on the formation of the secondary bonds. Such a "non stereochemically active" lone-pair is apparent in the anion $SbCl_5^{2-}$.[59,62] This square pyramidal ion displays weak secondary interactions in

the remaining octahedral position, close to the presumed direction of the lone pair. Stereochemical inactivity of the lone pair usually occurs when there is an excess of primary bonds over secondary interactions. In $SbCl_3$, which has only three primary bonds, the five secondary interactions avoid the presumed direction of the lone pair.

Where the lone pair exerts little or no steric control over the geometry of the secondary bonds it occupies a spherical *s-type* orbital. When as many as five primary bonds form to relatively large ligands, as in $SbCl_5^{2-}$, there is insufficient room for the lone pair to remain in the valence shell, and it moves inside the bonding pairs to occupy an *s-type* orbital. An extreme case arises in the $SbCl_6^{3-}$ anion, which has a regular octahedral structure but rather long Sb-Cl bonds of average length 2.643(6)Å. [63] The lone pair occupies a spherical *5s* orbital, which has no effect upon the orientation of the primary bonds. The Sb-Cl bonds approximate as three-centre four electron bonds formed from *5p* (of Sb) orbitals only, [64] in agreement with the Mossbauer work of Birchall *et al.* [65] The increased length of the Sb-Cl bonds, 2.643Å compared with those of $SbCl_3$ itself (2.340(2)Å and 2.368Å) [41] is in accordance with the greater coordination number of Sb in $SbCl_6^{3-}$.

There is a trend towards **decreasing stereoactivity of the lone pair** in the order **As > Sb >> Bi**, due to a greater **tendency of the lone pair to occupy an *s-type* orbital**, thus losing its steric influence. The unshared pair is stabilized by being able to distribute its electron density over the large surface of the heavy atom. [66] In $AsCl_3$ [33], $SbCl_3$ [41] and $BiCl_3$ [46] the difference in length between the primary bonds and the

secondary contacts decreases with increasing size of the central atom (Table 1.3), which implies a reduction in the stereochemical activity of the lone pair.

1.3.3. Pentahalides

All four Group 15 pentafluorides exist. They are powerful fluoride ion acceptors, forming EF_6^- anions or more complex species e.g. $E_2F_{11}^-$.

The chlorides of the group vary enormously in their stabilities. Only PCl_5 and $SbCl_5$ are stable at room temperature, although the stability of the latter extends only to 140°C. $AsCl_5$ was eventually synthesized in 1976 by the ultra-violet irradiation of $AsCl_3$ in liquid Cl_2 at -105°C. [67] It was shown, by means of Raman spectroscopy to have a trigonal bipyramidal structure.

$BiCl_5$ and EX_5 (E=As, Sb, Bi and X=Br, I) do not exist. This can be formally attributed to the inability of the halide ions to coexist with the +5 oxidation state of the Group 15 elements (compare the non-existence of FeI_3, CuI_2 and TlI_3).

The curious instability of $AsCl_5$ compared to that of PCl_5 and $SbCl_5$ can be attributed to the *"d- block contraction"*: The highest valence state of p-block elements following completion of the first (3d) transition series are, in general, unstable in comparison to the other members of the group. [3] Incomplete shielding of the nucleus by the d electrons leads to a lowering of the energy of the 4s orbital in $AsCl_3$. Hence it is more difficult to involve $4s^2$ electrons in bonding for the formation of $AsCl_5$, than it is for phosphorus or antimony. Similarly the energy of the $6s^2$ electrons in bismuth is low. This is probably

due to the" *lanthanoid contraction*," analogous to the effects experienced by arsenic. Table 1.4 shows that the sum of the fourth and fifth ionization energies of arsenic and bismuth are greater than for antimony.

Table 1.4 Ionization Energies of Arsenic, Antimony and Bismuth

	As	Sb	Bi
Ionization energies ($MJmol^{-1}$, sum of IV and V)	10.880	9.636	9.776

The pentavalent compounds of Group 15 generally adopt trigonal-bipyramidal (*tbp*) and square-pyramidal (*sp*) geometries. The *tbp* and *sp* configurations differ very little in energy and their interconversion is facile. The trigonal bipyramid is usually more stable for EX_5 molecules when X are separate groups; the square-pyramidal geometry is favoured when the X groups are connected to give two unsaturated five membered chelate rings, or in the presence of a more strained four-membered ring. [77,78]

Phosphorus pentafluoride is a trigonal bipyramidal [79] molecule with axial P-F bonds of length 1.571Å and equatorial fluorine atoms at a distance of 1.542Å. However all five fluorine atoms appear to be equivalent in the ^{19}F nmr spectrum of PF_5, [80] even at low temperatures: on the slower nmr time scale, rapid rotation of the axial-equatorial bonds via a square pyramidal intermediate results in the observed equivalence of the fluorine atoms. This rapid interchange of F-

ligands is known as *pseudorotation* via the *Berry Mechanism*. [81]

AsF_5 also has a *tbp* structure, [83] exhibiting stereochemical nonrigidity, whereas SbF_5, a viscous liquid at room temperature, is quite different. Even in the gas phase it associates by F bridges to form a cyclic trimer $(SbF_5)_3$. [84] In the liquid phase the SbF_5 moieties are linked by *cis* Sb-F-Sb bridges, resulting in polymeric chains of SbF_6 octahedra, [85] while in the solid state a tetramer forms [86] (Figure 1.5). BiF_5 is a crystalline solid, comprising infinite *trans* chains of BiF_6 octahedra. [87]

Figure 1.5: The $(SbF_5)_4$ Tetramer

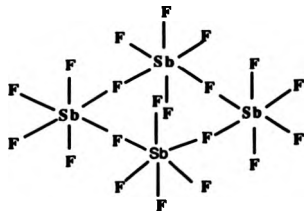

In the vapour and liquid phases PCl_5 has a molecular tbp structure; in the crystalline state it exists in the ionic form $[PCl_4][PCl_6]$, comprising tetrahedral PCl_4 cations and octahedral PCl_6 anions. [88] A well documented metastable solid form $[PCl_4]_2^+[PCl_6]Cl^-$ [89] also exists. The solution structure of PCl_5 depends upon the nature of the solvent. Disproportionation, according to equation 1, occurs in moderately polar solvents

such as MeCN and $PhNO_2$. [90] In highly polar solvents such as HCl, the ionization process (equation 2) competes with disproportionation.

$$2PCl_5 \rightleftharpoons [PCl_4]^+ + [PCl_6]^- \qquad (1)$$

$$PCl_5 \rightleftharpoons [PCl_4]^+ + Cl^- \qquad (2)$$

In non-polar solvents (such as benzene) PCl_5 is monomeric with a trigonal bipyramidal structure.

In vapour and liquid phases $SbCl_5$ exists in the monomeric *tbp* form. This geometry is retained in the crystal structure at -30°C. [91] At even lower temperatures there is spectroscopic evidence for dimerization, according to equation 3. [92]

$$2SbCl_5(\text{monomer}) \xrightleftharpoons{-76°C} Cl_4Sb\text{-}\mu(Cl)_2SbCl_4 \qquad (3)$$

PBr_5 is the only known pentabromide of the heavier Group 15 elements, in the gas phase it dissociates fully to PBr_3 and Br_2. This dissociation occurs in non polar solvents of low dielectric constant, while in more polar solvents such as MeCN, disproportionation is thought to occur, according to equation 4. [93]

$$2PBr_5 \rightleftharpoons [PBr_4]^+[PBr_6]^- \qquad (4)$$

Solid PBr_5 consists of $[PBr_4]^+$ and Br^- ions; [94] each Br^- ion is surrounded by four bromine atoms, each belonging to a different PBr_4^+ unit. Unlike PCl_6^- the $[PBr_6]^-$ anion seems to be unknown in the solid state. [95] The octahedral PBr_6^- anion is, however, stabilized by solvent molecules. This behaviour is analogous to that of phosphorus pentachloride in solvents of varying polarity. [90]

Antimony pentabromide has been isolated only as an adduct with ether, i.e. $(C_2H_5)_2O.SbBr_5$. The neutral ether ligand increases the electron density on Sb(V), and reduces its oxidising strength.

The synthesis of PI_5, formulated as $[PI_4]^+I^-$, was reported in 1978, [96] but it is probable that a mixture of PI_3 and I_2 was analysed. $PI_4^+AsF_6^-$ has been isolated [97] and characterised by Raman spectroscopy as the first example of a salt containing the discrete tetrahedral cation PI_4^+, a derivative of the unknown PI_5. It is thermodynamically unstable with respect to $PF_3(g)$, $AsF_3(l)$ and $I_2(s)$. Although $PI_4^+AlI_4^-$ has been reported, [98] the PI_4 and AlI_4 units are connected into a three dimensional structure by weak secondary iodine-iodine bonds. In the solid state the structure can be regarded as intermediate between molecular $PI_3/I_2/AlI_3$ and the ionic formulation given above. IF, SbF_5 and PI_3 together yield $PI_4^+SbF_6^-$, [97] which is less stable than its arsenic congener.

Stereochemical nonrigidity in pentavalent molecules increases in the order P < As < Sb (i.e. as the electronegativity of the central atom decreases). This is in accordance with a simple repulsion model which favours a trigonal bipyramidal geometry. [99] As repulsion effects are reduced in the order P > As > Sb, the energy difference favouring the *tbp* geometry decreases (hence so does the energy barrier between them).

Both AsF_5, SbF_5 and to a lesser extent PF_5 are very powerful fluoride ion acceptors, yielding EF_6^- ions or more complex species. The hexafluorophosphate(V) anion is frequently used as a non-complexing anion which has even less

coordinating ability than the ClO_4^- and BF_4^- anions. SbF_5 is used to generate SbF_6^-, another non-complexing anion, In Fe(TPP)($FSbF_5$).PhF [100] however, it is found to be a ligand covalently bound to iron, not the expected anion. Hexafluoroantimonate(V) likewise binds to some coordinatively unsaturated cations. [101]

BiF_5 has markedly weaker Lewis acidic properties than those of SbF_5, as illustrated by the structures of the adducts formed with xenon tetrafluoride. The antimony pentafluoride adduct is essentially ionic, $[XeF_3]^+[SbF_6]^-$, [102] with a bridging fluorine ligand 2.49Å from the XeF_3^+ unit. In the bismuth analogue [103] the μ(F-XeF) distance of 2.25Å is shorter and has a much greater covalent character. The structure is intermediate between the molecular $XeF_4.BiF_5$ and the ionic $[XeF_3]^+[BiF_6]^-$ formulations.

SbF_5 is the strongest Lewis acid of the Group 15 pentafluorides, and forms the strongest superacid with HSO_3F ("magic acid"). [104] The strong halide acceptor properties of the pentahalides are also exploited in their use as Friedel Crafts catalysts. [105] The elimination of HF by SbF_5 finds utility in the synthesis of fluoro-alkene derivatives in a novel approach to conjugated polymers. [106] The Lewis acidity of the pentafluorides will be discussed more fully later in this chapter.

The pentafluorides are extremely powerful fluorinating and oxidising agents, some typical reactions including:

$SbF_5 + ClCH_2PCl_2 \longrightarrow ClCH_2PF_4$

$BiF_5 + UF_4 \xrightarrow{150°C} UF_6$

$BiF_5 + Br_2 \xrightarrow{180°C} BrF_3 + BrF_5$

$BiF_5 + Cl_2 \xrightarrow{180°C} ClF$

SbF_3 (known as the Swarts reagent) and AsF_3 are also used as fluorinating agents:

$RCl \longrightarrow RF$

$R_3PS \longrightarrow R_3PF_2$

Antimony pentachloride behaves as a chlorinating and oxidising agent, *e.g.*

$Me_3As + SbCl_5 \longrightarrow Me_3AsCl_2 + SbCl_3$

$R_3P + SbCl_5 \longrightarrow [R_3PCl]^+[SbCl_6]^-$ (R=Ph, Et_2N, Cl)

The addition of small amounts of $SbCl_5$ to SbF_5 greatly reduces its viscosity by cleavage of the Sb-F-Sb bridges. This of importance in industrial applications of the Swarts reactions.

1.3.4. Mixed Pentahalides

Several covalent mixed pentahalides are known (e.g. PCl_4F, $SbCl_3F_2$, $SbCl_2F_3$). Others have ionic structures: the conductivity of $AsCl_2F_3$ in excess AsF_3 suggests the ionic formulation $[AsCl_4]^+[AsF_6]^-$.[73,74] In the vapour phase (below 55°C) $AsCl_3F_3$ monomers adopt a trigonal bipyramidal shape in which the two chlorines occupy equatorial positions.[75] The entire series of mixed chlorofluoroarsanes, $AsCl_nF_{n-1}$(n=1-5), have been synthesized from $AsCl_2F_3$.[68-72] The ionic mixed halides $[AsCl_4]^+[PCl_6]^-$ and $[AsCl_4]^+[SbCl_6]^-$[107] stabilize the +5 oxidation state of arsenic.

1.4.Group15 Halides as Acceptors:

1.4.1.Trihalides

EX_3 (X=halogen; E=P, As, Sb, Bi) compounds can behave both as ligands and acceptors: this duality leads to some interesting chemistry. PX_3 molecules are important π acid ligands, due to the polarity of the P-X bond (especially when X=F). The ligand PCl_3 is a good donor and forms purely σ bonded complexes with the boron halides. [108] Phosphorus trihalides also exhibit some Lewis acceptor behaviour, as shown by their formation of weak complexes with trimethylamine.

The trihalides of arsenic also show significant Lewis acidity, but it is with the Sb(III) and Bi(III) halides that extensive complex formation occurs. They form a great variety of adducts with neutral and anionic ligands. The compatability of donors for complexation can be rationalised by the Hard-Soft-Acid-Base (HSAB) rule. [109] SbX_3 and BiX_3 are hard acids, they form very stable complexes with chloride ion ligands. $SbCl_3$ forms very weak complexes with "soft" S-donor ligands. [118] The HSAB principle is a very useful rule of thumb for coordination chemistry, yet more and more complexes are being synthesized when the acid-base interactions are thought to be unfavourable (Chapter 5).

1.4.1.1.Group 15 Trihalide Adducts with Neutral Ligands

The trihalides of arsenic, antimony and bismuth form a great number of adducts with neutral ligands, yielding coordination numbers from 4 to 8.

Four Coordinate Structures

The majority of four coordinate mono-adducts, EX_3L (E=As,Sb,Bi; X=halogen; L=neutral ligand) retain stereochemical activity of the lone pair. The mono-adduct with aniline, $SbCl_3.PhNH_2$, [111] has a distorted trigonal bipyramidal geometry, the lone pair occupies one of the equatorial positions, as predicted by VSEPR. This is an example of a "hard" Lewis base (nitrogen donor) interacting with the hard Sb(III) (Lewis acid) centre. $AsCl_3.NMe_3$ [112] displays a similar interaction, although the As-N bond is very long (Figure 1.6). In both these structures the donor ligand occupies an axial position.

Figure 1.6: Structures of $SbCl_3.PhNH_2$ and $AsCl_3.NMe_3$

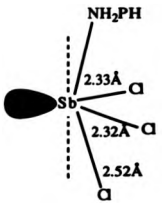

$SbCl_3.PhNH_2$.[111]

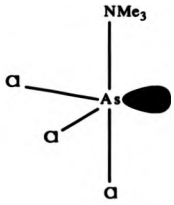

$AsCl_3.NMe_3$. [112]

This contrasts $SbCl_3$.dmit [113] (dmit=1, 3-dimethyl-2-(3H)-imidazolethione), in which both the ligand and the lone pair occupy equatorial positions (Figure 1.7).

Figure 1.7: Structure of $SbCl_3$.dmit. [113]

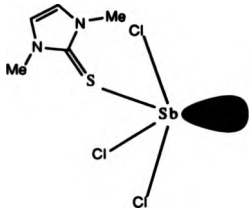

Oxygen donor adducts EX_3L (L=$POCl_3$ and $POMe_3$) have also been isolated. [114]

Five Coordinate Structures

Five coordinate structures fall into two classes; 1:1 complexes with bidentate ligands and 1:2 complexes with monodentate ligands. The distorted square-pyramidal species $SbCl_3.2PhNH_2$ [115] illustrates the latter possibility. The Sb atom lies below the basal plane of the square pyramid while the lone pair occupies the sixth coordination site. In $SbCl_3$.DEDTM [116] (Figure 1.8) the N, N'-diethyldithiomalonamide molecule bonds to $SbCl_3$ as a *cis* chelate ligand through the sulphur atoms. The Sb atom lies below the Cl(2), Cl(3), S, S plane, the sixth octahedral position is taken up by the lone pair.

Figure 1.8: $SbCl_3$.DEDTM [116]

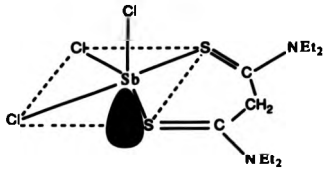

These structures contrast $[SbCl_5]^{2-}$ where the lone pair seems to be stereochemically inactive. [59,62]

Six Coordinate Structures

The six coordinate arrangement of ligands is highly favoured in the structures of the Group 15 trihalides. A good example is found in the polymeric $SbCl_3$.DMO adduct. [117] Each Sb atom binds strongly to three chlorine atoms (Sb-Cl; 2.35-2.40Å) and weakly to three oxygen atoms, resulting in a *regular octahedral* Sb geometry. In $SbCl_3.(DEDTO)_{1.5}$ each Sb atom is bound by three Cl atoms and three loosely bound sulphur atoms [118] to give a more *distorted octahedral* geometry. In both cases the lone pair seems to have very little stereochemical activity.

However, the lone pair is stereochemically active when the ligand contains "hard" donor atoms or "narrow bite" ligands. For example, $Bi(S_2CNEt_2)_3$, [119] features an octahedral coordination sphere. The lone pair acts through the centre of one of the faces, resulting in a *pseudo* seven-coordinate structure.

Seven Coordinate Structures

Seven coordination is seen in the monomeric $BiCl_3.(DEDTO)_2$ molecule. [120] The geometry approaches ideal pentagonal-bipyramidal, with two chlorine ligands in axial positions, and the remaining ligands in the equatorial plane. There is no vacancy in the Bi(III) coordination sphere for a stereochemically active lone pair. Such pentagonal bipyramidal geometry is usual in complexes of Group 15 trihalides with two bidentate ligands of large bite.

Eight Coordinate Structures

The compound $BiCl_3.18$-crown-6 [121] has the ionic formulation $2[BiCl_2.18\text{-crown-}6]^+[Bi_2Cl_8]^{2-}$. The bismuth cation is eight coordinate, involving the six oxygens of the crown ether and the two chlorine atoms in a bicapped trigonal prismatic geometry. The lone pair on bismuth(III) is thought to be active, pointing in the direction of the third potential capping position of the trigonal prism. Eightfold coordination of Sb(III) is also observed in the adduct $SbF_3.15$-crown-5. [122] The Sb atom is surrounded by three F atoms and the five oxygen atoms of the crown ether molecule. The analogous $SbCl_3.15$-crown-5 [123] features a stereochemically active lone pair, which points towards the centre of the crown ring. The three Sb-Cl bonds are pyramidally directed, the $SbCl_3$ molecule suffering very little structural change upon complexation to the crown molecule. The Sb-O distances vary from 2.787(5) to 2.997(4)Å, averaging 2.902Å (c.f. sum of covalent radii 2.2Å). These observations indicate weak $SbCl_3$-crown ether interactions. Even weaker interactions are found in $SbCl_3.18$-crown-6, [124]

where the mean Sb-O distance is 3.183Å, the lone pair is again stereochemically active.

Menshutkin Complexes

Aromatic donor ligands form a great number of complexes with Group 15 trihalides which vary enormously in their structures. These adducts involve weak interactions between the EX_3 molecule and the π cloud, and are known as *"Menshutkin"* complexes.

Smith and Davies [125] described adducts of antimony tribromide and trichloride with benzene and napthalene more than 100 years ago, and in 1912 Menshutkin [126] prepared and characterised several complexes between substituted aromatics and $SbCl_3$. Crystallographic investigations have more recently extended to complexes of both arsenic [127,128] and bismuth [129, 130,131] trichlorides and tribromides.

The 2:1 complex between $SbCl_3$ and napthalene [132] illustrates the bonding between the metal centre and the arene (Figure 1.9).

Figure 1.9: 2:1 Complex between $SbCl_3$ and Napthalene. [132]

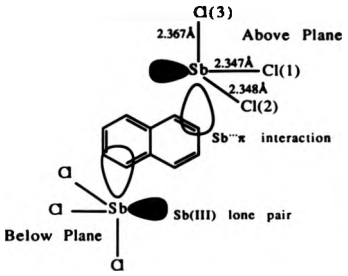

The two $SbCl_3$ moieties lie on opposite sides of the ring plane. The Sb atoms adopt distorted trigonal bipyramidal coordination: Cl(1), Cl(2) and the Sb lone pair lie in the equatorial plane, while the axial positions are occupied by Cl(3) and the electrons donated from the π-system of napthalene. The axial Sb-Cl(3) distance (2.367Å), is longer than the equatorial Sb-Cl(1), Sb-Cl(2) distances of 2.347 and 2.348Å respectively. The lone pair on antimony points over the aromatic ring, and is well positioned for interaction with the π*-orbitals. The complex exhibits η^3, *pseudo* π-allyl coordination. This contrasts the 1:1 hexaethylbenzene: trichloroantimony complex, [133] which shows centroid or hexahapto (η^6) coordination of the arene molecule (i.e. the lone pair on Sb(III) is oriented towards the centre of the ring).

Bismuth-arene complexes are more stable than those of arsenic and antimony. Metal-arene distances in Menshutkin complexes decrease in the order **As > Sb > Bi**. This is

surprising in the light of the standard covalent radii of As, Sb and Bi (1.21, 1.41 and 1.52Å), [134] reflecting an increasing metal-arene interaction in the order As < Sb < Bi. (This parallels the increased *s* character of the lone pair on the heavier atom, as suggested by the *"inert pair"* effect based on relativistic phenomena). [135]

$[Ph_4P]_2[Sb_2I_8].2MeCN$ [136] displays weak interactions between the phenyl groups of the cation and the antimony atoms of the anion, similar to those found in the Menshutkin complexes. The antimony atoms in the dimeric $[Sb_2I_8]^{2-}$ anion are square pyramidally coordinated by the iodine ligands, octahedral coordination being completed by η^2-bonded phenyl rings of the cation.

1.4.1.2.Complexes with Halide Ion Ligands

The trihalides of arsenic, antimony and bismuth combine with halide ions to form an extensive series of complex anions. Examples include: $[SbCl_4]^-$, [137] $[SbCl_5]^{2-}$, [138] $[BiCl_6]^{3-}$, [139] $[As_2Br_8]^{2-}$, [140] $[Sb_2Cl_9]^{3-}$, [141] $[As_4Cl_{16}]^{4-}$, [142] and $[Bi_4Cl_{18}]^{6-}$. [143] In the majority of these reactions the source of the halide ion is an organic molecule, RX, or an alkali metal halide, MX.

The conductivities of the trihalides are increased by addition of substances such as KF, Me_4NCl, SbF_5 and $FeCl_3$ which can donate or accept halide ions to give ionic species.

Arsenic and antimony trifluorides accept fluoride ions from MF, (M=Na, K, Rb, Cs) resulting in the formation of a variety of fluoroanions, Lithium fluoride fails to donate F^- ions doubtless due to the small size and polarizing power of the lithium cation. [144]

The stoichiometry of the resulting species is not particularly informative about their structures. This is due to oligomerisation of the resultant $[MF_4]^-$ ions which depends upon the nature of M. (No monomeric C_{2v} SbF_4^- anion (isoelectronic with SeF_4) exists).

The anion in $NaSbF_4$ [145] is based on a trigonal bipyramid of four primary Sb-F bonds and a lone pair. There are two secondary Sb···F contacts of 2.66 and 2.87Å which bridge the edges of the equatorial plane. This results in dimerisation of $\{SbF_4\}$ units. There is a third weaker contact of 3.33Å which caps one face of the bipyramid. In $KSbF_4$ [146] association of $\{SbF_4\}$ units occurs to give the tetrameric, cyclic anion $[Sb_4F_{16}]^{4-}$ (Figure 1.10). The geometry of the Sb(III) atom is slighty distorted from the EX_5A octahedral geometry of the SbF_5^{2-} anion and is intermediate between EX_3Y_3A and EX_5YA. Two of the equatorial Sb-F bonds are longer than the other two, and there is one long Sb···F contact of 2.94(2)Å, which caps an octahedral face.

Figure 1.10: The Tetrameric Cyclic Anion $[Sb_4F_{16}^-]$

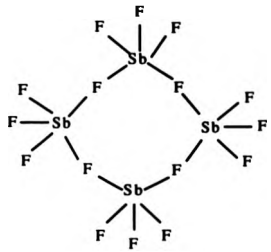

The SbF_5^{2-} anion in $(NH_4)_2SbF_5$ [147] has a short apical Sb-F bond (1.92Å) (compare 1.90 and 1.94(2)Å in SbF_3 itself), [40] which is trans to the lone pair, while the longer Sb-F bonds of average length 2.08Å form the base of the square pyramid. The Sb atom is slightly below the basal plane. This ion has a discrete structure, there are no secondary Sb···F contacts shorter than the Van der Waals radii (Figure 1.11). The K, Rb, Cs and Tl salts are isostructural with the ammonium salt.

Figure 1.11: The $[SbF_5]^{2-}$ Anion

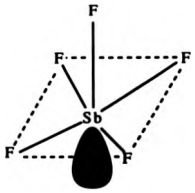

The mononuclear SbF_6^{3-} anion appears to be absent in the series of Sb(III) fluoroanions.

The structures of several salts of the $Sb_2F_7^-$ anion have been determined. [148,149,150] The ion consists of two SbF_3 groups bridged by a fluoride ion. In KSb_2F_7 [148] and $RbSb_2F_7$ [150] the Sb-F-Sb bridges are asymmetric (Sb-F lengths are 2.082 and 2.409(3)Å and 2.12 and 2.33Å respectively). In $CsSb_2F_7$, [149] however, the bridge is symmetrical with Sb-F distances of 2.240Å. In the three salts the environment of the Sb(III) atoms can be considered in two ways. A basic trigonal bipyramidal EX_4A geometry results if the bridging Sb-F bond is considered to be a primary bond. In this case the three (or four) secondary contacts cap two of the faces and bridge one (or two) of the edges. If the bridge is thought of as a secondary interaction the basic geometry is EX_3A tetrahedral. Four (or five) secondary contacts yield a partial $EX_3Y_3Y'_3A$ tricapped trigonal prismatic arrangement of atoms in which one or two of the Y' contacts are absent (Figure 1.12).

Figure 1.12: The $Sb_2F_7^-$ Anion in $CsSb_2F_7$

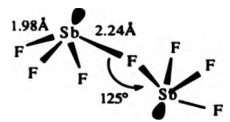

The anions $(SbF_3)_xF^-$, (x =3, 4) occur in $(NH_4)Sb_3F_{10}$, [151] $NaSb_3F_{10}$ [152] and KSb_4F_{13}. [153] The primary geometry of the Sb(III) atoms in the potassium salt is best described as

tetrahedral EX_3A, with three relatively short face-capping contacts of lengths 2.51 to 2.75Å, and three longer contacts of length 3.03 to 3.19Å. These bridge the edges of the tetrahedron, giving an overall $EX_3Y_3Y'_3A$ geometry. If the shortest of the secondary contacts (2.51Å) is considered as a primary bond, a basic EX_4A geometry results with two face-capping and three edge-bridging contacts. An overall $EX_4Y_3Y'A$ geometry describes the Sb(III) atoms in $NaSb_3F_{10}$. The structure of the ammonium salt seems to be quite different; the anion can be viewed either as an SbF_3 group interacting with an $Sb_2F_7^-$ moiety or as two SbF_3 groups interacting with an SbF_4^- anion. Sb(1) has an overall $EX_4Y_4Y'_3A$ geometry, while Sb(2) and Sb(3) have $EX_3Y_3Y'_2A$ and EX_4Y_3A geometries respectively.

The $Sb_2F_9^{3-}$ anion is found in $[Co(NH_3)_6]^{3+}[Sb_2F_9]^{3-}$;[154] it comprises two SbF_5 square pyramids which share a common F atom. The Sb(III) geometry is based on pentagonal bipyramidal (EX_6Y_3A) coordination, with the lone pair in an axial position surrounded by three longer contacts. The mixed Sb(III)/Sb(V) species $Sb_3F_{14}^-$ occurs in, for example, $[S_4N_4][Sb_3F_{14}][SbF_6]$,[155] $[S_8][Sb_3F_{14}][SbF_6]$[156] and $[I_4][Sb_3F_{14}][SbF_6]$.[157] The trimeric anion in the former salt consists of an angular $Sb^{III}F_2^+$ cation linked by trans asymmetric bridges to two $Sb^VF_6^-$ anions (Figure 1.13). The central Sb(III) atom has a trigonal bipyramidal geometry with the lone pair in an equatorial position. It forms four additional contacts to fluorine atoms in other SbF_6^- and $Sb_3F_{14}^-$ anions; these surround the lone pair to give overall distorted square-capped antiprismatic (EX_4Y_4A) coordination. Other salts of the

$Sb_3F_{14}^-$ anion have up to six secondary contacts to Sb(III), which bridge the edges or cap the faces of the trigonal bipyramid containing the lone pair as a vertex. Differences in secondary bond formation arise from the packing requirements of the cations in the lattice. Weak $Sb^{(III)}$...F interactions can cause $Sb_3F_{14}^-$ anions to form oligomeric chains or layers as in $[Te_2Se_4][Sb_3F_{14}][SbF_6]$. [158]

Figure 1.13: The $[Sb_3F_{14}]^-$ ion in $[S_4N_4][Sb_3F_{14}][SbF_6]$ [155]

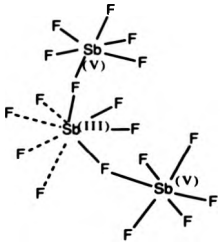

Other mixed $Sb^{(III)}/Sb^{(V)}$ species are known. The $Sb_4F_{17}^-$ anion in $[SeS]_2[Sb_4F_{17}][SbF_6]_3$ [159] can be formulated as $[SbF_6^-.SbF_2^+.F^-.SbF_2^+.SbF_6^-]$ or as $[SbF_6^-.Sb_2F_5^+.SbF_6]$. The central fluorine atom forms the crystallographic centre of symmetry; the $Sb_2F_5^+$ cation has a linear Sb-F-Sb bridge with Sb-F distances of 2.11Å. (Compare the analogous $Sb_2F_5^+$ cation in $[Se_4]^{2+}[Sb_2F_4]^{2+}[Sb_2F_5]^+[SbF_6]$ which has an asymmetric fluorine bridge, with Sb-F distances, 2.09(1) and 2.15(1)Å, and an Sb-F-Sb angle of 149.8(6)°). [160] In "$Sb_2F_4Cl_5$", [161] formulated

$[(Sb^{V}F_2Cl_3\text{-}F\text{-}Sb^{V}FCl_3\text{-}F\text{-}Sb^{III}Cl\text{-})_2F]^+[Sb_2Cl_5F_6]^-$ the cation contains a central Sb(III) atom bonded via F bridges to an Sb(V) atom, and which is weakly bound to terminal F atoms of the anion to give overall 8 coordination of the Sb(III).

$SbF_3.SbF_5$ mixtures yield several other mixed oxidation state species: crystal structures of the 1:1, 2:1, 3:1, 6:5, 5:3 and 3:4 adducts have been determined. [162-167] The 1:1 adduct [163] consists of $Sb_2F_4^{2+}$ cations and SbF_6^- anions. The cation, which has an asymmetric bridge (Sb-F lengths of 2.01Å and 2.15Å; F-Sb-F angle of 148°), may be considered as an SbF_3 molecule interacting with an SbF^{2+} cation (Figure 1.14).

Figure 1.14: The $[Sb_2F_4]^{2+}$ cation in $SbF_3.SbF_5$ (showing contacts shorter than 2.15Å)

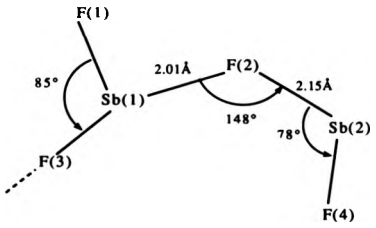

Sb(1) has an $EX_3Y_3Y'_2A$ geometry based upon a pyramidal EX_3A coordination, while Sb(2) is based upon an EX_5A pentagonal bipyramid. Three long contacts avoid the axial lone pair and cap three faces of the bipyramid (these are not shown

in Figure 1.14). The axial Sb(2)-F(4) bond (1.86Å) is shorter than the equatorial contacts, which range from 2.14 to 2.41Å. Bond angles in the equatorial pentagonal plane are close to the ideal 72°. The Sb^{III} atoms of the cation interact with fluorine atoms of the SbF_6^- anion to form a three dimensional polymeric structure. This $[Sb_2F_4]^{2+}$ unit contrasts the similar ion in $[Se_4]^{2+}[Sb_2F_4]^{2+}[Sb_2F_5]^+[SbF_6]_5^-$, [160] which is situated around a centre of symmetry. Here the Sb(III) atoms form primary bonds to two fluorine atoms related by the centre of symmetry to give planar Sb_2F_2 rings. There are additional bonds; a primary axial Sb-F bond and five further secondary fluorine contacts.

The unit cell of $Sb_{11}F_{43}$, (i.e. $6SbF_3.5SbF_5$) contains five SbF_6^- anions and a section of the polymeric Sb(III) chain cation $[Sb_6F_{13}]_n^{5+}$. [162] There are a large number of contacts between the Sb(III) atoms and the fluorine atoms of the SbF_6^- octahedra. If only the shorter Sb^{III}-F bonds are considered, the cation can be considered as separate SbF_2^+ and $Sb_2F_5^+$ units. The $Sb_2F_5^+$ unit has a linear symmetric fluorine bridge. By comparison, the $Sb_2F_5^+$ unit in the 3:1 adduct $3SbF_3.SbF_5$ [164] has a bent symmetric bridge (Sb-F-Sb angle,147.4°). It joins SbF_3 units by Sb-F bridges to form parallel strands of $[Sb_3F_8]^+_\infty$, associated by weak contacts of 2.716-3.056Å with the fluorine atoms of SbF_6^-. The component SbF_3 and $Sb_2F_5^+$ units are distinguished when only bonds shorter than 2.15Å are considered (Figure 1.15). The $Sb_2F_5^+$ unit has mirror symmetry.

Figure 1.15: The $Sb_2F_5^+$ cation in $(SbF_3)_3.SbF_5$. [164]

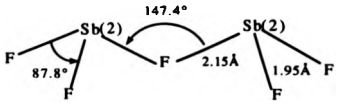

Bond angles around the Sb(III) atoms Sb(2) and Sb(3) are consistent with the presence of stereochemically active lone pairs. Sb(3) is square-pyramidal, the shortest Sb-F bond being trans to the lone pair. Four equatorial fluorine atoms form a plane 0.395(1)Å below Sb(3) (F_{eq}-Sb-F_{ax} < 90°). An additional contact of 2.833(7)Å with an F atom of SbF_6^- completes the monocapped octahedral (EX_3Y_3A) geometry. The coordination around Sb(2), including all contacts less than 3.00Å, is based upon a pentagonal bipyramid (EXY_5A).

By comparison $5SbF_3.3SbF_5$ consists of three dimensional cross-linked $[Sb_5F_{12}]_n^{3n+}$ cations and SbF_6^- anions. The cation consists of F-linked $Sb_2F_5^+$, $Sb_2F_3^{3+}$ and SbF_3 units. [166] The $Sb_2F_5^+$ component has a linear symmetric F bridge, similar to that found in $6SbF_3.5SbF_5$. [162] The $Sb_2F_3^{3+}$ component (Figure 1.16), has a cis planar configuration. This ion strongly interacts with two SbF_3 units to form the $Sb_4F_9^{3+}$ cation, if bonds ≤ 2.25Å are taken into consideration.

Figure 1.16: The $[Sb_2F_3]^{3+}$ cation in $5SbF_3.3SbF_5$.[162]

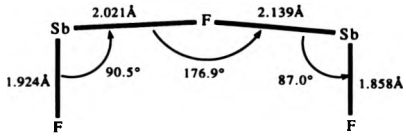

In all these fluoroanions the lone pair on Sb(III) exerts stereochemical influence over the geometry of the primary and secondary bond formation. The lone pair has less effect upon the stereochemistry of the complex halides of trivalent As, Sb, and Bi as

1) the coordination number on the central atom increases,
2) the atomic mass of the central atom increases and
3) the atomic mass of the halide increases.

1.4.2. Pentahalides

As previously mentioned the pentafluorides of arsenic, antimony and bismuth all exhibit Lewis acidic properties, and are powerful fluoride ion acceptors. Antimony pentachloride, the only stable pentachloride of As, Sb, and Bi, is also a powerful chloride ion acceptor. Acceptance of a halide ion increases the coordination number of the pentahalide to six, resulting in the formation of the octahedral, hexahalo anions $[EX_6]^-$ (E=P, As, Sb, Bi; X=halide).

Early crystal structure determinations of MEF_6 salts (M=Li, Na, K, Rb, Cs, Ag, Tl; E=As, Sb) show almost symmetrical octahedral anions. [168] (Preparation of these salts involved fluorination of the appropriate Group 15 trioxide E_2O_3 and metal halide using bromine trifluoride). Cation size influences the structure type; smaller cations such as lithium coordinate fluorines from six SbF_6^- groups, while larger cations such as caesium are coordinated by twelve fluorine atoms. Divalent metal fluorides react with AsF_5 in liquid HF [169] to give hexafluoroarsenates: $MF_2.2AsF_5$ (M=Mg, Ca, Co, Pb), $2MF_2.3AsF_5$ (M=Fe, Cu, Zn) and $MF_2.AsF_5$ (M=Ag and Sn).

The hexafluoro anions EF_6^- occur with a variety of quite elaborate cations. For example, $[Te_4Se_6][Te_2Se_8][AsF_6]_4(SO_2)_2$ [170] forms in SO_2 solution by condensing AsF_5 onto a mixture of Te, Se and S.

AsF_5 is used as a means of breaking the S-F bond in RSF_3, yielding the fluorosulfonium hexafluoroarsenates $RSF_2^+AsF_6^-$, R = Me_2N, CF_3. [171] Tribromosulfonium(IV) hexafluoroantimonate(V) $SBr_3^+.SbF_6^-$ has short contacts between the S atom of the cation and F atoms of surrounding

SbF_6^- anions, providing a distorted ψ-octahedral coordination around sulphur. [172] In addition, S-Br and Sb-F bonds and short Br-F contacts in the crystal yield nine and ten membered heterocycles.

The non-coordinating hexafluoroarsenate anion also stabilises the (iodocyano)iodonium, $[ICNI]^+$ cation, providing the first example of an N^+–I bond stable at room temperature. [173]

The pentahalides also form octahedral adducts with neutral ligands. In arsenic pentafluoride: *N* -methyl-S, S-difluorosulfoximine [174] the As-N bond length, 1.985Å is longer than the normal As-N bond length of 1.87Å, but is shorter than in $AsCl_3.NMe_3$ (2.286Å). [112] This is consistent with the more acidic arsenic(V) atom, whose acceptor ability is further enhanced by the F atoms.

Antimony and arsenic pentafluorides also form adducts with uranyl fluoride, UF_2O_2, [175] illustrating their powerful Lewis acidity. $UF_2O_2.3SbF_5$ comprises chains of UO_2 groups bridged to SbF_6^- units, with $Sb_2F_{11}^-$ side chains. Adducts of SbF_5 and BiF_5 with uranium tetrafluoride oxide, UF_4O are fluorine bridged with some ionic character, once again illustrating the great Lewis acidity of the pentafluorides, in the order Sb ≥ Bi. [176]

More complex anions such as $Sb_2F_{11}^-$ and $Sb_3F_{16}^-$ are formed by fluoride bridging. The former have been observed in many structures, [177] and consist of an SbF_6^- ion and an SbF_5 molecule joined by a fluorine bridge. Higher polymeric anions $[Sb_nF_{5n+1}]^-$, n=3,4, consisting of *cis* -bridged SbF_5 units can also be formed. [178] The $[Bi_2F_{11}]^-$ anion exists in adducts of noble gas

fluorides, and has been characterised, using Raman spectroscopy, as a linear species. [179]

Force constant calculations by Bougon *et al.* [180] suggest that the fluoride ion acceptor strengths increase in the order $BiF_5 < AsF_5 < SbF_5$. SbF_5 removes a fluoride ion from AsF_3 to yield AsF_2^+ and SbF_6^- ions. [181] There is some degree of cation-anion interaction resulting from fluorine bridging.

$Cp_2Ti[PF_6]_2$ is unstable with respect to Cp_2TiF_2 and PF_5, whereas the increased fluoride ion affinities of AsF_5, SbF_5 and BiF_5 stabilise the titanocene group in $Cp_2Ti[AsF_6]_2$, [182] $Cp_2Ti[SbF_6]_2$ [183] and $Cp_2Ti[BiF_6]_2$. [184] These represent the first well characterised F-coordinated metallocene hexafluoropnictate species. All these compounds are prepared by the reaction of $CpTiF_2$ with the corresponding pentafluoride, which behaves as a fluoride ion acceptor i.e.

$$Cp_2TiF_2 + 2EF_5 \longrightarrow Cp_2Ti[EF_6]_2 \quad E=As, Sb, Bi.$$

The AsF_6^- and SbF_6^- ions adopt regular octahedral geometry, while the hexafluorobismuthate unit has a distorted structure due to smaller differences between bridging (Ti···F···E) and non-bridging (E-F) lengths in the bismuth species.

Reaction of NiF_2 with the corresponding pentafluoride in anhydrous HF [185] yields $Ni[BiF_6]_2$ and $Ni[SbF_6]_2$. Addition of acetonitrile affords the ternary adducts $[Ni(MeCN)_6][BiF_6]_2$ [186] and $[Ni(MeCN)_6][SbF_6]_2$. [187] In the unsolvated hexafluoropnictates the SbF_6^- anion has an octahedral structure of C_3 symmetry, while BiF_6^- [186] has a distorted structure. Introduction of six acetonitrile ligands reduces the polarising effect of Ni(II), relieving these distortions.

The adducts $BiF_5.(SbF_5)_n$ (n=1.5, 2, 3) have been prepared; [188] they consist of SbF_5 and BiF_5 units joined by *cis* -bridged fluorine atoms to form tetramers (like solid $(SbF_5)_4$). [86] $(BiF_5)_nSbF_5$ ($n \geq 1$) on the other hand have *trans* -bridged polymeric BiF_5 [87] structures. No ionic species are present in these compounds although SbF_5 has been shown to be a better Lewis acid than BiF_5. [179,189]

In vapour, liquid and crystalline phases, $SbCl_5$ has a trigonal-bipyramidal structure [91] (Figure 1.17). Upon interaction with a donor group the coordination number increases to six, which results in the formation of an octahedral complex.

Figure 1.17: Trigonal Bipyramidal Shape of $SbCl_5$

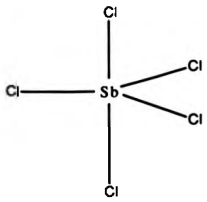

In particular $SbCl_5$ readily accepts a chloride ion to give the octahedral hexachloroantimonate(V) anion $SbCl_6^-$. Whereas ionic species occur with halide ion donors, molecular adduct formation occurs with nitrogen, oxygen and sulphur donors. [190] For example $S_4N_4.SbCl_5$ [191] has an octahedral Sb(V) atom which bonds five chlorine atoms and one nitrogen atom of the S_4N_4

ring (Figure 1.18). However with excess $SbCl_5$ in liquid SO_2 a redox reaction occurs to yield $[S_4N_4]^{2+}[SbCl_6]_2$, consisting of discrete $S_4N_4^{2+}$ cations and $SbCl_6^-$ anions.

Figure 1.18: $S_4N_4.SbCl_5$. [191]

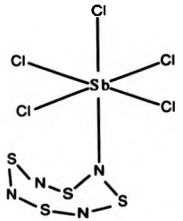

The adduct $SbCl_5.SeOCl_2$ was prepared in 1865, [192] but its structure was only elucidated 100 years later: [193] the central Sb(V) atom has a distorted octahedral geometry, adjacent chlorines bending towards the donor-acceptor bond.

The 1:1 adduct $S_8O.SbCl_5$ stabilises the cyclo-octa sulphur monoxide molecule; [194] upon coordination to $SbCl_5$ the exocyclic oxygen occupies the sixth coordination site on Sb(V) to give a distorted octahedron; Sb-Cl distances average 2.33Å, and Cl-Sb-Cl angles lie between 86 and 94°.

Antimony pentachloride reacts with a wide range of chlorine donors RCl, with the formation of a cationic species $[R^+]$ and the $[SbCl_6]^-$ anion. This chloride abstracting ability has been exploited in the formation of many hexachloroantimonate(V) salts and has been further investigated during the course of this work.

CHAPTER 2

Halide Abstracting Properties of Antimony Pentachloride

2.1.Introduction

One of the characteristic properties of Sb(V) is its ability to accept halide ions with consequent salt formation.

$RX + SbX_5 \longrightarrow [R][SbX_6]$ (R=organic group)

Antimony pentachloride finds use as a non-aqueous solvent because many covalent chlorides readily dissolve to give conducting solutions. [195] Auto-ionization is negligible, hence the formation of charged species results from halide transfer, which gives rise to the $SbCl_6^-$ anion; [196]

$$MCl_n + SbCl_5 \xrightarrow{\text{acceptor}} [MCl_{n-1}]^+[SbCl_6]^-$$

$SbCl_5$ is used in organic synthesis as a chloride abstractor. [197] Tertiary phosphines, $PRCl_2$ and PR_2Cl react with excess $SbCl_5$ to give phosphonium and chlorophosphonium salts.

$PFCl_2 + SbCl_5 + Cl_2 \longrightarrow [PFCl_3][SbCl_6]$

$Ph_3PCl_2 + SbCl_5 \longrightarrow [Ph_3PCl][SbCl_6]$

Infra-red data supports the existence of the $[PFCl_3]^+$ cation. [198]

Antimony pentachloride forms adducts with ICl_3 and ECl_4 (E = Se, Se, Te). The former consists of strongly interacting distorted $SbCl_6$ octahedra and angular ICl_2 groups; it is actually intermediate between $[ICl_2][SbCl_6]$ and $[SbCl_4][ICl_4]$. [3] This is a rare example where Sb(V) is described as being cationic.

Our interest in this property of Sb(V) lies in the development of non-redox halide abstraction as a direct route to reactive cationic metal species that may otherwise be inaccessible. Previous work [199] has resulted in the formation

of the ionic species $[TiCl_3(MeCN)_3]^+[SbCl_6]^-.CH_2Cl_2$. The structure consists of discrete *fac* - $[TiCl_3(MeCN)_3]^+$ cations and almost regular octahedral $[SbCl_6]^-$ anions. The dichloromethane molecule results from recrystallisation. The salts $[MCl_2(MeCN)_4][SbCl_6]$ are formed from MCl_3 (M=V, Cr, Fe).[199,200]

We have developed mono-, di- and tricationic metal species from anhydrous metal chlorides by use of increased stoichiometric ratios of $SbCl_5$. This programme has yielded the following hexachloroantimonate(V) salts (by the treatment of the anhydrous metal chloride with antimony pentachloride):

$[Mg(MeCN)_6][SbCl_6]_2$ **(I)**
$[Sn(MeCN)_6][SbCl_6]_2$ **(II)**
$[SnCl_3(MeCN)_3][SbCl_6]$ **(III)**
$[SnCl_2(MeCN)_4][SbCl_6]_2.MeCN$ **(IV)**
$[InCl_2(MeCN)_4][SbCl_6]$ **(V)**
$[In(MeCN)_6][SbCl_6]_3$ **(VI)**
$[ScCl_2(MeCN)_4][SbCl_6]$ **(VII)**
$[YCl_2(MeCN)_4][SbCl_6]$ **(VIII)**
$[LaCl_2(MeCN)_4][SbCl_6]$ **(IX)**
$[Ti^{III}Cl_2(MeCN)_4][SbCl_6]$ **(X)**
$[Ti^{IV}Cl_2(MeCN)_4][SbCl_6]_2$ **(XI)**

2.2.Discussion of Results

2.2.1.General Comments

Formulation of these adducts as monocationic, dicationic, and tricationic antimonate(V) salts is based upon ^{121}Sb NMR and UV spectroscopic identification of the $SbCl_6^-$ anion and accompanying microanalytical, electronic and infra-red spectroscopic data. In addition, conductivity measurements define the salts as 1:1, 1:2, or 1:3 electrolytes. The majority of the compounds give well defined melting points.

The ^{121}Sb NMR spectra ($I=5/2$) show a clearly resolved singlet in all complexes containing the $SbCl_6^-$ anion. These lie within the range δ=+0.14 to -0.55 ppm, with linewidths essentially the same as in the reference $[Et_4N][SbCl_6]$ δ=0, $W_{1/2}$, 190Hz. These contrast neat $SbCl_5$, δ=428.68 ppm; $W_{1/2}$ 7000 Hz. (Kidd and Matthews [201] report values of 8509 ± 20 ppm, $W_{1/2}$, 8000 Hz at 14.4 MHz). The ^{121}Sb nucleus has an electric quadrupole moment, hence its linewidth is dominated by the rate of quadrupolar relaxation. [202] The relatively narrow linewidths observed reflect the reduced rate of quadrupole relaxation of the ^{121}Sb nucleus in the highly symmetrical environment of the octahedral $SbCl_6^-$ anion.

Further identification of $SbCl_6^-$ comes from the presence of a diagnostic UV charge transfer band at λ_{max} *ca.* 36 765 cm^{-1} in acetonitrile solution.

All the salts studied exhibit a sharp doublet in the 2350-2250 cm^{-1} region of the infra-red spectra, characteristic of coordinated acetonitrile. ν(CN) bands at *ca.* 2320 and 2290 cm^{-1} compare with those at 2287 and 2251 cm^{-1} for the free ligand, implying strong binding to these cationic metal species.

Similarly ν(CN) stretching frequencies of aliphatic and aromatic nitriles increase by 80 ± 9 cm^{-1} in complexes with boron trichloride. [203]

The increase in ν(CN) on complex formation by nitriles (compare the decrease in ν(CO) in CO complexes) arises through coupling of the M-N and C≡N stretching vibrations: [204] σ-Donation to the metal raises ν(CN) as electrons are removed from the weakly antibonding 5σ, while π-backbonding tends to decrease the ν(CN) because the electrons enter the 2pπ* orbital. The peak at *ca.* 2290 cm^{-1} in the doublet profile comprises the C≡N stretch coupled to the M-N stretch. The other peak at *ca.* 2320 cm^{-1} has been assigned to either a combination band of the symmetric CH_3 deformation and the symmetric C-C stretch, [205] or to an overtone. [206] The increase in ν(CN) of the complexes do not correlate with the polarising power of the metal ion (i.e. a highly polarising M^{n+} does not give rise to a higher ν(CN)).

In the far IR region (450-200 cm^{-1}) the complexes commonly feature a broad intense band at *ca.* 345 cm^{-1}. This compares the exceptionally strong ν(SbCl) (F_{1u} bending mode (ν_3)) observed at 346 cm^{-1} in $[K][SbCl_6]$ [207] and at 348 cm^{-1} in $[PyH]^+[SbCl_6]^-$. [208] In the complexes which retain a metal-chlorine bond (III-V and VII-XI) ν(SbCl) is likely to include a pertinent ν(M-Cl) stretching component. [209] Absorptions in the far IR region are not only due to M-Cl vibrations. [210] For example the adduct $SnCl_4.2MeCN$ [211] has a weak band at approximately 420 cm^{-1} due to coordinated acetonitrile, (which itself has a medium band at 377 cm^{-1}, assigned to the δ(CCN) bending mode ν_8). [206] A similar weak band occurs at 400 cm^{-1}

in $SbCl_5$.MeCN. [208] Internal ligand vibrations absorb more weakly than ν(MX) stretching vibrations, but can be observed in complex metal ions fully solvated with acetonitrile. [212]

2.2.2.Magnesium system $[Mg(MeCN)_6]^{2+}[SbCl_6]_2$-(I)

Due to the negligible self-ionization of $SbCl_5$ itself, generation of hexachloroantimonate has occurred by halide transfer from electropositive magnesium. Double halide transfer occurs to form the fully solvated magnesium dication $[Mg(MeCN)_6]^{2+}$, which is counter-balanced by two $[SbCl_6]^-$ anions. Evidence for the formation of a 1:2 electrolyte in solution is verified by conductivity studies.

The only previous structural report of the $[Mg(MeCN)_6]^{2+}$ cation occurs in $[Mg(MeCN)_6][SbCl_4]_2$, [213] although it has been postulated in solution studies. [214] The structure of $[Mg(MeCN)_6]^{2+}$ $2[AlCl_4]^-$ [215] was not possible to solve due to crystal twinning and disorder, although the corresponding Fe^{II}/Fe^{III} structure was solved.

Similar halide transfer reactions occur in THF; removal of both chlorine atoms from $[MgCl_2(THF)_2]$ by $[MoOCl_3(THF)_2]$ leads to the formation of $[Mg(THF)_6][MoOCl_4(THF)]_2$. [216] $MgCl_2$ behaves similarly in the formation of a series of halogen-bridged magnesium species; $[Mg(THF)_6][TiCl_5(THF)]_2$, $[(THF)_4Mg(\mu\text{-}Cl)_2TiCl_4]$ and $[Mg_2(\mu\text{-}Cl)_3(THF)_6][TiCl_5(THF)]$: [217] The coupling of $MgCl_2$ and $MgCl^+$ from $[(THF)_4Mg(\mu\text{-}Cl)_2TiCl_4]$ leads to production of the bimetallic magnesium cation $[Mg_2(\mu\text{-}Cl)_3(THF)_6]$.

2.2.3.Tin(II) System $[Sn(MeCN)_6][SbCl_6]_2$-(II)

Reaction of $SnCl_2$ and $SbCl_5$ in MeCN also leads to double chloride abstraction yielding $[Sn(MeCN)_6][SbCl_6]_2$- (II). The formation of these species in solution is verified by spectroscopic identification of the hexachloroantimonate(V) anion and conductivity studies lending support to formulation of the salt as a 1:2 electrolyte. Reaction of $SnCl_2$ with an equimolar quantity of $SbCl_5$ results in an identical salt; formation of $[SnCl(MeCN)_5]^+[SbCl_6]^-$ does not occur.

$SnCl_2$ has great tendency to behave as a Lewis acid to form the $[SnCl_3]^-$ ion (isoelectronic with $SbCl_3$); it dissolves in solutions containing excess halide ions. Discrete $[SnCl_3]^-$ anions are found in $[Co(en)_3][SnCl_3]Cl_2$. [218] The *pseudo* trigonal bipyramidal $[SnCl_4]^{2-}$ ion is also found in $[Co(NH_3)_6][SnCl_4]Cl$ [218] and $[NH_4]_2[SnCl_3]Cl.H_2O$ [219] which appears to be intermediate between $SnCl_3^-$ and $SnCl_4^-$. The solid phases, for example Cs_4SnCl_6 [220] have been characterized. It can function simultaneously as both a Lewis acid and Lewis base in the complexes $B \rightarrow SnX_2 \rightarrow BF_3$ (X=Cl, Br, I; B=NMe_3, bipy, TMEDA and DMSO). [221]

The tin(II) ion $[Sn]^{2+}$ is found in acid perchlorate solutions, obtained by the reaction:

$Cu(ClO_4)_2 + Sn/Hg \rightarrow Cu + Sn^{2+} + 2ClO_4^-$

The "bare" Sn^{2+} cation occurs in $Sn(SbF_6)_2.2AsF_3$ formed from reaction of SnF_2 and SbF_5 in AsF_3. [222] This illustrates the fluoride donor ability of SnF_2 in combination with the powerful fluoride abstracting properties of antimony pentafluoride. The cation coordinates six F atoms from SbF_6^- and three F atoms from AsF_3, and distorts due to lone pair effects on Sn^{II}. Halide

abstraction by antimony pentachloride at room temperature provides a novel route to the solvated $[Sn(MeCN)_6]^{2+}$ cation. Rigorous oxygen free conditions are required in order to prevent oxidation to Sn(IV) species.

2.2.4. Tin (IV) Systems $[SnCl_3(MeCN)_3]^+[SbCl_6]^-$ (III) and $[SnCl_2(MeCN)_4]^{2+}[SbCl_6]_2^-$ (IV)

Addition of 1 equivalent of antimony pentachloride to $SnCl_4$ results in the formation of the monocationic species; $[SnCl_3(MeCN)_3]^+$ (III). Removal of a second halide ion is effected by a further equivalent of $SbCl_5$ to generate the highly reactive dication $[SnCl_2(MeCN)_4]^{2+}$ (IV). The conductivity data suggest that the species generated in solution are strong 1:1 and 1:2 electrolytes. Use of a great excess of $SbCl_5$ also gives the dication (IV), therefore it does not appear possible to remove more than two chlorides from $SnCl_4$.

Attempts to mount crystals of both III and IV in Lindemann tubes under argon for structural determination were unsuccessful. Hydrolysis occurred during manipulation under sodium-dried nujol, indicating that both products are highly air sensitive.

By analogy with its Ti(IV) counterpart the monocationic $[SnCl_3(MeCN)_3]^+$ species most likely comprises the *fac* isomer. (*Fac* MX_3L_3 (C_{3v}) should yield two IR active (M-Cl); *mer* MX_3L_3 (C_{2v}) three). [209] The presence of the exceptionally strong ν(Sb-Cl) at *ca* 345 cm^{-1} prevents full interpretation of the low IR bands.

$SnCl_4$ behaves as a Lewis acid, commonly forming anionic complexes *eg* the chloro anions $[SnCl_6]^{2-}$ and organotin halides

$[MeSnCl_4]^-$. Neutral species are also numerous; six-coordinate adducts of $SnCl_4$ and $SnBr_4$ with neutral ligands generally exhibit *cis* geometry, although the *trans* geometry is observed with bulky donor molecules.

Cationic complexies of Sn(IV) are much less known. Terdentate ligands like 2, 2', 2"-terpyridine promote the displacement of halide from tin resulting in the formation of ionic complexes such as $[Me_2Sn(terpy)Cl]^+[Me_2SnCl_3]^-$.[223] Ionization takes place more readily with bromine and iodine which bind Sn(IV) more weakly. Organotin chlorides can achieve high coordination number by intramolecular coordination of a donor atom remote in the organic ligand. When two nitrogen atoms are present on the organic group, ionization of halide from tin can occur in 2,6-bis[(dimethylamino)methyl] phenyldiorganotin bromide[224] (Λ_m = 84.8 Scm^2mol^{-1}). Halide abstraction by $SbCl_5$ provides a direct route for the generation of solvated tin (IV) chloride mono- and dicationic species.

2.2.5.Indium (III) Systems $[InCl_2(MeCN)_4]^+[SbCl_6]^-$ (V) and $[In(MeCN)_6]^{3+}[SbCl_6]_3^-$ (VI)

Removal of two chlorides from $MgCl_2$, $SnCl_2$ and $SnCl_4$ raises the possibility of further halide abstraction. Is it possible to remove $3Cl^-$ from $InCl_3$? Spectroscopic, analytical and conductivity measurements verify formation of the monocationic, $[InCl_2(MeCN)_4]^+[SbCl_6]^-$ (V) and tricationic $[In(MeCN)_6]^{3+}[SbCl_6]_3^-$ (VI) species, depending upon the stoichiometry of the reactants.

$$InCl_3 + xSbCl_5 \longrightarrow [InCl_{3-x}L_{6-(3-x)}]^{x+}[SbCl_6]_x \qquad (2)$$

(x=1, 2, 3; L=MeCN)

Hence equimolar quantities of $InCl_3$ and $SbCl_5$ in MeCN gives the monocation (V), 3 equivalents of $SbCl_5$ yield the tricationic species (VI). Use of a 1:2 molar ratio of reactants (x=2, equation 2) does not give $[InCl(MeCN)_5]^{2+}[SbCl_6]_2$; instead the tricationic complex (VI) forms (equation 3). This is confirmed by analytical, spectroscopic and conductivity measurements.

$$2[InCl(MeCN)_5][SbCl_6]_2 \rightleftharpoons [In(MeCN)_6][SbCl_6]_3 + [InCl_2(MeCN)_4][SbCl_6] \qquad (3)$$

Crystals of (V) and (VI) were unsuitable for X-ray diffraction studies.

Indium(III) cations form complexes with many nitrogen donor ligands. The $[In(NH_3)_6]^{3+}$ cation has been identified in liquid ammonia solution, [225] but attempts to prepare the perchlorate salt were unsuccessful. [226] Mixed complexes such as $[In(NH_3)_5Br]^{2+}$ have also been postulated in liquid ammonia. [226] Several cationic indium(III) salts with bidentate nitrogen donors have been prepared, *eg* $[In(bipy)_3]^{3+}$, $[In(en)_3]^{3+}$ as perchlorate [226] and nitrate [227] salts. There appears to be little reported work on the nitrile complexes of indium. Electrochemical oxidation of In metal leads to species $[InL_6][BF_4]_3$ [228] (where L = DMSO, MeCN).

The use of antimony pentachloride as halide abstractor in this study provides a direct facile route to the generation of indium(III) cations. $InCl_3$ can also behave as a halide abstractor, in reaction with PCl_5 at 300°C to give the ionic

product $[PCl_4][InCl_4]$. [229] The order of halide abstracting ability is therefore $SbCl_5 > InCl_3 > PCl_5$.

2.2.6.Scandium $[ScCl_2(MeCN)_4][SbCl_6]$(VII), Yttrium $[YCl_2(MeCN)_4][SbCl_6]$(VIII), and Lanthanum $[LaCl_2(MeCN)_4][SbCl_6]$(IX) Systems

Halide transfer from the trivalent chlorides of Sc, Y and La generates the hexachloroantimonate(V) ion. Crystals of the three salts (VII-IX) could not be obtained, hence analytical figures are based upon solid powder products. The scandium salt (VII), formulated as $[ScCl_2(MeCN)_4][SbCl_6]$, required rigorously dry conditions.

Other M-Cl shifts in the IR spectra of these complexes are obscured by the broad intense ν(SbCl) at *ca* 345 cm^{-1}.

There are few reports of M(III) complexes with monodentate nitrogen ligands. Ammine complexes of scandium are known; [230] IR studies of deuterated $ScCl_3/NH_3$ mixtures imply the presence of $[ScCl(NH_3)_5]Cl_2$. [231]

The ammonia complexes of lanthanide ions are not fully characterized. [232] N-bonded thiocyanate forms octahedral $[Ln(NCS)_6]^3$. [233]

In this study generation of cationic species of scandium, yttrium and lanthanum has been achieved, where both halide and monodentate nitrogen donor ligands complex to the metal.

2.2.7.Titanium (III) System $[TiCl_2(MeCN)_4][SbCl_6](X)$

The green crystals, which unfortunately were not of diffraction quality, analyse as $[TiCl_2(MeCN)_4][SbCl_6]$. The electronic spectrum reveals a charge transfer band at 36 900 cm^{-1} (which corresponds to the presence of the $SbCl_6^-$ anion), and visible bands at 15 380 cm^{-1} and 20 000 cm^{-1} which correspond to a d^1 metal ion in solution. The geometry of the resultant cation is likely to be *trans* in keeping with the *trans* geometry of similar $[TiCl_2L_4]^+$ cations (where L = H_2O, [235] THF [236]). The splitting of 4620 cm^{-1} compares a 4250 cm^{-1} splitting shown by *trans* $[TiCl_2(H_2O)_4]^+$ in Cs_2TiCl_5 $4H_2O$. [235] The bands at 14 970 and 19 220 cm^{-1} correspond to the $^2Eg \rightarrow {}^2A_{1g}$ and $^2Eg \rightarrow {}^2B_{1g}$ transitions respectively in a D_{4h} system.

The spectrochemical series places MeCN higher than H_2O; thus the band at 20 000 cm^{-1} for $[TiCl_2(MeCN)_4]^+(X)$, occurs at slightly higher energy than the corresponding band at 19 220 cm^{-1} shown by $[TiCl_2(H_2O)_4]^+$.

Ti(III) has great tendency to form cationic species: The complex $[Ti(MeCN)_6][BF_4]_3$ has been prepared by direct electrochemical oxidation. [228] *Trans* -$[TiCl_2(THF)_4]^+[ZnCl_3(THF)]^-$ has been synthesized by reaction of *mer* $TiCl_3.3THF$ and $ZnCl_2$ in THF under reflux. [236] Zinc dichloride here acts as chloride abstracting reagent towards $TiCl_3$. In a similar manner $SbCl_5$ and $TiCl_3.3MeCN$ in MeCN at room temperature give $[TiCl_2(MeCN)_4][SbCl_6]$ (X).

2.2.8.Titanium (IV) System $[TiCl_2(MeCN)_4]^{2+}[SbCl_6]_2$-(XI)

Generation of the 1:1 salt $[TiCl_3(MeCN)_3][SbCl_6]$ has been effected. [199] The preparation of the dicationic species was attempted by reaction of excess $SbCl_5$ with the isolated monocation. Analytical and spectroscopic data support the formation of the highly reactive dicationic species $[TiCl_2(MeCN)_4]^{2+}[SbCl_6]_2^-$ (XI). Recrystallisation of (XI) from MeCN afforded yellow *fac* -$[TiCl_3(MeCN)_3][SbCl_6].CH_3CN$ and extremely air-sensitive green crystals of the dication. The formation of the former on recrystallisation may be rationalized by the highly reactive nature of the dication (XI). The doubly charged Ti^{IV} centre is more highly polarising than the monocation due to its higher charge density, which may well be similar to that of Sb^V. The nature of the chloro-bridged intermediates which are proposed as precursors for the ionic halide transfer products are explained in Chapter 4, Section 4.4. By virtue of the highly polarising nature of the Ti^{2+} centre it may be possible that one of the chloro-bridged Sb^V units gives up one of its chlorides to Ti to regenerate the monocation. The dication $[TiCl_2(MeCN)_4]^{2+}$ is highly reactive towards ligand exchange reactions.

$TiCl_4$ generally behaves as a halide acceptor in the formation of $[TiCl_5]^-$, [238] $[TiCl_6]^{2-}$, [239] $[Ti_2Cl_9]^-$ and $[Ti_2Cl_{10}]^{2-}$. [240] salts. The formation of cationic species can only take place using powerful Lewis acidic reagents such as $SbCl_5$.

2.3.Conductivity Studies

Ionic formulation of the hexachloroantimonate(V) salts is based upon their behaviour as strong electrolytes in organic solvents, namely acetonitrile. The formation of ionic species in (I)-(XI) may actually only occur in MeCN solution. In the solid state thay may exist as chloro-bridged species (which only dissociate into ions in solution) or as ionic species. A precedent for the existence of such ternary systems as ions in the solid state is found in the structure of *fac* -$[TiCl_3(MeCN)_3][SbCl_6]$. [199] Therefore it would seem likely that (I)-(XI) are also ionic species in the solid state. The conductivity of $[TiCl_3(MeCN)_3][SbCl_6]$ was measured in this study and is consistent with a 1:1 electrolyte in MeCN solution.

Strong electrolytes have conductivities which depend only weakly on the concentration of the solute. As the concentration of solute decreases the molar conductivity rises to a limit which is called the molar conductivity at infinite dilution, Λ_o .

By contrast weak electrolytes have molar conductivities which depend markedly on solute concentration. The value of Λ_m is low until high dilutions are reached, at which point it increases to values which are comparable to those of strong electrolytes.

The conductivities of the salts were measured at different concentrations at 25.0 ± 0.1°C using the method described in Appendix 1. Acetonitrile was selected as the solvent on the basis of its high dielectric constant (36.2 at 25°C), low viscosity (0.325 $g^{-1}s^{-1}$ at 30°C), and low specific conductivity (5.9 x 10^{-8} Scm^{-1}). The use of acetonitrile as the solvent medium for

conductivity studies is appropriate for the compounds studied (which are solvated with MeCN).

The Onsager Law:

$\Lambda_o - \Lambda_m = (A + WB\Lambda_o)\, C^{1/2}$

makes the assumption that the counterion does not enter into the coordination sphere of the complex. ^{121}Sb nmr and UV spectroscopy indeed imply that $SbCl_6^-$ does not enter the coordination sphere and can be regarded as a non-complexing anion. Conductivity data are tabulated in Appendix 1.

$[SnCl_3(MeCN)_3]^+[SbCl_6]^-$ (III) and $[SnCl_2(MeCN)_4]^{2+}[SbCl_6]_2^-$ (IV)

Conductivity studies establish the ionic formulation of the ternary complexes $SnCl_4.SbCl_5.3MeCN$ (III) and $SnCl_4.2SbCl_5.4MeCN$ (IV). $[SnCl_3(MeCN)_3]^+[SbCl_6]^-$ (III) behaves as a 1:1 electrolyte in acetonitrile solution. $[SnCl_2(MeCN)_4]^{2+}[SbCl_6]_2^-$ (IV) behaves as a 1:2 electrolyte in acetonitrile solution.

Graphs of Λ_m (Scm^2mol^{-1}) versus $c^{1/2}$ (mol dm^{-3}) were plotted for $[SnCl_3(MeCN)_3][SbCl_6]$ (III) and $[SnCl_2(MeCN)_4][SbCl_6]_2$ (IV) (Figures 2.1 and 2.2).

Figure 2.1: Λ_m versus $C^{1/2}$ for $[SnCl_3(MeCN)_3][SbCl_6]$ **(III)**

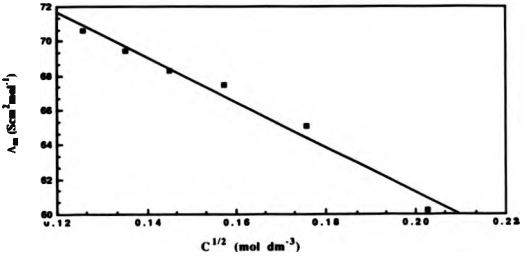

Figure 2.2. Λ_m versus $C^{1/2}$ for $[SnCl_2(MeCN)_4][SbCl_6]_2$ **(IV)**

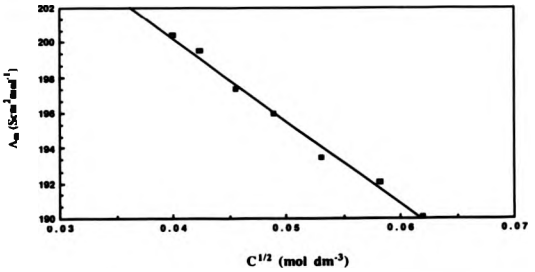

These graphs are extrapolated using linear least squares analysis to give Λ_o (Scm^2mol^{-1}), the molar conductivity at infinite dilution (Table 2.1).

According to the Onsager Law graphs of Λ_o-Λ_m (Scm^2mol^{-1}) versus $c^{1/2}$ (mol dm^{-3}) give slopes (A + $WB\Lambda_o$). (Figures 2.3 and 2.4).

Figure 2.3: Λ_o-Λ_m versus $c^{1/2}$ for $[SnCl_3(MeCN)_3][SbCl_6]$

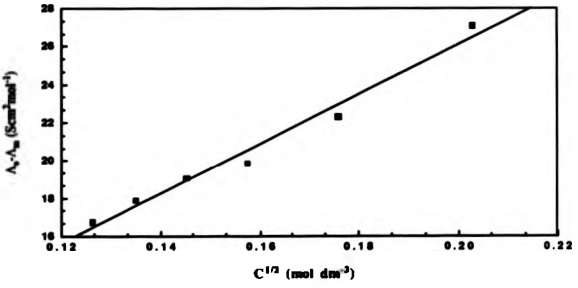

Figure 2.4. Λ_o-Λ_m versus $C^{1/2}$ for $[SnCl_2(MeCN)_4][SbCl_6]_2$

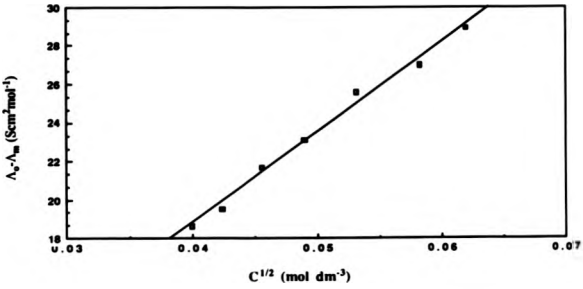

The slope of the plots are obtained using linear least squares analysis and directly reflect the electrolyte types of the complexes (Table 2.1, Figure 2.5).

Table 2.1 Conductivity Data for $[SnCl_3(MeCN)_3][SbCl_6]$(III) and $[SnCl_2(MeCN)_4][SbCl_6]_2$(IV)

Complex	Λ_o(Scm^{2}mol^{-1})	Slope ($A+WB\Lambda_o$)	Correlation Coefficient
$[SnCl_3(MeCN)_3][SbCl_6]$	87.3	130.70	0.980
$[SnCl_2(MeCN)_4][SbCl_6]_2$	219.1	469.67	0.991

Figure 2.5. Comparison of slopes of $[SnCl_3(MeCN)_3][SbCl_6]$(III) and $[SnCl_2(MeCN)_4][SbCl_6]_2$ (IV)

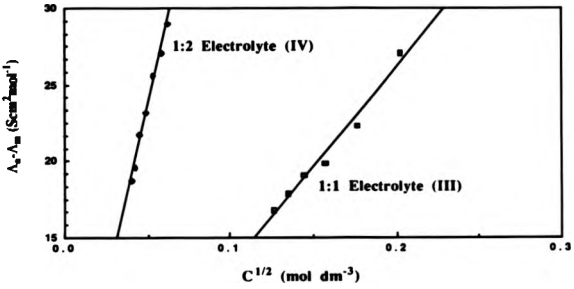

The slopes reflect the difference in electrolyte type between the two complexes. The 1:2 electrolyte $[SnCl_2(MeCN)_4][SbCl_6]_2$ yields a greater slope, 469.67 than $[SnCl_3(MeCN)_3][SbCl_6]$, 130.70. These values fall short of those obtained for comparable nickel salts in acetonitrile. [241] Accordingly the molar conductivities, Λ_m are also low, although of the same order for similar electrolyte types in acetonitrile [242] (Tables 2.2 and 2.3).

Table 2.2 Λ_m Values for $[SnCl_3(MeCN)_3][SbCl_6]$ (III) and $[SnCl_2(MeCN)_4][SbCl_6]_2$ (IV)

Complex	Λ_m at 10^{-3}M (Scm^2mol^{-1})	Expected Λ_m (at 10^{-3}M) (Scm^2mol^{-1})
$[SnCl_3(MeCN)_3][SbCl_6]$	77	120 - 160
$[SnCl_2(MeCN)_4][SbCl_6]_2$	203	220 - 300

Table 2.3 Expected Λ_m Ranges for Different Electrolytes in MeCN

Electrolyte Type	Λ_m range at 10^{-3}M (Scm^2mol^{-1})
1:1	120-160
1:2	220-300
1:3	340-420
1:4	(500)

$[Sn(MeCN)_6][SbCl_6]_2$ (II)

The ionic formulation of the title compound is based on spectroscopic observations and conductivity data.

A graph of Λ_m versus $C^{1/2}$ yields a value of 184.9 Scm^2mol^{-1} for Λ_o, the molar conductivity at infinite dilution (correlation coefficient, 0.823, Figure 2.6).

Figure 2.6. Λ_m versus $C^{1/2}$ for $[Sn(MeCN)_6][SbCl_6]_2$ (II)

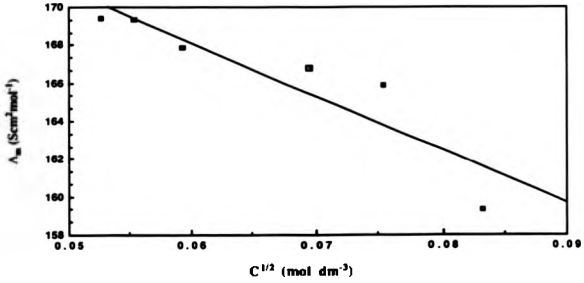

This value is used to plot Λ_o-Λ_m versus $C^{1/2}$ (Figure 2.7), from which a slope of 280.25 is obtained. This value compares with that of 469 for the complex $[SnCl_2(MeCN)_4][SbCl_6]_2$ (IV), also a 1:2 electrolyte.

Figure 2.7. Λ_o-Λ_m versus $C^{1/2}$ for $[Sn(MeCN)_6][SbCl_6]$ (II)

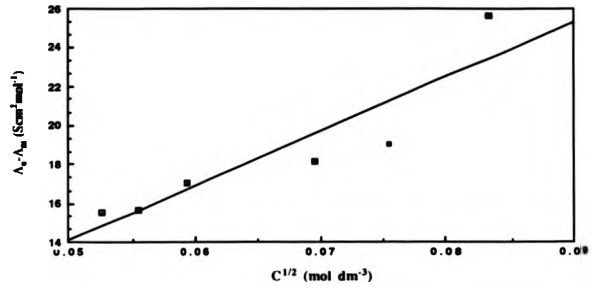

As with the Sn(IV) complex (IV) the molar conductivity of (II) (170 Scm^2mol^{-1}) falls below the expected Λ_m range for a 1:2 electrolyte in acetonitrile. The low Λ_o values obtained for the Sn(IV) and Sn(II) salts compared to the other hexachloroantimonate salts may be due to differences in the electrical conductivities of the metal cations themselves. The slopes for all three complexes are compared in Figure 2.8.

Figure 2.8. Λ_o-Λ_m versus $C^{1/2}$ for (II), (III) and (IV)

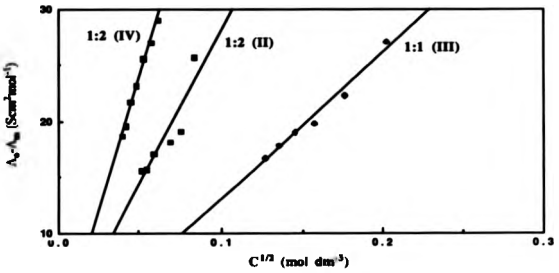

[$InCl_2(MeCN)_4$][$SbCl_6$] (V) and [$In(MeCN)_6$][$SbCl_6$]$_3$ (VI)

The ternary complexes $InCl_3.SbCl_5.4MeCN$ (V) and $InCl_3.3SbCl_5.6MeCN$ (VI) are formulated as ionic species on the basis of spectroscopic data. Conductivity measurements establishes them as 1:1 and 1:3 electrolytes respectively in acetonitrile solution. Plots of Λ_m versus $c^{1/2}$ (Figures 2.9 and 2.10) give Λ_o values of 181.4 Scm^2mol^{-1} and 383.1 Scm^2mol^{-1} for [$InCl_2(MeCN)_4$][$SbCl_6$] and [$In(MeCN)_6$][$SbCl_6$]$_3$ respectively. (Correlation coefficients of 0.989 and 0.958 were obtained).

Figure 2.9. Λ_m versus $C^{1/2}$ for $[InCl_2(MeCN)_4][SbCl_6]$ **(V)**

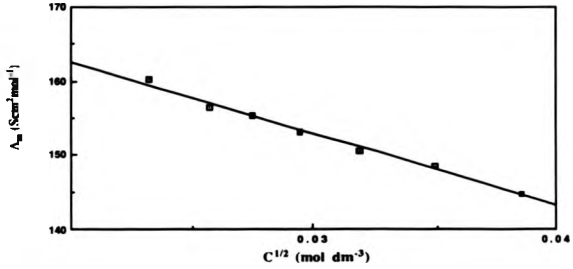

Figure 2.10. Λ_m versus $C^{1/2}$ for $[In(MeCN)_6][SbCl_6]_3$ **(VI)**

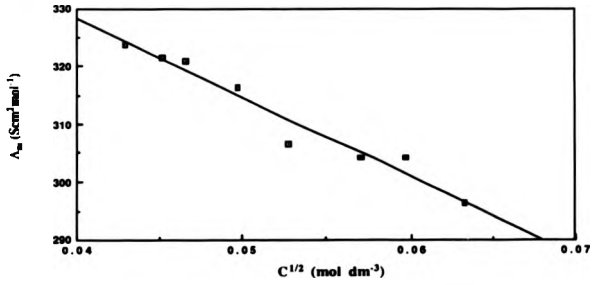

Λ_o-Λ_m versus $C^{1/2}$ plots (Figures 2.11 and 2.12) have slopes of 971.1 and 1370.1 respectively, reflecting the difference in electrolyte type of the two complexes (Figure 2.13).

Figure 2.11. Λ_o-Λ_m versus $C^{1/2}$ for $[InCl_2(MeCN)_4][SbCl_6]$ (V)

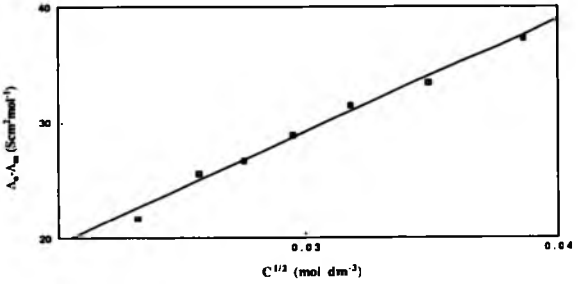

Figure 2.12. Λ_o-Λ_m versus $C^{1/2}$ for $[In(MeCN)_6][SbCl_6]_3$ **(VI)**

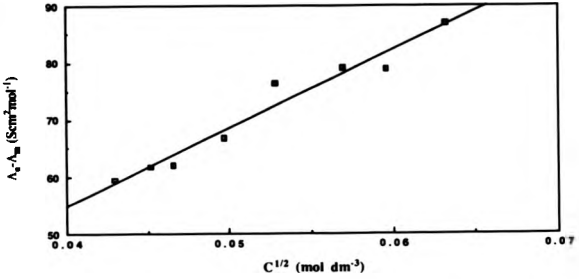

These slopes exceed those for the Sn^{IV} and Sn^{II} complexes.

Figure 2.13. Comparison of Slopes for $[InCl_2(MeCN)_4][SbCl_6]$ (V) and $[In(MeCN)_6][SbCl_6]_3$ (VI)

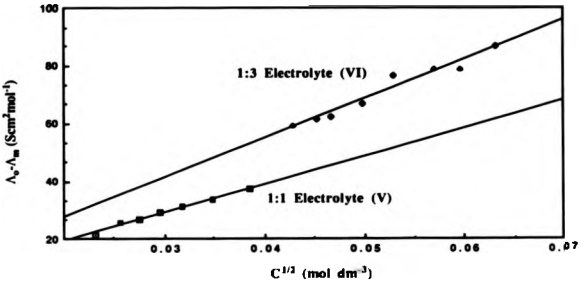

Molar conductivites of 150.5 and 323.7 Scm^2mol^{-1} at 10^{-3}M for $[InCl_2(MeCN)_4][SbCl_6]$ (V) and $[In(MeCN)_6][SbCl_6]_3$ (VI) lie well within the usual range for 1:1 and 1:3 electrolytes (Table 2.3).

The formulation of (I) as $[Mg(MeCN)_6][SbCl_6]_2$ is based upon spectroscopic results, and is further confirmed by conductivity data which characterise the complex as a strong 1:2 electrolyte.

A plot of Λ_m versus $C^{1/2}$ (Figure 2.14) gives a Λ_o value of 339.01 Scm^2mol^{-1} (correlation coefficient, 0.992).

Figure 2.14. Λ_m versus $C^{1/2}$ for $[Mg(MeCN)_6][SbCl_6]_2$ (I)

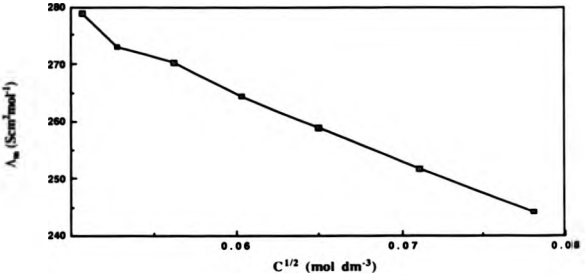

The Λ_o-Λ_m versus $C^{1/2}$ plot (Figure 2.15) has a slope of 1224.6.

Figure 2.15. Λ_o-Λ_m versus $C^{1/2}$ for $[Mg(MeCN)_6][SbCl_6]_2$(I)

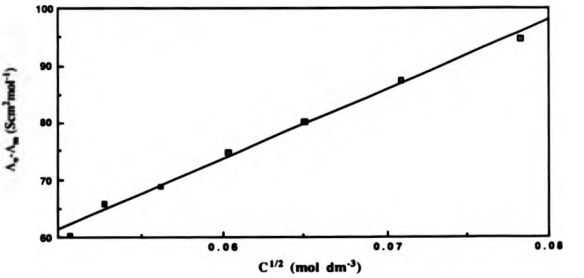

This value compares well with slopes obtained for $[InCl_2(MeCN)_4)][SbCl_6]$ and $[In(MeCN)_6][SbCl_6]_3$ and again exceeds those of the tin(IV) and tin(II) salts.(Table 2.4).

Table 2.4 Conductivity data for In^{III} and Mg^{II} salts

Complex	Λ_o (Scm^2mol^{-1})	Slope ($A + WBA_o$)	Λ_m at $10^{-3}M$ (Scm^2mol^{-1})
$[InCl_2(MeCN)_4]^+$ $[SbCl_6]^-$	181.9	971.12	150.5
$[Mg(MeCN)_6][SbCl_6]_2$	339.1	1224.6	278.9
$[In(MeCN)_6][SbCl_6]_3$	383.1	1370.1	323.7

The molar conductivity of $[Mg(MeCN)_6][SbCl_6]$ (I), 278.9 Scm^2mol^{-1} at 25.0 ± 0.1°C, lies within the expected range for a 1:2 electrolyte (220-300 Scm^2mol^{-1}) (Table 2.3).

2.4.Summary

In all the systems studied $SbCl_5$ shows no tendency to donate its chloride ions to form cationic $SbCl_4^+$ species; but it accepts halide ions from MCl_n, to give mono-, di-, or tricationic metal species, depending upon the stoichiometry of the reactants (Equation 4).

$$MCl_n + xSbCl_5 \longrightarrow [MCl_{n-x}L_{6-(n-x)}]^{x+}[SbCl_6]_x \quad (4)$$

(n=2, 3, 4; x=1, 2, 3; L=MeCN)

CHAPTER 3

Halide Exchange Reactions of Bismuth(III) Chloride.

3.1.Introduction

The work described in this chapter deals with the halide transfer reactions of bismuth(III) chloride. As discussed in Chapter 2 the removal of a chloride ion from a covalent M-Cl bond (M = metal or metalloidal) can be effected by antimony pentachloride. To expand on this theme of halide abstraction the behaviour of $BiCl_3$ in such systems has been investigated.

What is of particular interest here is that as well as showing acceptor behaviour (*i.e.* the formation of complex anions of several types $[BiCl_5]^{2-}$, [243] $[BiCl_6]^{3-}$, [139] $[Bi_2Cl_8]^{2-}$, [243] $[Bi_2Cl_9]^{3-}$, [244] and $[Bi_4Cl_{18}]^{6-}$) [143] bismuth(III) chloride can act as a halide ion donor with the formation of cationic species, e.g. $[BiCl_2(18\text{-crown-}6)]_2^{+}$ $[Bi_2Cl_8]^{2-}$. [245] Bismuth clusters and even 'naked' Bi^{+} cations are known. [246,247] Thus bismuth trichloride exhibits duality in its behaviour; in some instances it behaves as a Lewis acid, while in others it can behave as a Lewis base.

Both anionic and cationic bismuth species can be found in the same compound; this is illustrated by $(BiCl_3)_3.7tu$ (tu = thiourea) [248] and $(BiCl_3)_3.4tsc$ (tsc = thiosemicarbazide). [249] These complexes comprise $[Bi_2Cl_4tu_6]^{2+}[BiCl_5tu]^{2-}$ and $[Bi_4Cl_{10}(tsc)_6]^{2+}$ $[BiCl_6]^{3-}$ Cl^{-} respectively. Also the complex $2BiCl_3.18\text{-crown-}6$ [245] has the ionic formulation $[BiCl_2(18\text{-crown-}6)]_2^{+}$ $[Bi_2Cl_8]^{2-}$.

Aluminium trichloride has been used to abstract chloride ions from bismuth(III) chloride, [250] similar to the use of antimony pentachloride as Lewis acid to generate $[BiCl_2(MeCN)_4][SbCl_6]$ (XIV) and $[Bi(MeCN)_6][SbCl_6]_3$ (XV). Reaction of $BiCl_3$ with Al_2Cl_6 in the presence of toluene or

hexamethylbenzene yields $C_6H_5MeAlBiCl_6$ and $C_6Me_6AlBiCl_6$ respectively. The arenes stabilize $\{[BiCl_2][AlCl_4]\}_2$ by coordinating to the vacant site generated on the bismuth ion.

The results discussed below illustrate the generation of both cationic and anionic bismuth species, according to the following scheme:

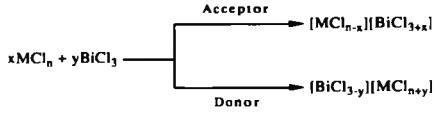

(where MCl_n are anhydrous metal chlorides).

All reactions were performed in acetonitrile, whose strongly coordinating properties allow occupancy of coordinatively unsaturated sites generated on metal centres (on M or Bi) following halide expulsion.

3.2.Discussion of Results: Bismuth Cations

3.2.1.1 $[BiCl_2(MeCN)_4][SbCl_6]$ (XIV)

1:1 stoichiometric addition of $SbCl_5$ to $BiCl_3$ in acetonitrile provides colourless crystals of poor definition which analyse as $BiCl_3.SbCl_5.4MeCN$. Of several possible formulations the ionic structure $[BiCl_2(MeCN)_4][SbCl_6]$ (XIV) is proposed on the basis of spectroscopic and conductivity data (this formulation is supported in solution phase).

The ^{121}Sb nmr spectrum consists of a singlet δ=0.05ppm, $W_{1/2}$=182Hz. The electronic spectrum shows an intense charge transfer band, λ_{max} 37 037 cm^{-1}; both are diagnostic of $SbCl_6^-$ anions in solution. [202] Other charge transfer bands at λ_{max} 44 250 and 31 545 cm^{-1} in the electronic spectrum are assigned to the cationic complex $[BiCl_2(MeCN)_4]^+$.

The infra-red spectrum has a sharp doublet profile ν(CN) 2300 and 2260 cm^{-1}, typical for coordinated MeCN. The far IR region (400-200 cm^{-1}) has a broad intense band at 348 cm^{-1}, ν(SbCl) (*cf* [K][$SbCl_6$], 346cm^{-1} (ν_3)).[207] The medium-broad bands at 280 cm^{-1} and 250-255 cm^{-1} are tentatively assigned as Bi-N stretching and Bi-NCMe wagging modes.

Further confirmation of the ionic nature comes from conductivity measurements in acetonitrile where Λ_m=115.8 Scm^2mol^{-1} at 25°C. 1:1 electrolytes have molar conductivities, Λ_m =120-140 Scm^2mol^{-1} in acetonitrile under similar conditions. [242] A *cis* or *trans* geometry for the cation in XIV (Figure 3.1) cannot be defined without structural analysis, as pertinent ν(BiCl) frequencies are masked by the intense ν(SbCl).

Figure 3.1. Proposed Structure of $[BiCl_2(MeCN)_4]^+$

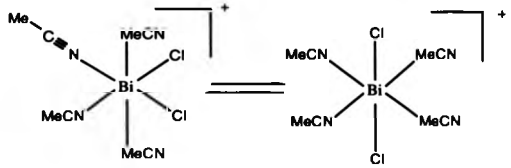

cis *trans*

2,2,1,2,1[Bi(MeCN)$_6$][SbCl$_6$]$_3$,2MeCN (XV)

Addition of 1:3 stoichiometric quantities of $SbCl_5$ to $BiCl_3$ in acetonitrile provide colourless crystals of poor definition which analyse as the ternary complex $BiCl_3.3SbCl_5.8MeCN$. The ionic formulation $[Bi(MeCN)_6][SbCl_6].2MeCN$ (XV) is proposed on the basis of spectroscopic and conductivity data.

The ^{121}Sb nmr spectrum consists of a singlet δ=0.16ppm, $W_{1/2}$=190.5 Hz, and the electronic spectrum has an intense charge transfer band at 35 714 cm^{-1}, both of which are diagnostic of $SbCl_6^-$ anions in solution. The other charge transfer band at 44 843 cm^{-1} can be assigned to $[Bi(MeCN)_6]^{3+}$.

The infra-red spectrum has a doublet profile ν(CN) 2296, 2276 cm^{-1} which corresponds to coordinated acetonitrile, a further band at ν(CN) 2258 cm^{-1} is assigned to uncoordinated MeCN in the lattice. The presence of a broad intense band at 340 cm^{-1} is indicative of $SbCl_6^-$ in the solid state, (*cf* [K][$SbCl_6$], ν(SbCl), 346 cm^{-1}). As in $[BiCl_2(MeCN)_4]^+[SbCl_6]^-$ (XIV) the

bands at 280 and 240-245 cm^{-1} are tentatively assigned to Bi-N stretching and Bi-NCMe wagging modes.

Further confirmation of the ionic nature of the complex comes from conductivity measurements in acetonitrile where Λ_m = 199 Scm^2mol^{-1} at 25°C. Although this value is seemingly rather low for a 1:3 electrolyte, the values of Λ_o (molar conductivity at infinite dilution, 245.6 $Scm^{-1}mol^{-1}$ for (XV) and 142.1 Scm^2mol^{-1} for (XIV)) and the slopes of the two plots (868.1 for (XV) and 486 for (XIV)) (Figure 3.7) reflect the difference in electrolyte type between the two complexes.

Use of 1:2 stoichiometric quantitites of $BiCl_3$ and $SbCl_5$ respectively does not result in the removal of two chloride ions from $BiCl_3$ to give $[BiCl(MeCN)_5][SbCl_6]_2$, but gives the monocationic product, $[BiCl_2(MeCN)_4][SbCl_6]$ (XIV).

As illustrated in Chapter 2 antimony pentachloride always behaves as a Lewis acid towards metal chlorides forming $SbCl_6^-$ salts. The ionic formulations of (XIV) and (XV) are in accord with chloride ion transfer from electro-positive Bi(III). The polar solvent acetonitrile assists ion formation via occupancy of uncoordinated metal sites generated by halide abstraction.

The stoichiometry of the reactants evidently influences the number of halide ions removed. To summarize; equimolar and 1:2 stoichiometric quantities give the 1:1 electrolyte, while reaction of 1:3 stoichiometric quantitites of $BiCl_3$ with $SbCl_5$ gives the 1:3 electrolyte $[Bi(MeCN)_6][SbCl_6]_3.2MeCN$ as a result of triple halide abstraction.

The generation of Bi(III) chlorocations is somewhat unexpected in the light of its rather high ionization energy,

4779 KJmol^{-1} ($Bi \rightarrow Bi^{3+}$, sum of I, II, III) yet bismuth(III) does exhibit the ability to form both cationic and anionic complexes.

Bismuth Anions

3.2.2.1.$[Mg(MeCN)_6]_2[Bi_4Cl_{16}]$ (XII)

Treatment of $MgCl_2$ (1mol) with $BiCl_3$ (2 mol) in acetonitrile provides the colourless ternary complex $2MgCl_2.4BiCl_3.12MeCN$ (XII) identified by X-ray crystallography as the ionic salt $[Mg(MeCN)_6]_2[Bi_4Cl_{16}]$. In this instance Bi(III) acts as the chloride abstracting agent towards the electropositive Mg(II), with subsequent formation of the tetranuclear anion $[Bi_4Cl_{16}]^{4-}$. The magnesium cation is octahedrally coordinated by six acetonitrile ligands to yield $[Mg(MeCN)_6]^{2+}$, whose structure has been previously described. [213] Other members of the octahedral $[MgL_6]^{2+}$ series which have been structurally characterised include those with $L=C_2H_5OH$, [251] THF, [216] and H_2O. [252]

In the infra-red spectrum of (XII) the characteristic sharp doublet ν(CN) 2322, 2290 cm^{-1}, (*cf* 2287, 2251 cm^{-1} for the free ligand), confirms strong attachment of MeCN to the Mg^{2+} ion. Bands at 405 and 340-350 are tentatively assigned as ν(Bi-Cl) and those at 276, 250-255 cm^{-1} to ν(Mg-N) str/ν(Mg-NCC) wag modes respectively.

The intense charge-transfer band in the ultraviolet spectrum at λ_{max} 30 959 cm^{-1} is associated with the $[Bi_4Cl_{16}]^{4-}$ anion. [253] The molar conductivity Λ_m 207 Scm^2mol^{-1} in dimethylformamide solution is slightly above the range expected for 1:2 electrolytes (Table 3.3). [242]

Formation of the hexakis solvato Mg(II) cation in (XII) and in previous studies,

$MgCl_2/SbCl_3/MeCN \longrightarrow [Mg(MeCN)_6][Sb_2Cl_8]$ [213]

$MgCl_2/SbCl_5/MeCN \longrightarrow [Mg(MeCN)_6][SbCl_6]$ (I)

establishes $MgCl_2$ as a suitable double chloride ion source in Group 15 halide exchange systems. By careful control of the stoichiometry of the $MgCl_2/BiCl_3/MeCN$ system (equation 1) other complex anions may be isolated.

$$mMgCl_2 + 4BiCl_3 \xrightarrow{MeCN} [Mg(MeCN)_6]_m[Bi_4Cl_{12+2m}]^{2m-} \quad (1)$$

m=2 gives $[Bi_4Cl_{16}]^{4-}$ (XII), whilst m=3 leads to the $[Bi_4Cl_{18}]^{6-}$ anion which has been reported in the literature. [143] The product isolated using 3:4 stoichiometric quantities of $MgCl_2$ and $BiCl_3$ is the ternary complex $3MgCl_2.4BiCl_3.18MeCN$ (XIII), *vide infra*.

3.2.2.2.Discussion of the Structure of $[Mg(MeCN)_6]_2[Bi_4Cl_{16}]$ (XII)

Complete lists of bond lengths and bond angles, crystal data, collection and refinement conditions, thermal parameters and atomic coordinates is given in Appendix 2.

The unit cell of $[Mg(MeCN)_6]_2[Bi_4Cl_{16}]$ contains discrete $[Mg(MeCN)_6]^{2+}$ cations and discrete centrosymmetric $[Bi_4Cl_{16}]^{4-}$ anions. A view of the anion with two cations is shown in Figure 3.2 with the atomic numbering scheme.

The cation has distorted octahedral geometry with Mg-N distances ranging from 2.20(2) - 2.25(3) Å. These distances are slightly longer than those previously found (2.14 - 2.18Å). [213]

Selected bond lengths and angles are given in Table 3.1. The $[Bi_4Cl_{16}]^{4-}$ anion contains a crystallographic centre of symmetry. Of the eight independent chlorine atoms, five are terminal, while two, [Cl(2), Cl(6)], bridge two bismuth atoms, and one, [Cl(1)], bridges three.

Each bismuth atom achieves a coordination number of six. Bi(1) is bonded to two terminal chlorine atoms [mutually *cis* at 2.453(18), 2.516(20) Å], two μ^2 chlorine atoms [*trans* at 2.678(13), 2.730(14) Å], and two μ^3 chlorine atoms [*cis* at 3.009(16), 3.034(16) Å]. On the other hand Bi(2) is bonded to three terminal chlorine atoms in the *fac* configuration [2.426(16), 2.528(14), 2.552(16) Å], as well as two μ^2 chlorine atoms [*cis* at 2.974(17), 2.976(13)Å] and one μ^3 chlorine atom at 2.930(14) Å. The terminal Bi-Cl bonds (to the atoms Cl(3), Cl(4), Cl(5), Cl(7) and Cl(8)) are shorter than any of the bridging bonds. They are similar to the corresponding lengths observed in $BiCl_3$ [46] [2.468(4) - 2.518 (7)Å].

The Bi-Cl-Bi bridges are asymmetric, distances to Bi(1) are significantly shorter, 2.678(13) Å, than those to Bi(2), 2.976(13) Å. This may reflect the fact that Bi(2) is bonded to three terminally bound chlorine atoms, while Bi(1) has only two such bonds.

With this wide variation in the bond lengths around each Bi(III) centre the Cl-Bi-Cl angles deviate by up to 10° from those of a regular octahedron (Table 3.1).

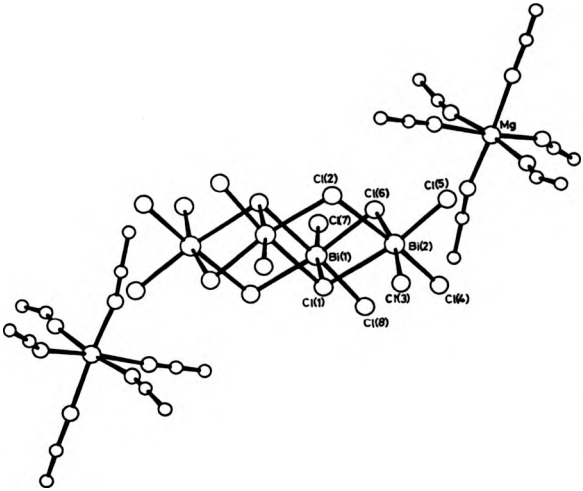

Figure 3.2. Crystal Structure of $[Mg(MeCN)_6]_2[Bi_4Cl_{16}]$

Table 3.1. Selected Bond Lengths and Angles for $[Mg(MeCN)_6]_2[Bi_4Cl_{16}]$. (esd's in Parentheses).

Bond Lengths (Å)		Bond Angles (°)	
Bi(1)-Cl(1)	3.009(16)	Cl(1)-Bi(1)-Cl(7)	172.1(5)
Bi(1)-Cl(6)	2.678(13)	Cl(8)-Bi(1)-Cl(1i)	167.8(6)
Bi(1)-Cl(7)	2.453(18)	Cl(1)-Bi(1)-Cl(8)	86.0(5)
Bi(1)-Cl(8)	2.516(20)	Cl(1)-Bi(1)-Cl(6)	82.1(4)
Bi(1)-Cl(1i)	3.034(16)	Cl(2)-Bi(2)-Cl(4)	176.0(5)
Bi(2)-Cl(1)	2.930(14)	Cl(1)-Bi(2)-Cl(5)	172.4(5)
Bi(2)-Cl(2)	2.974(17)	Cl(4)-Bi(2)-Cl(5)	93.9(5)
Bi(2)-Cl(3)	2.528(14)	Bi(1)-Cl(1)-Bi(2)	95.8(5)
Bi(2)-Cl(4)	2.426(16)		
Bi(2)-Cl(5)	2.552(16)		
Bi(2)-Cl(6)	2.976(13)		

Bi-Cl bonds *trans* to terminal halogens are weaker (longer) than those *trans* to bridging halogens. A more strongly bound group (with a shorter bond length) limits the amount of electron density available for the bonding of the position *trans* to itself. This is illustrated as follows: the terminal Bi(2)-Cl(5), 2.552(16)Å is trans to μ^3-Cl(1), length 2.930(14)Å. The terminal Bi-Cl bond, Bi(2)-Cl(4), of length 2.426(16) Å is *trans* to μ^2-Cl(2), length 2.974(17) Å. Also the terminal Bi(2)-Cl(3), 2.528(14) Å is shorter than the μ^2-bridging Bi(2)-Cl(6) bond, 2.976(13) Å which is *trans* to it. It is also noted that the longer bridging bonds of 2.976(13) and 2.974(17)Å are *trans* to the shorter terminal bonds of 2.528(14) and 2.426(16) Å respectively, and *vice versa* that

the shortest bridging bond of 2.930(14) Å is *trans* to the longest terminal bond, 2.552(16) Å. The lengthening of a bond *trans* to a somewhat shorter bond is consistent with the population of antibonding orbitals. Force constants calculated from low frequency vibrational spectra imply similar differences between bond lengths observed in the bromo- and iodobismuthates, BiX_4^-, BiX_5^{2-}, BiX_6^{3-} and $Bi_2X_9^{3-}$.[254]

3.2.2.3.[Mg(MeCN)$_6$]$_3$[Bi$_4$Cl$_{18}$] (XIII)

The ternary complex $3MgCl_2.4BiCl_3.18MeCN$ is formulated as the ionic title compound (XIII) on the basis of analytical, spectroscopic and conductivity data.

The infra-red spectrum contains two sharp ν(MeCN) bands at 2320, 2289 cm^{-1} characteristic of the Mg(II) cation, two bands at 230-240 and 273 cm^{-1} assigned to ν(Mg-N) stretch/ ν(Mg-NCC) wag modes and two strong bands at 401, 335-345 which can be assigned to ν(Bi-Cl) modes.

The intense charge transfer band in the vis-uv spectrum at λ_{max} 31 055 cm^{-1} is associated with the $[Bi_4Cl_{18}]^{6-}$ anion. The molar conductivity in dimethylformamide Λ_m=251.8 Scm^2mol^{-1} is within the usual range (Λ_m=200-250 Scm^2mol^{-1}) for 1:3 electrolytes in DMF.

The anion in (XIII) $[Bi_4Cl_{18}]^{6-}$ is likely to have a similar structure to that in $[pyr]_6[Bi_4Cl_{18}]^{6-}$,[143] which comprises two pairs of edge-shared octahedra joined symmetrically by apex-apex fusion of their axial chlorides (TYPE E, Figure 3.11).

3.2.3. $MgCl_2/BiCl_3$/MeCN Reactions - other Stoichiometries

Further reactions have been carried out to investigate the effect of stoichiometry upon the $MgCl_2/BiCl_3$ system.

Using 0.25 equivalents of $MgCl_2$ (m=1, equation 1) the reaction flask contained unreacted bismuth(III) chloride. Thin-layer chromatography of the product revealed the presence of unreacted $BiCl_3$ and a product with R_f=0 in MeCN and DMF on SiO_2 and Al_2O_3. This product is $[Mg(MeCN)_6]_2[Bi_4Cl_{16}]$ on the basis of analytical, spectroscopic, conductivity and m.p. data. Formation of $[Bi_4Cl_{14}]^{2-}$ (according to equation 1) would clearly involve generation of halide deficient bismuth centres. Aggregation to form such a cluster is impossible if their six coordinate geometry is maintained.

According to equation 1 reaction of equimolar quantities of $MgCl_2$ and $BiCl_3$ (m=4) gives $[Mg(MeCN)_6]_4[Bi_4Cl_{20}]^{8-}$. Instead, unreacted $BiCl_3$ is found in the reaction flask. Thin layer chromatography revealed the presence of unreacted $BiCl_3$ and a product with zero R_f. On the basis of analytical, conductivity, spectroscopic and m.p. data, this second product is the 3:1 electrolyte $[Mg(MeCN)_6]_3[Bi_4Cl_{18}]$ (XIII) instead of the 4:1 salt $[Mg(MeCN)_6]_4[Bi_4Cl_{20}]^{8-}$. (The latter anion would comprise four $BiCl_6$ octahedra fused apex-apex, each bismuth centre having four terminal chlorines and two μ^2 bridging chlorines, type G, Figure 3.11. Its high negative charge of -8 is probably too much to hold together).

Treatment of $MgCl_2$ (1 mol) with $BiCl_3$ (3 mol) gives a colourless semi-crystalline material; excess unreacted bismuth(III) chloride is found in the reaction vessel. Thin-

layer chromatography of the product revealed the presence of unreacted $BiCl_3$ and a product with zero R_f. This product is $[Mg(MeCN)_6]_2[Bi_4Cl_{16}]$ on the basis of analytical, spectroscopic, conductivity and m.p. data. Reaction at this stoichiometry could potentially give $[Bi_3Cl_{11}]^{2-}$, but a discrete trimeric structure of this sort is forbidden due to the apparent desire of bismuth(III) to attain six coordination. The minimum number of chlorides required to retain six coordinate Bi centres would be twelve, this would lead to a cluster of three highly distorted face-sharing octahedra which share a common μ^3-chloro apex, or three face-sharing $BiCl_6$ octahedra each joined by three μ^3 chlorines. This $[Bi_3Cl_{12}]^{3-}$ anion could potentially form by reaction of 2:3 molar ratios of $MgCl_2$ and $BiCl_3$. But in a reaction of this stoichiometry excess unreacted $BiCl_3$ was found in the reaction vessel. Thin layer chromatography, analytical, spectroscopic, conductivity and m.p. data revealed the presence of unreacted $BiCl_3$ and $[Mg(MeCN)_6]_2[Bi_4Cl_{16}]$.

Although the trimeric anions $[Bi_3Cl_{14}]^{5-}$ [255] and $[Bi_3Cl_{16}]^{7-}$ [256] have been postulated on the basis of the stoichiometry of the reactants used and analytical data, their existence has not been proved.

There is no apparent reason why only tetramers form in these reactions: Monomeric $[Mg(MeCN)_6][BiCl_4]_2$ and $[Mg(MeCN)_6][BiCl_5]$ and dimeric $[Mg(MeCN)_6][Bi_2Cl_8]$ bismuth anions could potentially form with these stoichiometries, but only the formation of tetrameric anions was observed. This can be associated with the large size of the $[Mg(MeCN)_6]^{2+}$ cation in these complexes.

3.2.4.Other MCl_n reactions with Bismuth(III) Chloride

$TiCl_4$ System (XVI)

Equimolar quantities of bismuth trichloride and titanium tetrachloride in acetonitrile yield a mixture of $TiCl_4.2MeCN$ and $BiCl_3.3MeCN$. The infra-red spectrum reveals the presence of coordinated acetonitrile. There is a distinct doublet profile to each of the sharp ν(CN) bands at 2305 and 2295 cm^{-1}, which presumably results from some site irregularity concerning the ligand environment.

In the electronic spectrum the charge-transfer band at 30 769 cm^{-1} corresponds to the presence of $BiCl_3$.[253] Thin-layer chromatography revealed the presence of bismuth trichloride.

Recrystallisation from MeCN isolates yellow crystals of $TiCl_4.2MeCN$. Charge transfer bands in the ultra-violet visible spectrum at 45 662, 39 682 and 33 557 cm^{-1} are almost identical to those (at 45 871, 39 682 and 33 783 cm^{-1}) for the synthesized adduct. Bands at 2310 and 2290 cm^{-1} in the infra-red spectrum correspond to coordinated acetonitrile, whose doublet profile is observed at ν(CN) 2310 and 2285 cm^{-1} in the synthesized adduct. Bands at 380 and 315 cm^{-1} in the far infra-red region also closely correspond to those at 387 and 315 cm^{-1} in $TiCl_4.2MeCN$.[210]

$BiCl_3$ is therefore not a powerful enough Lewis acid to cleave the covalent Ti-Cl bond to form a bismuth-chloro anion and $TiCl_4$ does not abstract Cl^- from $BiCl_3$. This contrasts the behaviour of $SbCl_5$ which has adequate Lewis acidic strength to abstract a chloride ion from $TiCl_4$, giving the ionic species $[TiCl_3(MeCN)_3][SbCl_6]$.[199]

$TiCl_3$ System (XVII)

$BiCl_3$ likewise fails to act as a Lewis acid towards $TiCl_3$. The purple solid obtained is a mixture of the two adducts, $TiCl_3.3MeCN$ and $BiCl_3.3MeCN$. The infra-red spectrum reveals the presence of coordinated acetonitrile, ν(CN) at 2305 and 2290 cm^{-1}. The charge transfer band at 31 515 cm^{-1} is due to $BiCl_3$.[253] The band at 17 029 cm^{-1} in the visible region corresponds to the $^2B_{1g} \rightarrow {}^2B_{2g}$ transition of a d^1 ion in solution.[257]

VCl_3 (XVIII), $CrCl_3$ (XIX) and $SnCl_4$ (XXI) show similar behaviour to $TiCl_4$ and $TiCl_3$ towards $BiCl_3$. In all three cases the acetonitrile adducts $VCl_3.3MeCN$, $CrCl_3.3MeCN$ and $SnCl_4.2MeCN$ respectively form, which were identified spectroscopically.

$FeCl_3$ System (XX)

Reaction of equimolar quantities of $FeCl_3$ and $BiCl_3$ yields an orange coloured solid which is a mixture of $FeCl_3.2MeCN$ and $BiCl_3.3MeCN$. The presence of coordinated acetonitrile is observed in the infra-red spectrum, which has ν(CN) bands at 2305 and 2290 cm^{-1}. The weak band at 2260 cm^{-1} reveals the presence of some uncoordinated acetonitrile.

Inspection of the electronic spectrum reveals charge transfer bands at 47 778, 41 946, 35 087(sh), 32 154, and 28 011 cm^{-1}. These bands are almost identical to those observed at 47 400, 41 600, 37 400(sh), 32 000 and 27 000 cm^{-1} for $[Et_4N][FeCl_4]$ in acetonitrile, [258] which correspond to charge transfer bands of the tetrahedral tetrachloro-ferrate anion, $[FeCl_4]^-$.

The formation of $[FeCl_4]^-$ from the acetonitrile adduct of $FeCl_3$. has occurred. Hathaway and Holah [258] have noted that the ultraviolet spectrum of $FeCl_3.2MeCN$ is identical to that of $[Et_4N][FeCl_4]$, and that solvolysis occurs to produce the $[FeCl_4]^-$ ion. A series of equilibria, summarised as:

$$2FeCl_3 + n(solvent) \rightleftharpoons [Fe^{III}Cl_2L_x]+[Fe^{III}Cl_4]^- \qquad (2)$$

has been suggested to account for the formation of $[FeCl_4]^-$ in acetonitrile solution. The presence of $[FeCl_4]^-$ has resulted from solvolysis of $FeCl_3.2MeCN$, not by halide transfer from bismuth trichloride to give $[BiCl_2(MeCN)_4][FeCl_4]$.

3.3.Conductivity Data

Conductivity measurements on $[Mg(MeCN)_6]_2[Bi_4Cl_{16}]$ (XII), $[Mg(MeCN)_6]_3[Bi_4Cl_{18}]$ (XIII), $[BiCl_2(MeCN)_4][SbCl_6]$ (XIV) and $[Bi(MeCN)_6][SbCl_6]_3$ (XV) confirm their existence as ionic species in solution. The existence of these species as ions may only occur in solution. But the structural evidence for $[Mg(MeCN)_6]_2[Bi_4Cl_{16}]$ (XII) as an ionic product implies that $[Mg(MeCN)_6]_3[Bi_4Cl_{18}]$ (XIII) also exists as an ionic product in the solid state. The conductivities of individual complexes were measured at different concentrations (at 25.0 ± 0.1°C) using the method described in Appendix 1.

Both acetonitrile and dimethylformamide were used as solvents for the bismuth complexes. The use of acetonitrile as a solvent for conductivity measurements has been described (Chapter 2). Due to the low solubilities of (XII) and (XIII) in acetonitrile, dimethylformamide was selected as the solvent for conductivity studies of these compounds. DMF has a high dielectric constant (36.7 at 25°C) and low specific conductivity ($0.6 - 2.0 \times 10^{-7}$ Scm^{-1}) but it has a greater viscosity than acetonitrile (0.796 $g^{-1}\,s^{-1}$ at 25°C).

Conductivity of $[BiCl_2(MeCN)_4][SbCl_6]$ (XIV) and $[Bi(MeCN)_6][SbCl_6]_3$ (XV)

Ionic formulation of the ternary compounds $BiCl_3.SbCl_5.4MeCN$ and $BiCl_3.3SbCl_5.8MeCN$ as (XIV) and (XV) is based upon spectroscopic and conductivity measurements. The conductivity of these salts were measured in acetonitrile. The title compounds were found to behave as strong electrolytes whose conductivities vary with concentration according to the Onsager Law (Appendix 1).

The conductivities of both salts were measured as a function of increasing concentration. Graphs of Λ_m (Scm^2 mol^{-1}) versus $c^{1/2}$ (mol dm^{-3}) for each salt appear in Figures 3.3 and 3.4.

Figure 3.3. Graph of Λ_m versus $C^{1/2}$ for $[BiCl_2(MeCN)_4][SbCl_6]$ (XIV)

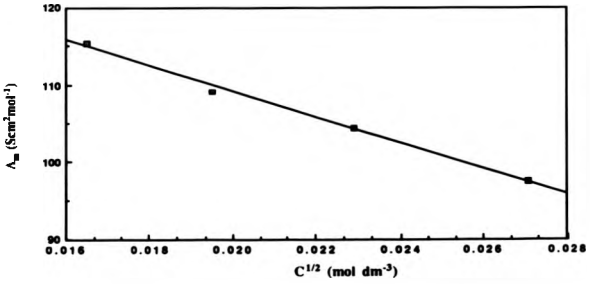

Figure 3.4. Graph of Λ_m versus $C^{1/2}$ for $[Bi(MeCN)_6][SbCl_6]_3$ (XV)

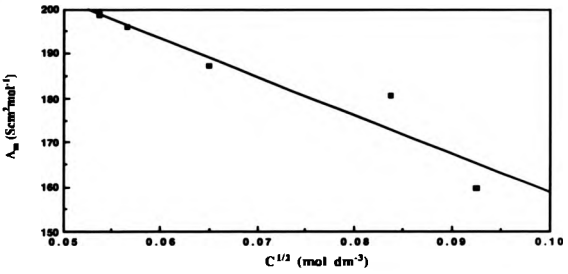

Using linear least squares analysis, values of molar conductivity at infinite dilution, Λ_o, of 142.18 and 245.65 Scm^2mol^{-1} were obtained for the title compounds XIV and XV respectively. These values were used to plot graphs of Λ_o-Λ_m versus $c^{1/2}$ for both salts (Figures 3.5 and 3.6).

Figure 3.5. Graph of Λ_o-Λ_m versus $C^{1/2}$ for (XIV)

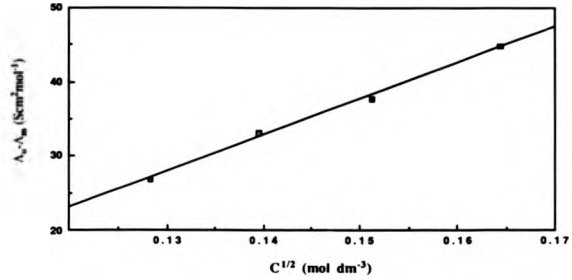

Figure 3.6. Graph of Λ_o-Λ_m versus $C^{1/2}$ for (XV)

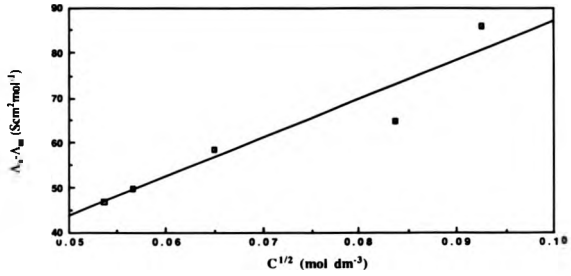

These graphs yield slopes characteristic of the electrolyte type of the complexes (see Table 3.2 and Figure 3.7).

Figure 3.7. Comparison of Λ_o-Λ_m versus $C^{1/2}$ for (XIV) and (XV)

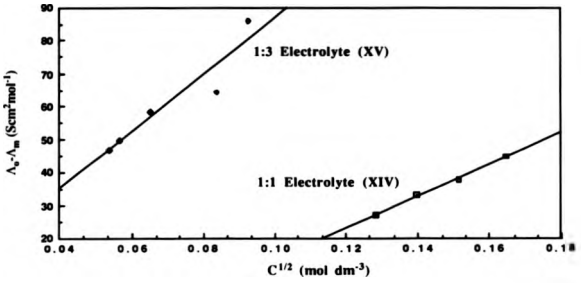

Table 3.2. Conductivity Data for (XIV) and (XV)

Complex	Λ_o (Scm^{2}mol^{-1})	Slope	Λ_m (Scm^{2}mol^{-1})	Corr Coeff
(XIV)	142.2	486.6	115.7	0.99
(XV)	245.6	868.6	199	0.90

The molar conductivity 115.7 Scm^{2}mol^{-1} for $[BiCl_2(MeCN)_4][SbCl_6]$ (XIV) lies within the range expected for a 1.1 electrolyte (120-160 Scm^{2}mol^{-1}) in acetonitrile. The value for Λ_m obtained for $[Bi(MeCN)_6][SbCl_6]_3$ (XV) is low for a 1:3 electrolyte (expected range= 340-420 Scm^{2}mol^{-1}).

Figure 3.8 shows a comparison of Λ_o-Λ_m versus $c^{1/2}$ graphs for (XV) and another 1:3 electrolyte studied, namely $[In(MeCN)_6][SbCl_6]_3$ (VI).

Figure 3.8. Comparison of Λ_o-Λ_m versus $C^{1/2}$ for the 1:3 electrolytes (VI) and (XV)

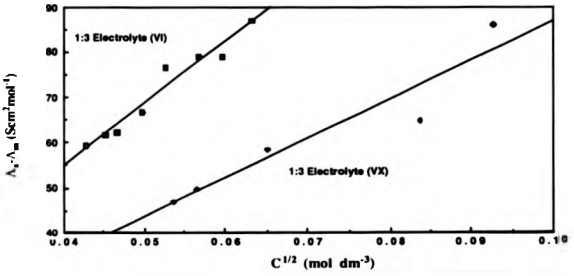

The graphs have comparable slopes, although conductivity values obtained for the indium[III] salts, (V) and (VI), (Chapter 2) have markedly higher values than their bismuth[III] congeners (XIV) and (XV). This is associated with the lower electrical conductivity of Bi(III) (0.00867 x 10^6 Scm^{-1}) compared to In(III) (0.116 x 10^6 Scm^{-1}), which is attributed to the larger size of Bi(III). There is scant data available on the conductivity of bismuth cations in solution for comparative purposes.

Conductivity of $[Mg(MeCN)_6]_2[Bi_4Cl_{16}]$ (XII) and $[Mg(MeCN)_6]_3[Bi_4Cl_{18}]$ (XIII)

Conductivity measurements of both these complexes were made in dimethylformamide, as both were found to be insoluble even in refluxing acetonitrile. We assumed that DMF replaces MeCN as coordinating ligand in DMF solution based upon its greater donor capacity towards metal ions. However the molar weight of $[Mg(MeCN)_6]_2[Bi_4Cl_{16}]$ was used to calculate the concentration in DMF.

The molar conductivity, Λ_m, of $[Mg(DMF)_6]_2[Bi_4Cl_{16}]$ (XII) in DMF is 172 Scm^2mol^{-1} (at $10^{-3}M$). This value based on a single conductivity measurement.

Conductivity of $[Mg(DMF)_6]_3[Bi_4Cl_{18}]$ (XIII)

Formation of the above species in DMF solution is assumed, however, the molecular weight of $[Mg(MeCN)_6]_3[Bi_4Cl_{18}]$ was used to calculate the concentration in DMF. A graph of Λ_m versus $C^{1/2}$ for (XIII) is given in Figure 3.9.

Figure 3.9. Graph of Λ_m versus $C^{1/2}$ for (XIII)

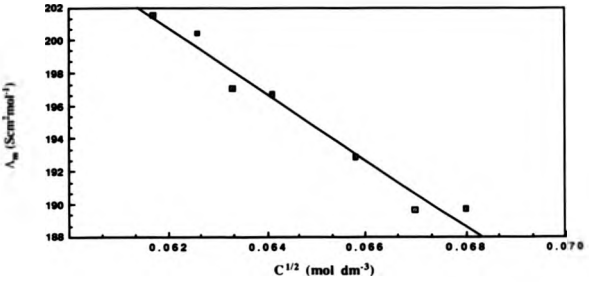

A value of 326.17 $Scm^2\ mol^{-1}$ obtained for Λ_o (correlation coefficient, 0.97) was then used to plot a graph of Λ_o-Λ_m versus $C^{1/2}$. The slope has a value 2022.6 (Figure 3.10).

Figure 3.10. Graph of Λ_o-Λ_m versus $C^{1/2}$ for (XIII)

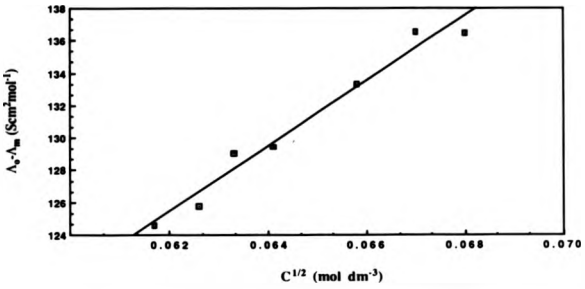

The molar conductivity of the title compound (XIII), 202 $Scm^2\ mol^{-1}$, lies within the range observed for a 1:3 electrolyte in dimethylformamide (Table 3.3).

Table 3.3. Expected Λ_m Values of Electrolyte Types in DMF

Electrolyte Type	Λ_m range ($Scm^2\ mol^{-1}$) in DMF (10^{-3}M)
1:1	65 - 90
1:2	130 - 170
1:3	200 - 240
1:4	300?

3.4.The Structural Relationship of the $[Bi_4Cl_{16}]^{4-}$ Anion with Other Complex Bismuth(III)-Chloro Anions

Figure 3.11 places the structure of $[Bi_4Cl_{16}]^{4-}$ in context with other known (and idealised) structures of tetranuclear halo-bismuth(III) anions. For such species, all Bi(III) centres are invariably six coordinate, with or without a formal lone pair of electrons showing stereochemical activity. It is possible to rationalise some of the structures as aggregates of the dinuclear $[Bi_2Cl_8]^{2-}$ [243,245] unit. This basic building block can be regarded as an edge-edge dimer of formal ψ-square based pyramidal $[BiCl_4]^-$ units with retention of lone pair activity. [TYPE A]

Transverse dimerisation of two such units leads to a structure [TYPE B] which, curiously, is unknown for $[Bi_4Cl_{16}]^{4-}$. Examples of this structural type from Group 15 are, however, provided by $[Et_4N]_4[Sb_4Cl_{16}]^{4-}$ [260] and the $[As_4Cl_{16}]^{4-}$ unit in $(S_5N_5)_4[As_8Cl_{28}].2S_4N_4$. [142] Other examples include $[TeCl_4]_4$, [261] $[SeBr_4]_4$ [262] and $[Et_3PtCl_4]_4$. [263] In this cubic structure each MX_6 octahedron shares three edges and the formal lone pairs associated with the M(III) centres can be accommodated in the tetrahedral 'hole' in the centre of the cubic array. Each metal atom binds three terminal and three μ^3 halide atoms.

An alternative structural arrangement for $[Bi_4Cl_{16}]^{4-}$ is based upon a tetrahedral Bi_4 array in which each metal centre has three terminal Bi-Cl bonds with the four remaining halogen atoms located as triply bridging groups in the centres of the four faces [TYPE C]. This structural type is unknown.

Direct super-positioning (apex-apex, eclipsed) of two $[Bi_2Cl_8]^{2-}$ units would provide the hypothetical $[Bi_4Cl_{16}]^{4-}$ [TYPE

D] featuring a rectangular Bi_4 array incorporating both single and double halogen bridges, but with retention of two lone pairs. Removal of these lone pairs of electrons (formal) by the addition of first one and then another halide ion gives the hypothetical $[Bi_4Cl_{17}]^{5-}$ and the symmetrical $[Bi_4Cl_{18}]^{6-}$ [TYPE E] species respectively. An example of the latter is provided by $[pyrH]_6[Bi_4Cl_{18}]$[6-] [143] in which two pairs of edge-edge octahedra are joined symmetrically by apex-apex fusion of their axial chlorines. As mentioned previously the ternary complex $3MgCl_2.4BiCl_3.18MeCN$ (XIII) most likely contains this anion structure.

An alternative structure for $[Bi_4Cl_{18}]^{6-}$ is based on a tetrahedral Bi_4 array [TYPE F]. In addition to three terminal Bi-Cl bonds per metal centre there are single halogen bridge bonds along the six edges of the tetrahedron as depicted. Type F is unknown.

Further halide addition leads to $[Bi_4Cl_{20}]^{8-}$ with the idealised tetranuclear array [TYPE G] in which the four MX_6 octahedra are fused apex-apex with a full complement of four single halogen bridge bonds and four terminal halogens for each Bi centre (*cf* the tetrameric penta-fluorides $[MF_5]_4$ M=Mo, Nb, Ta). [264]

The structure of $[Bi_4Cl_{16}]$ in (XII) can be regarded as the super-positioning of two $[Bi_2Cl_8]^{2-}$ units but with lateral displacement such that the Bi centres do not sit directly over one another (TYPE H, Figure 3.12). This cluster of four $BiCl_6$ octahedra has two pairs of non-equivalent Bi atoms (1 and 2) resulting from fused octahedra which share two (Bi(2)) or three (Bi(1)) common edges. There are three types of halogen

environment: 10 Cl atoms bind only one Bi centre (terminal); four more bind two Bi centres (μ^2) and two bind three Bi centres (μ^3). This discrete centrosymmetric structure is adopted by $[Ti(OMe)_4]_4$,[265] $[HL]_4^+[Sb_4Br_{16}]^{4-}$ [266] (L=2-amino-1,3,4-thiadiazole) and $[Cp_2Fe]_4[Bi_4Br_{16}]^{4-}$,[267] but this is the first report of any $[Bi_4Cl_{16}]^{4-}$ anion structure. $[Bi_4Br_{16}]^{4-}$ and $[Sb_4Br_{16}]^{4-}$ also consist of four edge-sharing distorted octahedra, joined by six bridging halogens, two of which bridge three metal centres (μ^3) while the other four bridge two metal centres (μ^2).

There is a general consensus that the condensation of MX_4^- units (M=As, Sb, and Bi) into dimers, trimers, tetramers, oligomers or polymers (and the retention or loss of lone pair activity) is dependent upon the nature of the cation present. Bi(III) complex anions can be regarded as archetypal in this respect; large cations promote the formation of large anions.[268] All previous cases however, have involved alkyl ammonium or related cations for which $N\text{-}H_{cation}\cdots X_{anion}$ hydrogen bonding is invariably present. To what extent, if any, such auxiliary H-bonding influences the resulting structure is an open question. Unquestionably the bulky 'metallo' cation $[Mg(MeCN)_6]^{2+}$ undergoes no H-bonding or direct ion-ion interactions in $[Mg(MeCN)_6]_2[Bi_4Cl_{16}]$.

A more relevant factor is the stoichiometry of the $MgCl_2/BiCl_3/MeCN$ reaction systems. $3MgCl_2/4BiCl_3$ results in the formation of the $[Bi_4Cl_{18}]^{6-}$ anion. Other stoichiometric ratios give only $[Mg(MeCN)_6]_2[Bi_4Cl_{16}]^{4-}$ or $[Mg(MeCN)_6]_3[Bi_4Cl_{18}]^{6-}$.

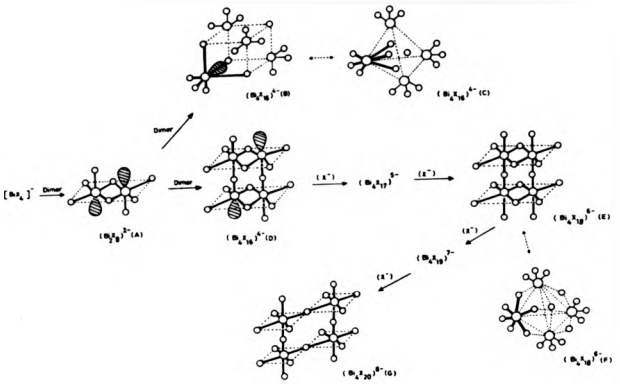

Figure 3.11. Structures of Tetranuclear Halo-Bismuth Anions

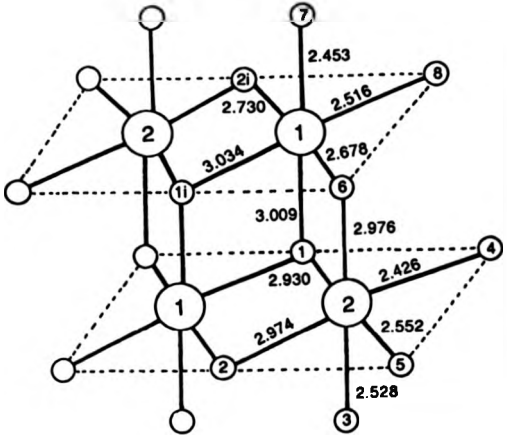

Figure 3.12. Schematic Structure of the $[Bi_4Cl_{16}]^{4-}$ Anion

3.5.Other Bismuth(III) Halo Anions

Condensation of BiX_4^- units seems to be influenced by the nature of the cation present: and large anions seem to form in the presence of large cations. For example the tetranuclear anion structures $[Bi_4X_{16}]^{4-}$ and $[Bi_4X_{18}]^{6-}$, where X=Cl, Br, occur in association with "bulky" counterions, such as $[Cp_2Fe]$, [267] $[Mg(MeCN)_6]^{2+}$ **(XII)**, **(XIII)** and $[PyrH]^+$. [143]

Monomeric $[BiX_4]^-$ units do not exist; instead infinite chains of $[BiX_4]_n^{n-}$ units are present in the structures of stoichiometrically formulated species. For example, quinolinium tetraiodobismuthate consists of infinite zigzag chains of $[BiI_4]_\infty^-$ with $[C_9H_7NH]^+$ cations situated between them. [269] The bismuth atoms have a distorted octahedral coordination. Similar skew-octahedral chains are observed in the 2-picolinium salts of $[BiBr_4]$ and $[BiI_4]$, individual $[BiX_4]^-$ units being linked by double halogen bridges. [270] Infinite chains of distorted edge-sharing $BiCl_6$ octahedra are found in ferricenium tetrachlorobismuthate, the cations stack between the polymeric anions. [271]

The $[BiX_5]^{2-}$ unit is found in $[C_5H_{10}NH_2]_2[BiBr_5]^{2-}$, [272] and is present as the tetragonal $BiCl_5^{2-}$ group in bismuth subchloride. [243] The $[BiCl_6]^{3-}$ anion is found in $Cs_2Na[BiCl_6]$ as a discrete regular octahedral group. [139]

Dimerization also occurs to form $[Bi_2X_8]^{2-}$, $[Bi_2X_9]^{3-}$ and $[Bi_2X_{10}]^{4-}$ units. The $[Bi_2Cl_8]^{2-}$ unit [243,245] consists of two square-pyramidal $BiCl_4^-$ units, which share a basal edge. The lone pairs are fully active giving a ψ-octahedral geometry to each bismuth atom. Face-sharing triply-bridged bioctahedral units $Bi_2X_9^{3-}$ are found in complexes such as $Cs_3Bi_2Cl_9$. [244] By

comparison $[Bi_2Br_{10}]^{4-}$ found in $K_4[Bi_2Br_{10}].4H_2O$, [268] $[Sr(H_2O)_8]_2[Bi_2Br_{10}]$ and $Na_7[BiBr_6][Bi_2Br_{10}]$ [273] consist of two edge sharing BiX_6 octahedra, with no evidence of lone-pair activity. There is no Cl analogue of the $[Bi_2Br_{10}]^{4-}$ unit.

There is no crystallographic evidence for the formation of trinuclear anions, and the tetranuclear anions tend to be found in combination with larger cations than Group 1 and 2 metal ions.

3.6. Summary

Halide abstraction from electropositive magnesium dichloride has been effected by bismuth trichloride. Previous studies of complex bismuth anions have used aqueous HBr and HCl as the source of halide ion and bismuth oxide or hydroxide as the source of Bi(III). This study represents the first example of bismuth(III) chloride acting as a Lewis acid (halide abstracting reagent) to generate cationic metal species directly from MCl_n. By virtue of its electropositive nature $MgCl_2$, is a suitable double chloride ion source for $BiCl_3$. Failure of $BiCl_3$ to remove chloride ions from the other transition metal halides to form ionic species confirms that $BiCl_3$ is a weaker Lewis acid than $SbCl_5$. This point is well illustrated by the generation of cationic bismuth species upon treatment with $SbCl_5$.

CHAPTER 4

Sb(III) and As(III) as Lewis Acids

4.1.Introduction

The use of Sb(V) and Bi(III) as Lewis acids towards metal chlorides has been reported in Chapters 2 and 3. To expand on this theme of halide abstraction, arsenic and antimony trihalides have been used in conjunction with various metal halides in an attempt to generate cationic metal species by a direct route.

The ability of antimony(III) and arsenic(III) to act as halide acceptors is a recognised feature of their chemistry. A range of complex halide ions have been isolated and structurally characterised, whose structures often depend upon the source of halide ion which necessarily reflects the cation choice. The following complex anions have been isolated. $[MX_4]^-$, [137,140,274-276,213] in each case the metal ion is octahedrally coordinated by halide ions due to the formation of a polymeric anion chain in which monomeric units are joined by halogen bridges. The MX_4^- unit is not monomeric (C_{2v}).

$[MX_5]^{2-}$ [137,277-280], the geometry of this anion is based upon a square pyramid. Secondary interactions can occur between neighbouring anions to form infinite chains of $SbCl_5^{2-}$, for example, in dianilinium pentachloroantimonate(III), [137] while in the 4, 4'-dipyridylium complex [279] the anions build up dimers, with average Sb-Cl bridging distances of 3.19Å. In K_2SbCl_5 [278] the equivalent Sb-Cl distance is 3.881Å. By contrast such interionic interactions are further reduced in $[NH_4]_2[SbCl_5]$ [277] where $SbCl_5^{2-}$ exists as a discrete ion, the lone pair on antimony occupies one of the octahedral sites in the antimony(III) coordination sphere.

$[MX_6]^{3-}$ anions are are also known, they are found in $[Co(NH_3)_6]^{3+}[SbCl_6]^{3-}$ [281] and $(C_5H_5NH)_6Sb^{III}Sb^{V}_3Br_{24}$. [282] There appears to be very little or no stereochemical lone pair activity on the trivalent group 15 atom, instead it can be regarded as occupying a spherical *s* orbital, not available for describing primary bonds. If no *d*-orbital participation is invoked the bonds can be described approximately as three-centre four-electron bonds formed from *p* orbitals only. [283] Conspicuous absentees from the MX_5^{2-} and MX_6^{3-} anions are those of the arsenic halides.

As observed in the case of Bi(III) dimerization of "monomeric" MX_4^- units occurs to produce $[M_2X_8]^{2-}$ and $[M_2X_9]^{3-}$. Examples of these anion types are observed for both antimony(III) and arsenic(III) halides. The $[M_2X_8]^{2-}$ ion types are similar for the Sb(III) [260,284] and As(III) [140] halides. The metal atoms have *pseudo*-octahedral coordination, one octahedral site being occupied by the lone pair to form two square-based pyramids joined by a basal edge.

The $[M_2X_9]^{3-}$ anions can be found as discrete or polymeric [140,244] dimer units with limited lone pair activity on M. In certain structures they are observed as two discrete, face-sharing distorted octahedra, [140] while in others they form a chain of infinite apex-apex fused octahedra, which are connected to the cations by N-H···Cl hydrogen bonds. [141]

A rather more unusual complex anion is found by reaction of tris(dimethylamino)cyclopropenylium iodide with antimony triiodide, producing the polymeric $[Sb_3I_{10}]_\infty^-$. [285] The distorted SbI_6 octahedra are linked edge to edge to form a polyanion. Distortion is due to differences in the magnitude of

the stereochemical effect of the non-bonding pairs at the three independent Sb atoms.

Finally, tetrameric units $[M_4X_{16}]^{4-}$ have been structurally characterised for both As(III) [142] and Sb(III) [260] halides. Both have a cubane type M_4 unit of four edge-bridged octahedra; each metal centre is octahedrally coordinated to three terminal and three μ_3 bridging chlorides. The bromide analogue $[HL]_4[Sb_4Br_{16}]$ [266] (L=2-amino-1, 3, 4-thiadiazole), by comparison does not have the same anion structure. Lateral displacement of $Sb_2Br_8^{2-}$ dimer units has occurred in the formation of the tetramer, similar to that observed in $[Mg(MeCN)_6]_2[Bi_4Cl_{16}]$ (XII). Intramolecular hydrogen bonding, N-H···Br occurs between NH_2 and NH groups of the cation and eight Br atoms of the anion. Stabilisation of the $[As_4Cl_{16}]^{4-}$ anion [142] occurs by the additional bonding of four $\{AsCl_3\}$ units via Cl bridges to form four additional distorted octahedra, while in $[Et_4N]_4[Sb_4Cl_{16}]$ [260] there appears to be no intramolecular bonding between the cations and anions. The structure $[Fe(Cp)(CO)_2Cl]_4[SbCl_3]_4$ [286] has a Sb_4Cl_4 cubanelike framework, with four antimony and four chlorine atoms occupying alternate corners of a tetragonally distorted cube. The iron atoms of the cation bond to chlorine atoms of the Sb_4Cl_4 anion. In all these tetranuclear anion structures the lone pair on the M^{III} atom is thought to point to the central cavity of the cube.

The majority of these arsenic and antimony(III) halide anions are synthesized by direct mixing with a quaternary ammonium (or related) salt. Many have hydrogen bonds, N-H···X between cations and anions which have a stabilising effect on the complex anion. [141,276]

As an alternative approach, the use of metal halides as the source of halide ion for the production of antimonate(III) and arsenate(V) species has been investigated. Preliminary observations [287] indicate that arsenic trichloride is not capable of removing a halide ion from metal halides to form ionic species such as:

$$MCl_n + AsCl_3 \longrightarrow [MCl_{n-1}][AsCl_4] \quad (1)$$

Where M=Ti(IV) the above reaction in acetonitrile results in the formation of the bis(acetonitrile) adduct $TiCl_4.2MeCN$. Therefore it was an obvious step to attempt the oxidation of As(III) to As(V), using chlorine as oxidising agent, in order to generate cationic metal species resulting from halide transfer to As(V) and formation of the hexachloroarsenate anion $AsCl_6^-$.

Arsenic pentachloride has only been isolated at -105°C [67] by the ultraviolet irradiation of $AsCl_3$ in liquid Cl_2. A number of its complexes are known, [288,289] which represent the use of complexing agents to stabilise high oxidation states:

$$AsCl_3 + Cl_2 + MCl_n \longrightarrow [AsCl_4]^+[MCl_{n+1}]^- \quad (2)$$

M=Al, Ga, Sb

$$AsCl_3 + Cl_2 + Q^+Cl^- \longrightarrow [Q]^+[AsCl_6]^- \quad (3)$$

Q+=Et_4N, PPh_4

$$AsCl_3 + xD + Cl_2 \longrightarrow AsCl_5.yD + [x-y]D \quad (4)$$

The instability of $AsCl_5$ is due to the instability of the highest valence state of p-block elements following completion

of the first (3d) transition series. Incomplete shielding of the nucleus leads to the "d-block contraction", which causes a lowering of the 4s orbital in $AsCl_3$. Hence the large promotional energy required by the $4s^2$ electrons to enter a vacant d orbital makes the formation of $AsCl_5$ difficult.

Isolation of the tetraphenylphosphonium hexachloroarsenate(V) salt [289] was achieved by ozonation or chlorination of $[PPh_4]_2[As_2Cl_8]$ at -40°C, *i.e.* an intermediate trivalent As(III) anion was isolated before oxidation to the pentavalent state.

The behaviour of antimony pentachloride and bismuth trichloride with antimony trichloride provides observations on the relative Lewis strengths of the chlorides of the group.

4.2.Oxidation of As(III) to As(V)

As previously mentioned, preliminary observations indicate the failure of $AsCl_3$ to remove a halide ion from $TiCl_4$. Therefore the oxidation of As(III) to As(V) was carried out using chlorine as oxidising agent.

Titanium and tin tetrachlorides were chosen as covalent chlorides, while zinc and magnesium chlorides were selected as rather more electropositive metal chlorides. Tetramethylammonium chloride was also used as a source of halide ion in these oxidation reactions in an attempt to produce an $AsCl_6^-$ standard for ^{75}As nmr purposes. The following results were obtained.

Discussion of Results: Oxidation of As(III) to As(V)

4.2.1.[Me_4N][$AsCl_6$](XXII)

Isolation of the title compound (XXII) from reaction of Me_4NCl with $AsCl_3$ in Cl_2 follows a very similar procedure to the synthesis of $Et_4N^+AsCl_6^-$. [288a] Full dissolution of tetramethylammonium chloride in acetonitrile is indicative of its incorporation into an ionic product which is soluble in MeCN.

Formulation of the compound as (XXII) is based upon analytical, conductivity, infra-red and electronic spectroscopic data. The high melting point 230-233°C (with decomposition) is indicative of the incorporation of the tetramethylammonium cation into the product (compare Me_4NCl; m.p. > 300°C). The presence of the broad intense band at 350 cm^{-1} in the far infra-red spectrum is assigned to $\nu_3(AsCl)[F_{1u}$ bending mode]. [288a,290] Charge transfer bands at 38 759, 37 453 and 36 900 cm^{-1} in the electronic spectrum are associated with the hexachloroarsenate(V) anion.

The conductivity of this salt was measured in dimethylformamide, due to its greater solubility in this solvent compared with that in acetonitrile: its existence as a 1:1 electrolyte *i.e.* Λ_m=99.14 Scm^2mol^{-1} at 10^{-3}M at 25.0 ± 0.1°C is confirmed. The molar conductivity range for a 1:1 electrolyte in DMF is 65-90 Scm^2mol^{-1}.

4.2.2.[$Mg(MeCN)_6$][$AsCl_6$]$_2$(XXIII)

Immediate precipitation of solid material was observed upon addition of $MgCl_2.2MeCN$ to a chlorine saturated solution of $AsCl_3$ in MeCN, this solid is proposed as the title compound (XXIII) on the basis of infra-red and electronic spectroscopy;

analytical and conductivity data. A clear m.p. of 66-68°C distinguishes the compound from the bis(acetonitrile) adduct $MgCl_2.2MeCN$ m.p. > 300°C.

The doublet profile in the infra-red spectrum at ν(CN) 2316 and 2286 cm^{-1} is characteristic of acetonitrile coordinated to a metal centre (compare the corresponding bands at 2287 and 2251 cm^{-1} for the free ligand). Other hexakis(acetonitrile) magnesium(II) cations isolated in these studies have ν(CN) doublets, for example, at 2320 and 2289 cm^{-1}. Acetonitrile coordination to magnesium raises the ν(CN) by 29 and 35 cm^{-1} due to coupling of the M-N and C≡N stretching frequencies. This can be compared to increases in ν(CN) stretching frequencies, upon ligand coordination, of 23, 29 and 25, 29 cm^{-1} observed for the Ti(IV) and Sn(IV) species respectively. This is due to the electropositive nature of magnesium compared to Ti(IV) and Sn(IV). Zinc, also electropositive causes an increase of 29 and 33 cm^{-1} to ν(CN), which is similar to that observed for magnesium.

The band at 406 cm^{-1} is assigned to the δ(CCN) bending mode ν_3 of coordinated acetonitrile. (Compare bands at 407, 405 and 401 cm^{-1} for other hexakis(acetonitrile) magnesium(II) cations). The broad intense band at 345 cm^{-1} is tentatively assigned to ν(AsCl), this band is close to the corresponding band at 350 cm^{-1} for (XXII). The similar bands at 333 cm^{-1} [290] and 352 cm^{-1} [288a] for $[Et_4N][AsCl_6]$ have been assigned as the F_{1u} bending mode (ν_3) of the As-Cl bond. [$MgCl_2.2MeCN$ has ν(MCl) at 315 and 250 cm^{-1}].

The charge transfer bands at 36 764, 37 453 and 38 759 cm^{-1} in the electronic spectrum are associated with the

hexachloroarsenate(V) anion, and are very similar to those observed at 38 759, 37 453 and 36 900 cm^{-1} in $[Me_4N][AsCl_6]$.

The conductivity was measured in DMF solution, due to the insolubility of the compound in acetonitrile. Low solubility in acetonitrile of (XXIII) compares with the low solubility of the hexakis(acetonitrile) magnesium(II) salts with tetranuclear bismuth chloro-anions (Chapter 3). The molar conductivity, Λ_m=157.67 Scm^2mol^{-1} (at 10^{-3}M at 25.0 ± 0.1°C) of (XXIII) confirms its existence as a 1:2 electrolyte. Similar electrolyte types have molar conductivities in the range 130-170 Scm^2mol^{-1} in DMF solution.

4.2.3.$ZnCl_2$ Reaction (XXIV)

The oxidation of $AsCl_3$ to $AsCl_5$ with chlorine was carried out but halide transfer to $AsCl_5$ from $ZnCl_2$ proved to be unsuccessful. The white solid obtained from this reaction is the bis(acetonitrile) adduct, $ZnCl_2.2MeCN$. The melting point , 95-98°C is very similar to that of 108-109°C for the synthesized adduct. The doublet profile in the infra-red spectrum at 2316 and 2284 cm^{-1} is characteristic of acetonitrile coordinated to a metal centre. The sharp band at 402 cm^{-1} corresponds to the δ(CCN) bending mode of coordinated acetonitrile. Bands at 383, 347, 310 and 245 cm^{-1} are assigned to ν(MCl) stretching and bending modes, compare those observed at 400, 390, 355, 320, 265 and 240 cm^{-1} for the synthesized adduct.

4.2.4.$TiCl_4$ Reaction (XXV)

The oxidation of $AsCl_3$ to $AsCl_5$ using Cl_2 as oxidising agent was carried out but halide transfer from $TiCl_4$ to $AsCl_5$ was unsuccessful. The bright yellow crystals isolated from this reaction correspond analytically to the bis(acetonitrile) adduct, $TiCl_4.2MeCN$. The m.p. of these crystals, 150-152°C is very similar to the m.p.'s of the bis adducts isolated from the reactions of $TiCl_4/BiCl_3/MeCN$; 148-151°C and $TiCl_4/SbCl_3/MeCN$; 158-160°C. The synthesized adduct itself has a m.p. of 150-152°C. Bands in the IR and UV spectrum are very similar to those observed in the synthesized adduct.

4.2.5.$SnCl_4$ Reaction (XXVI)

The oxidation of $AsCl_3$ to $AsCl_5$ using Cl_2 as oxidising agent was carried out but halide transfer from $SnCl_4$ to $AsCl_5$ has proved to be unsuccessful. The colourless crystals isolated from this reaction analyse for chloride as the bis(acetonitrile) adduct, $SnCl_4.2MeCN$. Halide abstraction by arsenic has not occurred. The m.p.,110-112°C is very close to that of the synthesized adduct, 112-114°C. [291]

The ν(CN) bands in the infra-red spectrum at 2312 and 2280 cm^{-1} correspond to acetonitrile coordinated to a metal centre. The band at 410 cm^{-1} is assigned to the δ(CCN) bending mode ν_8 of coordinated MeCN. The bands at 392, 366, 334 and 303 cm^{-1} in the far infra-red region are very similar to those observed at 397, 303, 367, 333-345 and 305 cm^{-1} for $SnCl_4.2MeCN$. [259]

4.2.6. ^{75}As NMR Studies

Several attempts were made to identify the ^{75}As nmr signal in DMSO solution, using AsO_4^{3-} as external reference in solutions of $[Me_4N]^+[AsCl_6]^-$(XXII) and $\{Mg(MeCN)_6\}[AsCl_6]_2$ (XXIII). Failure to locate any signal using a ^{75}As nmr probe does not rule out the presence of the hexachloroarsenate(V) anion, but is more likely a result of the relatively large electric quadrupole moment of the nucleus, which causes ^{75}As linewidths to be rather broad, and the short relaxation times [292] of this nucleus. Dove *et al* [293] have reported the ^{75}As resonance of $AsCl_6^-$ as a singlet at δ=-391.8ppm (ca 0.1M concentration) relative to Et_4NAsF_6 at δ=0ppm in MeCN (at an operating frequency of 42.83 Hz). The signal is seen to reduce in intensity in a MeCN solution containing AsF_6^- and is replaced by the resonances of $AsCl_nF_{6-n}^-$, n<5, indicative of the instability of the $AsCl_6^-$ anion.

4.2.7. Conclusions

The results of these reactions indicate that $AsCl_3$ can be oxidised to $AsCl_5$, but halide transfer from Ti(IV), Sn(IV) and Zn(II) chlorides to $AsCl_5$ does not take place. Instead the products of these reactions are simply the bis(acetonitrile) adducts. By contrast, oxidation of $AsCl_3$ to $AsCl_5$ by chlorine and generation of $AsCl_6^-$ by halide transfer occurs in the presence of Me_4NCl and $MgCl_2$ at room temperature. $AsCl_3$ is oxidised to $AsCl_5$ in the presence of Cl_2. $AsCl_5$ is unstable at RT and halide transfer from these two chloride ion donors to $AsCl_5$ takes place to give $AsCl_6^-$. The symmetrical $AsCl_6^-$ anion stabilizes the +5 oxidation state of arsenic. The failure of Ti, Sn and Zn

chlorides to donate chloride ions to $AsCl_5$ compared to the ability of $MgCl_2$ to do so illustrates the superior role of $MgCl_2$ as a source of halide ion in these reactions.

The use of Me_4NCl as source of chloride ion for transfer to As(V) was to produce an $AsCl_6^-$ standard for ^{75}As nmr purposes, and follows previous methods for the generation of hexachloroarsenate(V) by the addition of an ionic chloride containing a bulky cation. [288a] Stabilisation of the higher oxidation state of As primarily relies upon a large lattice energy contribution to the stability of the arsenic(V) salt. The stability of the $AsCl_6^-$ anion is also increased by complexation, but this contribution to the stability of the salt is minor compared to lattice energy effects. Similar strategy for isolation and structural determination of $AsCl_6^-$ is observed by the use of the bulky tetraphenylphosphonium cation. [289]

Another method for the stabilisation of arsenic(V) relies on the use of neutral ligands which are capable of π bonding and of increasing the electron density on the metal. This reduces the oxidising strength of arsenic in the +5 state. Ligands such as R_3PO have been used to this end. [288a]

Lewis acid halides $FeCl_3$, $AlCl_3$, $GaCl_3$ [294] and $SbCl_5$ [295] have been used to form cationic arsenic(V) species according to conductivity measurements. Stabilisation of the As(V) state by generation of the tetrachloroarsenate(V) cation has been achieved. By contrast the compound $PCl_5.AsCl_5$ has been formulated as $PCl_4^+AsCl_6^-$; [295] although later studies propose that its formula lies between PCl_5 and $PCl_5.AsCl_5$, $[x\ AsCl_6^-.(1-x)PCl_6^-]$ [290]. Raman studies [296] indicate that this compound decomposes to $AsCl_3$, Cl_2 and PCl_5.

The oxide chloride of arsenic(V), $AsOCl_3$ has been isolated by ozonolysis of $AsCl_3$. At room temperature it decomposes to $(As_2O_3Cl_4)_n$ of unknown structure. In the same study arsenic trichloride reacts with fluorine at -78°C to give $AsCl_4^+AsF_6^-$. [297]

The use of $MgCl_2$ as a source of chloride ion to stabilise the pentavalent state of arsenic following oxidation of $AsCl_3$ with Cl_2 in our studies represents a novel route to the generation of the hexachloroarsenate(V) anion. In this present study and in previous studies [213] $MgCl_2$ is established as a suitable double chloride ion source in Group 15 halide exchange systems, *i.e.*

$$MgCl_2 + 2SbCl_5 \xrightarrow{MeCN} [Mg(MeCN)_6][SbCl_6]_2 \qquad \textbf{(I)}$$

$$MgCl_2 + 2BiCl_5 \xrightarrow{MeCN} [Mg(MeCN)_6]_2[Bi_4Cl_{16}] \qquad \textbf{(XII)}$$

$$3MgCl_2 + 4BiCl_3 \xrightarrow{MeCN} [Mg(MeCN)_6]_3[Bi_4Cl_{18}] \qquad \textbf{(XIII)}$$

$$MgCl_2 + 2SbCl_3 \xrightarrow{MeCN} [Mg(MeCN)_6][SbCl_4]_2 \qquad (213)$$

Thus the use of $MgCl_2$ to generate cationic metal species seemed an obvious choice, due to its electropositive nature. Solvent choice is also an important factor in the generation of the bulky $[Mg(MeCN)_6]^{2+}$ cation to stabilise the $[AsCl_6]^-$ anion. The stability of As(V) in $[Mg(MeCN)_6][AsCl_6]_2$ is therefore enhanced by complexation and a large lattice energy contribution, whereby As(V) behaves as a Lewis acid towards $MgCl_2$ generating ionic species.

$$MgCl_2 + AsCl_3 + Cl_2 \xrightarrow{MeCN} [Mg(MeCN)_6][AsCl_6]$$

To our knowledge this represents the first example of the use of an electropositive metal halide as the source of halide to generate the hexachloroarsenate anion.

4.3.Sb(III) as a Lewis Acid

The usual preparation of antimonate(III) salts involves direct mixing with a quaternary ammonium (or related) salt. As an alternative approach we have investigated the use of metal halides as the source of halide ion in an attempt to generate antimonate(III) salts involving cationic metal species. Previous studies [213] have resulted in the formation of the ternary complex $MgCl_2.2SbCl_3.6MeCN$, identified as $[Mg(MeCN)_6][SbCl_4]_2$. This was obtained from the reaction of $SbCl_3$ with $MgCl_2$ in acetonitrile solution.

A variety of different metal chlorides have been used as the source of halide ion in reactions with $SbCl_3$ in acetonitrile. Several covalent chlorides were used, namely: $TiCl_4$, $SnCl_4$ and $TiCl_3$. Iron(III) and In(III) chlorides were selected on the basis of their Lewis acidic tendencies. While Sb(V) and Bi(III) chlorides were chosen as a means of demonstrating the relative Lewis acidic strengths of the group 15 chlorides. The following results were obtained.

4.3.1.Discussion of Results: Sb(III) as Lewis Acid

$TiCl_4$ Reaction (XXVII)

Reaction of $TiCl_4$ with $SbCl_3$ in acetonitrile results in the formation of the adducts $TiCl_4.2MeCN$ and $SbCl_3.3MeCN$, which have been spectroscopically identified using IR and UV tecniques. Halide transfer from Ti^{IV} to Sb^{III} has not occurred.

Recrystallisation from MeCN gave bright yellow crystals of $TiCl_4.2MeCN$, m.p. 158-160°C. $TiCl_4.2MeCN$. Bands observed in the electronic and infra-red spectrum confirm the formation of the bis(acetonitrile) adduct.

$TiCl_3$ Reaction (XXVIII)

Reaction of $TiCl_3$ with $2SbCl_3$ in MeCN results in the formation of the two acetonitrile adducts, $TiCl_3.3MeCN$ and $SbCl_3.3MeCN$, which have been identified using IR and UV-Visible spectroscopy. Halide transfer from Ti^{III} to Sb^{III} has not occurred.

$FeCl_3$ Reaction (XXIX)

Reaction of equimolar $FeCl_3$ with $SbCl_3$ in MeCN gives a yellow solid which is a mixture of $FeCl_3.2MeCN$ and $SbCl_3.3MeCN$. Halide transfer from Sb^{III} to Fe^{III} or *vice versa* has not occurred.

Peaks at 2320 and 2295 cm^{-1} in the infra-red spectrum correspond to coordinated acetonitrile. In the far infra-red region the broad intense band at 378 cm^{-1} is assigned to v(FeCl). The bands at 350 and 250 cm^{-1} are assigned to v(SbCl) (compare bands at 352 and 259 cm^{-1} in $SbCl_3$ itself).

The charge transfer bands at 41 841, 37 313(sh), 32 051 and 27700 cm^{-1} in the electronic spectrum are attributed to the $[FeCl_4]^-$ anion in solution, they correspond closely to bands observed at 41 600, 37 400, 32 000 and 27 700 cm^{-1} in $[Et_4N][FeCl_4]$.[258]

The dissociation of $FeCl_3.2MeCN$ to $FeCl_2^+FeCl_4^-$ in MeCN accounts for the presence of $FeCl_4^-$ in the electronic spectrum.

$InCl_3$ Reaction (XXX)

Reaction of $InCl_3$ with $3SbCl_3$ in acetonitrile results in the formation of a mixture of the tris(acetonitrile) adducts of $SbCl_3$ and $InCl_3$. Halide transfer has not occurred between In^{III} and

Sb^{III}. Group 13 halides generally behave as Lewis acids, the trihalides interact with other metal chlorides to form mixed halides with halogen bridges, many of which are quite volatile.

$SnCl_4$ Reaction (XXXI)

Reaction of $SnCl_4$ with $2SbCl_3$ in MeCN results in the formation of the two acetonitrile adducts $SnCl_4.2MeCN$ and $SbCl_3.3MeCN$. Halide transfer from Sn^{IV} to Sb^{III} has not occurred.

Bands at 2304 and 2276 cm^{-1} in the infra-red spectrum correspond to coordinated acetonitrile. In the far infra-red spectrum bands at 408, 392 and 360 cm^{-1} assigned to $\nu(SnCl)$ and those at 334 and 304 cm^{-1} assigned to $\nu(SnN)$ are very similar to those observed in $SnCl_4.2MeCN$. [259] Recrystallisation from MeCN gave colourless crystals $SnCl_4.2MeCN$.

$SbCl_5$ Reaction (XXXII)

Reaction of equimolar $SbCl_5$ with $SbCl_3$ in acetonitrile solution results in the formation of the highly air-moisture sensitive ternary complex $SbCl_3.SbCl_5.4MeCN$. This product is formulated as an ionic product on the basis of infra-red, electronic and nmr spectroscopic data.

The bands at 2310 and 2280 cm^{-1} in the infra-red spectrum correspond to coordinated MeCN. These ligands necessarily bond to the Sb^{III} centre as there is strong evidence for the formation of the six coordinate hexachloroantimonate(V) anion.

The presence of a broad intense band at 346 cm^{-1} in the far infra-red spectrum is indicative of $SbCl_6^-$. Compare the exceptionally strong $\nu(SbCl)$ 346 cm^{-1} [F_{1u} bending mode (ν_3)]

observed for $[K][SbCl_6]$.[207] The intense charge transfer band at λ_{max} 37 313 cm^{-1} is diagnostic of $SbCl_6^-$ species in solution. The clearly resolved singlet at δ=-0.17ppm ($W_{1/2}$=175Hz) in the ^{121}Sb nmr spectrum provides further confirmation of $SbCl_6^-$. (Compare the external reference $[Et_4N][SbCl_6]$ δ=0, $W_{1/2}$=190Hz). The intense band at 260 cm^{-1} in the far infra-red spectrum is assigned to ν(SbCl); compare the similar band at 259 cm^{-1} of $SbCl_3$ itself.

In the knowledge that the presence of the $SbCl_6^-$ ion arising from the self-ionisation of $SbCl_5$ is unlikely, halide transfer has occurred from Sb^{III} to Sb^V: the ternary complex (XXXII) may be formulated as $[Sb^{III}Cl_2(MeCN)_4]^+[Sb^VCl_6]^-$. However this simple stoichiometric formulation is rather unlikely. The cation species may well be multinuclear, analogous to the fluoro species derived from $SbF_3.SbF_5$ adducts of differing stoichiometries (Chapter 1). These have no coordinated solvent molecules and synthesis usually involves the reduction of SbF_5 by PF_3 in arsenic trifluoride.[162-167] The solid-state nature of the ternary species $SbCl_3.SbCl_5.4MeCN$ is an obvious candidate for an X-ray structural study, but suitable crystals could not be obtained.

Conductivity measurements in acetonitrile solution imply that the product is a 1:1 electrolyte, Λ_m=141.75 Scm^2mol^{-1} at $10^{-3}M$.

A similar reaction is found in that of Ph_3SbCl_2 with $SbCl_5$ in carbon tetrachloride. Chloride ion transfer to $SbCl_5$ occurs to give the ionic species $[Ph_3SbCl]^+[SbCl_6]^-$,[298] although the cation contains antimony in the pentavalent state.

There are very few examples where $Sb^{III}Cl_3$ behaves as a Lewis base, this more unusual feature of its chemistry is observed in the unstable, light-sensitive products $[Ni(CO)_3SbCl_3]$ and $[Fe(CO)_3(SbCl_3)_2]$. [299]

Antimony(III) chloride behaves as a chloride ion donor in the 1:1 adduct $SbCl_3.GaCl_3$ [300] (synthesis in liquid SO_2). This comprises very distorted tetrahedral $GaCl_4^-$ anions which strongly interact with $SbCl_2^+$ cations via Ga-Cl···Sb bridges to give a polymeric chain. In this instance halide transfer has occurred from Sb^{III} to Ga^{III} but a strong covalent interaction exists between the ions $[SbCl_2]^+[GaCl_4]^-$. The product cannot be formally regarded to contain the $SbCl_2^+$ cation.

This study represents the behaviour of Sb^{III} as a chloride ion donor in the presence of the very powerful Lewis acid $SbCl_5$.

BiCl$_3$ Reaction (XXXIII)

Reaction of equimolar $BiCl_3$ with $SbCl_3$ in acetonitrile results in the formation of the two tris(acetonitrile) adducts $BiCl_3.3MeCN$ and $SbCl_3.3MeCN$. Halide transfer from Sb^{III} to Bi^{III} or *vice versa* has not occurred.

The bands at 2300 and 2260 cm^{-1} in the infra-red spectrum correspond to coordinated MeCN. In the far infra-red spectrum bands at 350 and 250 cm^{-1} are tentatively assigned to ν(BiCl). The charge transfer bands at 45 045, 42 918, 34 965 and 31 847 cm^{-1} are due to the presence of $BiCl_3.3MeCN$. Similar bands are observed at 46 882, 43 478, 35 014 and 32 258 cm^{-1} in the electronic spectrum of $BiCl_3$ in MeCN.

4.3.2.Conductivity Studies

Acetonitrile was chosen as the solvent for conductivity studies. Using the technique described in Appendix 1 the conductivity of (XXXII) was measured over a series of dilutions at 25.0 ± 0.1°C to allow application of the Onsager Law for solutions of strong electrolytes.

Reaction of $SbCl_5/SbCl_3$/MeCN (XXXII)

The ternary complex $SbCl_5.SbCl_3.4MeCN$ is formulated as an ionic product in solution on the basis of spectroscopic data which identify the $SbCl_6^-$ anion, also conductivity studies imply that the complex behaves as a 1:1 electrolyte in MeCN.

Initially the graph of $\Lambda_m(Scm^2mol^{-1})$ versus $c^{1/2}$(mol dm^{-3}) was plotted (Figure 4.1).

Figure 4.1. Λ_m versus $c^{1/2}$ for $SbCl_3.SbCl_5.4MeCN$

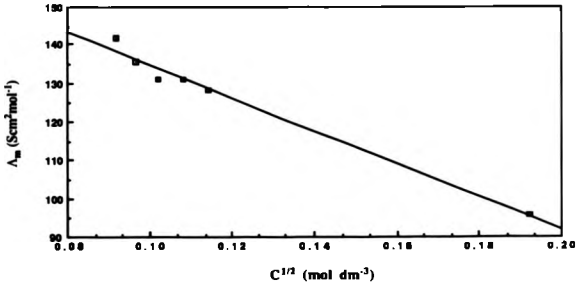

This graph was extrapolated to give Λ_o, the molar conductivity at infinite dilution, using linear least squares analysis (Λ_o=177.50 Scm^2mol^{-1} at 25.0 ± 0.1°C, correlation coefficient, 0.984). This value is used to plot a graph of Λ_o-Λ_m versus $c^{1/2}$ (Figure 4.2) to give a slope which necessarily reflects the electrolyte type of the complex. The slope has a value of 428.1.

Figure 4.2. Λ_o-Λ_m versus $c^{1/2}$ for $SbCl_3$,$SbCl_5$,4MeCN

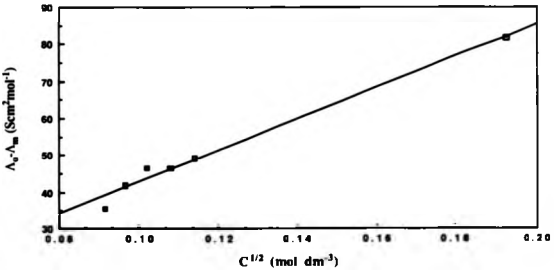

Λ_m, the molar conductivity at 10^{-3}M is 141.75 Scm^2mol^{-1}. This value is within the range, 120-160 Scm^2mol^{-1}, expected for a 1:1 electrolyte in acetonitrile solution. [242]

4.3.3.Conclusions

The results of these reactions in most cases illustrate the failure of $SbCl_3$ to generate cationic metal species by halide abstraction, by contrast with $SbCl_5$ which removes at least one halide ion from the corresponding metal chlorides. The rapacious Lewis acidity of Sb^V is illustrated by the generation of cationic Sb^{III} and Bi^{III} species and the stable $SbCl_6^-$ anion by halide removal from $SbCl_3$ and $BiCl_3$ *i.e.*

$$SbCl_3 + SbCl_5 \xrightarrow{MeCN} SbCl_3.SbCl_5.4MeCN \qquad \textbf{(XXXII)}$$

$$BiCl_3 + SbCl_5 \xrightarrow{MeCN} [BiCl_2(MeCN)_4][SbCl_6] \quad \textbf{(XIV)}$$

The reaction of Sb^{III} with Bi^{III} in MeCN gives the acetonitrile adducts. This serves to illustrate their similar Lewis acidic strengths, which is further confirmed by their identical behaviour towards the various metal chlorides chosen.

4.4.Mechanism of Halide Transfer

Many of the reactions investigated in this study illustrate the transfer of chloride ions from MCl_n to a group 15 chloride and the formation of ionic species. Comparisons of the behaviour of $AsCl_3$, $SbCl_3$, $BiCl_3$ and $SbCl_5$ towards different MCl_n provides insight into the relative Lewis acidic strengths of these chlorides.

The choice of acetonitrile as solvent for these reactions is based upon its strongly coordinating aprotic properties: M-Cl/Sb-Cl solvolysis side reactions are avoided. Its powerful donor properties ensures occupation of coordinatively

unsaturated sites generated on the metal centres following halide removal, and the attainment of a six coordinate geometry for M. The resultant formation of ionic products is assisted by this polar solvent.

The transfer of halide ion(s) from M to E (E=As^{III}, Sb^{III}, Bi^{III}, Sb^{V}) is thought to proceed by a molecular mechanism which involves halogen bridged intermediates. The generation of $[Mg(MeCN)_6][SbCl_6]_2$(I) is used as an example. In this $MgCl_2/SbCl_5$/MeCN system halogen-bridged intermediates of binuclear (A) and/or trinuclear (B) nature can be proposed (Figure 4.3) involving the edge or face sharing fusion of octahedral units.

In MeCN solution asymmetric cleavage of chloride bridges at 1 generates (I) which implies that Sb(V) is the preferred halogen acceptor. Vacant sites on $[Mg]^{2+}$ are occupied by six MeCN ligands. The solvent plays a very important role in the stabilisation of the cationic species; it assists ionic formation via occupancy of co-ordinatively unsaturated metal species implicit with halide expulsion. The unlikely situation where asymmetric cleavage at 3 occurs would result in the formation of $[SbCl_4]^+$. This is dismissed on the basis of the rapacious Lewis acidity of $SbCl_5$. (Symmetric cleavage at 2 gives the starting materials).

In this case multiple halide abstraction has occurred, so both binuclear and trinuclear halogen bridged intermediates can be proposed. With a binuclear species sequential removal of chloride from $MgCl_2$ to give $MgCl^+$(solvated) is implied, a second molecule of $SbCl_5$ approaches the $MgCl^+$(solvated) species to abstract its chloride to give the fully solvated

$[Mg(MeCN)_6]^{2+}$ cation. The $MgCl^+$ cation has actually been structurally identified in $[MgCl(THF)_5][AlCl_4]$.[309]

Figure 4.3. Proposed Intermediates of $[Mg(MeCN)_6][SbCl_6]_2$

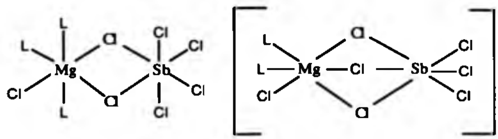

A

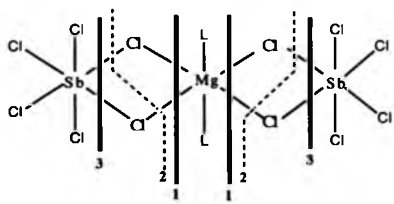

B

(The number and arrangement of coordinated ligands, L=MeCN around the Mg centre is variable).

By contrast, a trinuclear intermediate as in B may be involved, whereby simultaneous removal of both chlorides from $MgCl_2$ occurs to give (I). In complexes where triple halide abstraction takes place, i.e. $[In(MeCN)_6][SbCl_6]_3$ (VI) and $[Bi(MeCN)_6][SbCl_6]_3$ (XV), more complex multinuclear bridged

species can be envisaged to enable simultaneous chloride abstraction from MCl_3.

Another consideration of the halide transfer mechanism is associated with the positions of the MeCN ligands on the metal centre. Whether chloride ligands *trans* to MeCN are removed in preference to those *trans* to another chloride is an open question. Compare the "trans effect" and similar "trans influence" of ligands on metal centres. The expected *trans* geometry of the $[TiCl_2(MeCN)_4]^+$ cation in **(X)** implies that the MeCN ligands exert such a trans effect on the removal of chloride from *mer* $TiCl_3.3MeCN$.

The use of covalent chlorides as chloride ion donors in the reactions investigated rules out the preformation of any ionic species in MeCN. In fact most of these chlorides form molecular adducts in MeCN. Even $MgCl_2$, which is an ionic compound, has limited solubility in MeCN. Its conductivity was measured and was found to be negligible in MeCN. Therefore the dissociation of $MgCl_2$ into ions does not occur. The autoionization of these group 15 chlorides is also negligible; the formation of ionic species in these reactions has occurred by halide transfer from MCl_n to the group 15 Lewis acid ECl_n by a molecular mechanism.

Where halide transfer to $BiCl_3$ has occurred similar halogen bridged intermediate species are envisaged, the lone pair on Bi^{III} may or may not be active before oligomerization to a tetranuclear Bi_4 unit occurs.

4.5. Variations in the Lewis Acidity of Group 15 Chlorides

From these studies it is apparent that there are variations between the acceptor strength of arsenic, antimony and bismuth chlorides. Antimony pentachloride is by far the most powerful Lewis acid of the chlorides of this group. In all reactions (I-XI) $SbCl_5$ removes at least one chloride ion from MCl_n to generate partially or fully solvated metal cations and $SbCl_6^-$. The formation of cationic Sb^{III} and Bi^{III} species upon reaction with $SbCl_5$ in (XIV), (XV) and (XXXII) shows that $SbCl_5$ exceeds $SbCl_3$ and $BiCl_3$ in chloride acceptor strength. The failure of $BiCl_3$, $SbCl_3$ and $AsCl_3$ to abstract chloride ions from those chlorides which form cations with Sb^V provides further confirmation of their weaker Lewis acidity. The only chloride from which As^{III}, Sb^{III} and Bi^{III} will remove chloride ions is $MgCl_2$, to give $[Mg(MeCN)_6][AsCl_6]_2$ (XXIII), $[Mg(MeCN)_6][SbCl_4]_2$,[213] $[Mg(MeCN)_6]_2[Bi_4Cl_{16}]$ (XII) and $[Mg(MeCN)_6]_3[Bi_4Cl_{18}]$ (XIII) respectively. All other chlorides used gave the acetonitrile adducts (A) rather than halide transfer products (HT) (Table 4.1).

Table 4.1. The Formation of Halide Transfer Products with MCl_n and the Group 15 Chlorides

MCl_n	As(V)	Sb(V)	Sb(III)	Bi(III)
$MgCl_2$	HT	HT	HT	HT
$ZnCl_2$	A	HT	A	A
$TiCl_3$		HT	A	A
$TiCl_4$	A	HT	A	A
VCl_3		HT		A
$CrCl_3$		HT		A
$FeCl_3$		HT	A	A
$InCl_3$		HT	A	A
$SnCl_4$	A	HT	A	A
$SbCl_3$		HT		A
$BiCl_3$		HT	A	

Such variations between the chloride donor ability of $MgCl_2$ compared to MCl_n (n=2, M=Zn; n=3, M=Ti, V, Cr, Fe, In; n=4, M=Ti, Sn) is attributed to a number of factors: The electronegativity of M, the size and charge of M^{n+} (polarizability). According to Pauling's electronegativity scales magnesium has by far the lowest electronegativity compared to other M, such that it is more likely to donate chloride to ECl_n to become a cation. There is a correlation between the size (using Shannon and Prewitts effective ionic radii, [22] coordination number 6) and the charge of M^{n+} and its chloride donor ability. This is also related to the chloride ion acceptor ability of ECl_n (Table 4.2).

Table 4.2. Ratio of Charge to Effective Ionic Radii (charge density) for M^{n+}

M	Charge	Ionic Radii (pm)	Charge Density (charge/ionic radii)
Mg	2	86	0.023
Zn	2	88	0.022
Ti	3	81	0.037
V	3	78	0.038
Cr	3	75.5	0.0397
Fe	3	69 (low spin)	0.0434 (L.S)
		78.5 (high spin)	0.0382 (H.S)
In	3	94	0.0319
Ti	4	74.5	0.0536
Sn	4	83	0.048
As	3	72	0.0416
As	5	60	0.0833
Sb	3	90	0.033
Sb	5	74	0.067
Bi	3	117	0.0256

It must be remembered that these values relate to the effective ionic radii and size of M^{n+}, so are appropriate for the formation of $[Mg(MeCN)_6]^{2+}$, $[In(MeCN)_6]^{3+}$ and $[Bi(MeCN)_6]^{3+}$ but are used as guidelines for predicting the behaviour of MCl_n

in the formation of $[MCl_{n-x}L_{6-(n-x)}]^{x+}$, when the charge of $[M]^{x+}$ is not the same as its oxidation state.

The chloride ion donor and acceptor ability of M deduced from these studies parallels the trends observed in electronegativity and charge density data, i.e. the higher the charge density and electronegativity the greater is the Lewis acidity (acceptor ability) of M. This is a direct measure of the "hardness" of M.

On the basis of these data it is understood why $MgCl_2$ is a suitable source of chloride ion for Group 15 halide transfer reactions compared to other MCl_n; the electronegativity and charge density of trivalent As, Sb and Bi all exceed that of Mg, while their charge densities are lower than those of other M. This latter point explains the failure of As^{III}, Sb^{III} and Bi^{III} to behave as Lewis acids towards MCl_n other than $MgCl_2$.

To compare, Sb^{V} has a high charge density which is greater than all the metals used and explains its behaviour as a powerful Lewis acid towards them, and equally to Sb^{III} and Bi^{III}. In addition to the reduced electron density around Sb^{V}, which causes an increased acceptor strength, the superiority of $SbCl_5$ over $SbCl_3$ as a Lewis acid is associated with an increase in stability in changing from a trigonal bipyramidal to an octahedral geometry after chloride acceptance. The formation of ionic products is favoured due to a lattice energy contribution.

It is apparent from this study that $BiCl_3$ and $SbCl_3$ have very similar chloride acceptor strengths, the following series can be drawn up in order of decreasing Lewis acidity:

$$SbCl_5 >> SbCl_3 \approx BiCl_3 > AsCl_5 > AsCl_3$$

Chloride ion removal from $MgCl_2$ by $AsCl_5$ and the formation of a stable product $[Mg(MeCN)_6][AsCl_6]$ (XXIII) requires the presence of Cl_2 to oxidise $AsCl_3$ to $AsCl_5$. Its Lewis acidity is not adequate to effect halide ion transfer in the trivalent state, unlike $SbCl_3$ and $BiCl_3$.

It was observed that the reaction of $AsCl_3/Cl_2$ with $ZnCl_2$ (XXIV) fails to give halide transfer products: Zn and Mg have very similar charge density (Table 4.2) but the electronegativity of Zn (1.65) is greater than that of Mg (1.31). Also the 2nd ionization energy of Zn (1726 $kJmol^{-1}$) is higher than for Mg (1450 $kJmol^{-1}$).

CHAPTER 5

Titanium Tetrachloride [a) Lewis Acid and b) Cation Formation]

$TiCl_4$ is a colourless liquid which is rapidly hydrolysed in the air. The role of $TiCl_4$ as a Lewis acid is well established; [301] it complexes with chloride ions to form a series of chloro-anions and forms a large number of addition compounds with other ligand types. The most common coordination number of Ti(IV) is six, although compounds of different coordination number are known. For example, $(\eta^5\text{-}C_5H_5)_2TiCl_2$, [302] distorted tetrahedral (if the centre of the ring is considered as the coordination site), TiO(porphyrin), [303] square pyramidal and $TiCl_4(diars)_2$ (diars=*o*-phenylenebis(dimethylarsine), [304] dodecahedral.

a) 5.1.$TiCl_4$ as a Lewis Acid

5.1.1.Introduction

The formation of Ti(IV) complex chloro-anions is an established feature of its chemistry; $TiCl_5^-$ and $TiCl_6^{2-}$ anions have been isolated [305,306] by reaction of Et_4NCl with $TiCl_4$ in thionyl chloride.

The dinuclear anions $[Ti_2Cl_{10}]^{2-}$ and $[Ti_2Cl_9]^-$ have been prepared by reaction of PCl_3 and PCl_5 with $TiCl_4$ in $SOCl_2$ and $POCl_3$ respectively. [240] The $[Ti_2Cl_{10}]^{2-}$ anion comprises an edge-bridged bioctahedral unit. This anion is also formed as a by-product of the reaction of trithiazyl chloride, $(NSCl)_3$ with $TiCl_4$ in CCl_4. [307] By comparison the $[Ti_2Cl_9]^-$ anion provided the first example of a first row transition metal in the +4 formal oxidation state to assume the geometry of a face-shared bioctahedron (Figure 5.1).

Figure 5.1. The $[Ti_2Cl_9]^{2+}$ Anion

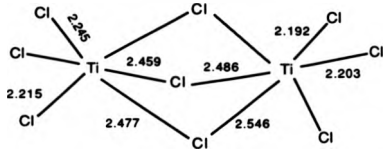

Isolation of the double salt $[PCl_4]_3[TiCl_6][PCl_6]$ was achieved by reaction of a large excess of PCl_5 with $TiCl_4$ in CH_3NO_2 and $POCl_3$.[239] Attempts to prepare the simple salt $[PCl_4][TiCl_6]$ have been unsuccessful.

Interest in the chemistry of $TiCl_4/MgCl_2$ systems stems from the knowledge that Ziegler-Natta catalysts of the type $MgCl_2$/electron donor/$TiCl_4$/$AlEt_3$ are very effective in the polymerization of ethylene and propylene.[308] Extremely active catalysts can be prepared by milling $MgCl_2$ and $TiCl_4$ together, polymerization is then effected using $AlEt_3$ as an activator. $MgCl_2$ acts as the catalyst support, its unique behaviour as such has been attributed to the similarity of its crystal structure to that of α or γ $TiCl_3$, and the similar ionic radii (Pauling) of Ti^{4+} and Mg^{2+} (0.68 and 0.65Å respectively), which illustrates the compatibility of these two catalyst components. Sobota *et al*[309] have suggested that the key to the unusual role played by $MgCl_2$ as a support for super-high-activity Ziegler-Natta catalysts lies in the reaction:

$AlCl_3 + [MgCl_2(THF)_2] \longrightarrow [MgCl(THF)_5][AlCl_4].THF$ (1)

Elimination of $AlCl_3$ from the catalyst composition (equation 2) prevents the formation of $AlEtCl_2$, which is thought to poison the catalyst. $AlEtCl_2$ is formed during the catalyst synthesis, as a by-product of the alkylation of $TiCl_3$.

$AlEt_2Cl + AlCl_3 \longrightarrow 2AlEtCl_2$ (2)

Several groups have investigated the chemistry of $TiCl_4/MgCl_2$ systems in different oxygen donor solvents as models for Ziegler/Natta catalyst sites: Bassi *et al* have used EtOAc, [310] and $ClCH_2CO_2Et$ (ethylchloroacetate). [311] Sobota's group have carried out similar reactions in THF. [217] These studies gave bimetallic complexes which incorporate halogen-bridging. Although titanium(IV) is very oxophilic the solvent molecules bind to the magnesium centre, which implies that Ti(IV) is the preferred halogen acceptor in these halogen bridged structures.

Reaction of $MgCl_2$ in EtOAc with equimolar $TiCl_4$ in EtOAc at 60°C yields $TiMgCl_6(EtOAc)_4$ [310] which has the following chloro-bridged structure (Figure 5.2).

Figure 5.2. Structure of $TiMgCl_5(EtOAc)_4$

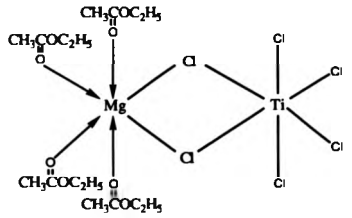

Complex formation has changed the metal geometry of titanium from tetrahedral to octahedral.

Reaction of $MgCl_2$ with equimolar $TiCl_4$ in ethylchloroacetate gives $TiMgCl_5(O_2CCH_2Cl).(ClCH_2CO_2Et)_3$ (Figure 5.3). [311]

Figure 5.5. Structure of $TiMgCl_5(OOCCH_2Cl).(ClCH_2CO_2Et)_3$

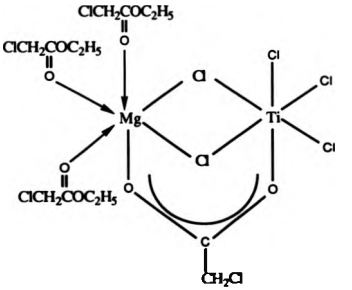

In this structure the Ti(IV) atom is octahedrally coordinated by five chlorine atoms and an oxygen atom of a $ClCH_2CO_2$ residue. This unit has resulted from the loss of the ethyl group from ethylchloroacetate. Six coordination is observed for Mg(II) which is surrounded by two bridging chlorine atoms, the carbonyl oxygen atoms of three $ClCH_2CO_2Et$ and an oxygen atom of the $ClCH_2CO_2$ residue. The two octahedra share an edge via the two chlorine bridges and are further connected by the CO_2 group of the $ClCH_2CO_2$ residue.

Reaction of Mg(OH)Cl with $TiCl_4$ in EtOAc gives $TiMgCl_5OH(EtOAc)_4$ [312] (Figure 5.4).

Figure 5.4. Structure of $TiMgCl_5(OH)(EtOAc)$

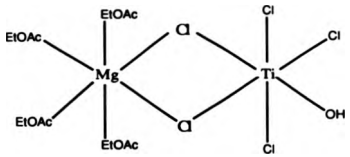

This structure consists of two slightly distorted octahedra; Ti(IV) being coordinated by five chlorines and a hydroxyl ligand, and Mg(II) by the carbonyl oxygens of four EtOAc molecules and two bridging Cl atoms. The two octahedra share an edge defined by the double chlorine bridge between Ti and Mg as in $TiMgCl_6(EtOAc)_4$. [310] The presence of both OH and Cl ligands on the titanium centre is unusual due to the hydrolytic nature of Ti-Cl bonds.

Reactions of $MgCl_2$ with $TiCl_4$ in THF, in varying stoichiometries results in the formation of a variety of products: [217]

$$2[TiCl_4(THF)_2] + [MgCl_2(THF)_2] \xrightarrow[20°C]{THF} \underset{a}{[Mg(THF)_6][TiCl_5(THF)]_2} \quad (3)$$

$$a + [MgCl_2(THF)_2] \xrightarrow[20°C]{THF} \underset{b}{[(THF)_4Mg(\mu\text{-}Cl)_2TiCl_4]} \quad (4)$$

$$b + [MgCl_2(THF)_2] \xrightarrow[20°C]{THF} \underset{c}{[(THF)_3Mg_2(\mu\text{-}Cl)_3(THF)_3][TiCl_5(THF)]} \quad (5)$$

Complete halide transfer from Mg^{II} to Ti^{IV} has occurred in reaction of a 1:2 molar ratio of $[MgCl_2(THF)_2]$ with $[TiCl_4(THF)_2]$ (equation 3) to give the $[Mg(THF)_6]^{2+}$ cation and $[TiCl_5(THF)]^-$ anions. Reaction of this product, a, with equimolar $MgCl_2$ (equation 4) gives the binuclear chlorine-bridged structure b (Figure 5.5), which is similar to that found in $TiMgCl_6(EtOAc)_4$. [310] With an equimolar ratio of $[MgCl_2(THF)_2]$ and b (equation 5) the product is c which comprises the homobimetallic cation $[(THF)_3Mg_2(\mu\text{-}Cl)_3(THF)_3]^+$ (Figure 5.6) and the pseudo octahedral $[TiCl_5(THF)]^-$ anion. [238] This cation consists of two face-sharing octahedra joined by three chlorine bridges, a similar cation structure is observed with $[MoOCl_4THF]^-$. [216]

Figure 5.5. Structure of $TiMgCl_6(THF)_4$

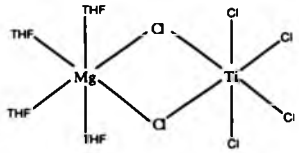

Figure 5.6. Structure of $[(THF)_3Mg(\mu\text{-}Cl)_3Mg(THF)_3]$

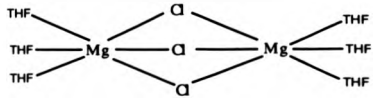

Other bimetallic halogen-bridged magnesium species are known; direct reaction between $MgCl_2(THF)_2$ and $FeCl_3$ in THF yields $[MgCl(THF)_5][FeCl_4]$ [309] and $[FeCl_2(\mu\text{-}Cl)_2Mg(THF)_4]$. [313] The former species is light sensitive and undergoes reduction to the bimetallic compound. Structural characterisation of $[MgCl(THF)_5]^+$ [309] provides evidence for the existence of the previously postulated $MgCl^+$ cation. Reduction of Fe^{III} to Fe^{II} is thought to be caused by THF, which reacts with $FeCl_3$, with ring-opening and polymerizeration.

All reactions in this research have used MeCN as solvent for halide transfer. Reasons for this choice of solvent are based upon its strongly coordinating aprotic properties (Chapter 4, Section 4.4). The results presented in Chapters 2, 3 and 4

indicate the success of MeCN as solvent media for halide transfer reactions involving arsenic, antimony and bismuth chlorides. Solvolysis side reactions are avoided and unsaturated sites generated on the metal centres following halide removal are occupied by MeCN ligands. It was therefore an obvious choice to study the reaction of $MgCl_2$ with $TiCl_4$ in MeCN to investigate what effect, if any, the use of a more polar nitrogen donor solvent has upon the reaction. Complete or single halide transfer may take place, or the formation of bridged species, similar to those observed in EtOAc, $ClCH_2CO_2Et$ and THF, may occur.

5.1.2.Discussion of Results

Reaction of $TiCl_4$ with $MgCl_2$ in MeCN (XXXIV)

Isolation of air sensitive bright yellow crystals from the reaction of equimolar $TiCl_4$ with $MgCl_2$ in MeCN gave the ternary complex $TiCl_4.MgCl_2.6MeCN$ (X-ray structural determination pending).

The doublet at 2304 and 2276 cm^{-1} in the infra-red spectrum corresponds to coordinated acetonitrile. In the far infra-red region the band at 412 cm^{-1} is assigned to δ(CCN) of coordinated MeCN. The broad intense peak at 330 cm^{-1} is assigned to a Ti-Cl stretching mode. Similar peaks are observed at 324 and 321 cm^{-1} in $[Me_4N]_2[TiCl_6]$ and $[Et_4N]_2[TiCl_6]$ respectively, [305] and at 330 cm^{-1} in aqueous $H_2[TiCl_6]$. [306] (Compare ν(TiCl) peaks at 387s, br and 318w for $TiCl_4.2MeCN$). [210] In the electronic spectrum the intense band at 43 668 cm^{-1} (shoulder at 38 461 cm^{-1}) is associated with $Cl(\pi)\rightarrow Ti$ charge transfer transitions. [314] The peak observed at 43 800 cm^{-1} for $TiCl_6^{2-}$ [301] is similar (Compare peaks at 45 871, 39 682 and 33 783 cm^{-1} for $TiCl_4.2MeCN$).

Conductivity studies show that the product behaves as a 1:1 electrolyte in MeCN solution (Λ_m=73 Scm^2mol^{-1} at $10^{-2}M$; Λ_o=110.8 Scm^2mol^{-1}).

Conductivity of $MgCl_2.TiCl_4.6MeCN$

The conductivity of this ternary species was measured at 25.0 ± 0.1°C over a range of concentrations, using the method detailed in Appendix 1. A graph of Λ_m (Scm^2mol^{-1}) versus $c^{1/2}$ ($moldm^{-3}$) was plotted (Figure 5.7) from which a value for Λ_o of 110.8 Scm^2mol^{-1} was obtained by extrapolation.

Figure 5.7.Graph of Λ_m versus $c^{1/2}$ for $MgCl_2.TiCl_4.6MeCN$

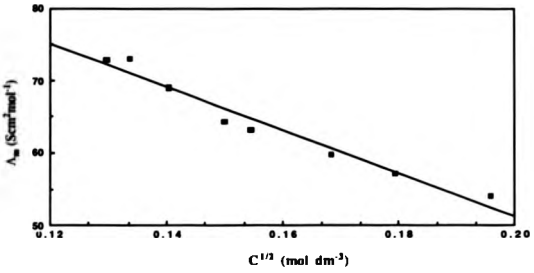

This value was used to plot Λ_o-Λ_m versus $c^{1/2}$ which gives a slope of 298.11 (Figure 5.8).

Figure 5.8. Graph of Λ_o-Λ_m versus $c^{1/2}$ for $MgCl_2.TiCl_4.6MeCN$

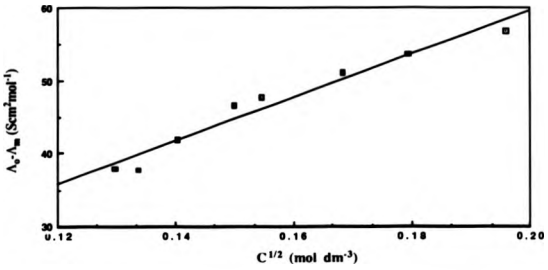

Λ_m=73 Scm^{2}mol^{-1} at 10^{-2}M. These values are low by comparison with the expected range for 1:1 electrolytes in MeCN (Λ_m=120-160 Scm^{2}mol^{-1}), [242] but are of similar magnitude to those observed for the 1:1 electrolytes $[SnCl_3(MeCN)_3][SbCl_6]$ (III) and $[TiCl_3(MeCN)_3][SbCl_6]$. A molar conductivity of 98 Scm^{2}mol^{-1} at 10^{-3}M was recorded (Λ_o=116.26 Scm^{2}mol^{-1}) for the latter complex.

The exact nature of the ternary species $MgCl_2.TiCl_4.6MeCN$ is unknown. There are three possible structures for a species of this stoichiometry:

i) a neutral chloro-bridged product $[L_4Mg(\mu\text{-}Cl)_2TiCl_4]$ (Figure 5.9, L=MeCN) like those where L=THF [217] and EtOAc. [310] Analytical figures indicate six solvent molecules rather than four, so in this case two uncoordinated solvent molecules must

be present in the lattice. It can be envisaged that such a bimetallic species could undergo some degree of dissociation in MeCN to give a conducting solution.

ii) single halide transfer from Mg^{II} to Ti^{IV} would involve symmetric cleavage of chloro-bridges according to **2** (Figure 5.9) to give $[MgCl(MeCN)_5][TiCl_5(MeCN)]$.

iii) double halide transfer from Mg^{II} to Ti^{IV} would involve asymmetric cleavage of the chloro-bridges at **1** (Figure 5.9) to give $[Mg(MeCN)_6][TiCl_6]$. Similarly Sobota *et al* [217] suggest an ionic formulation $[Mg(MeCN)_6][ZrCl_6]$ for $ZrCl_4.MgCl_2.6THF$ based upon elemental analysis.

Figure 5.9. Chloro-Bridged $TiCl_4/MgCl_2/MeCN$ Species

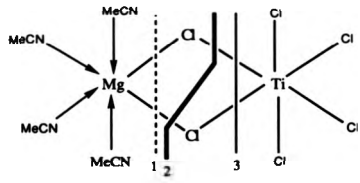

It is unlikely that asymmetric cleavage of the bridges according to **3** occurs, as this would imply that Mg^{II} is the preferred halogen acceptor.

These Ti/Mg chloro-bridged species are models for the halogen bridged intermediates of the ionic products resulting

from halide transfer to a Group 15 chloride (Chapters 2, 3 and 4).

The solvent used may play a crucial role in the type of product formed *i.e.* equimolar quantities of reactants in EtOAc and THF give the chloro-bridged products $[L_4Mg(\mu\text{-}Cl)_2TiCl_4]$, L=THF, EtOAc. Both these ligands have oxygen donor atoms, while MeCN contains nitrogen as its donor atom (all three ligands can be classed as "hard" by virtue of their donor atoms).

Differences in polarity of these solvents could reflect the different products formed. Dipole moments increase in the order THF < EtOAc < MeCN (1.63, 1.78 and 3.92 Debye respectively). Thus MeCN is more likely than THF and EtOAc to give ionic rather than bridged species where transfer of chloride(s) from Mg^{II} to Ti^{IV} occurs (solvent assisted cleavage of the chloro bridges may take place as shown in Figure 5.9, and vacant sites in the metal coordination spheres are occupied by polar MeCN following halide transfer).

5.2. Ti-Cl Bond Lengths

Table 5.1 shows variations in the Ti-Cl bond lengths of various $Ti^{(IV)}$ chloro species.

Table 5.1.Selected $Ti^{(IV)}$-Cl Bond Lengths

Compound	Bond Ti-Cl_b	Distances(Å) Ti-Cl_t	Ref
$TiCl_4$(gas)		2.18(4)	315
$TiCl_4$(solid)		2.20	315
$TiMgCl_6$ $(EtOAc)_4$	2.466-2.493(2)	2.255-2.326(2)	310
$TiMgCl_5$ (O_2CCH_2Cl) $(ClCH_2CO_2Et)_3$	2.441-2.457(2)	2.242-2.246(6)	311
$[PCl_4][Ti_2Cl_9]$	2.459-2.546(7) (av. 2.493)	2.188-2.245(7)	240
$[Mg(POCl_3)_6]$ $[Ti_2Cl_{10}]$	2.520(4)	2.267	316
$[TiCl_3(MeCN)_3]$ $[SbCl_6]$		2.176-2.195	199
$[(THF)_3Mg$ $(\mu\text{–}Cl)_3$ $Mg(THF)_3]$ $[TiCl_5(THF)]$		2.249-2.318	238
$[Mg(POCl_3)_6]$ $[TiCl_6]$		2.340	316

Several points can be made from the lengths observed in Table 5.1.

Terminal, Ti-Cl_t, lengths are consistently shorter than bridging, Ti-Cl_b, lengths. This is consistent with the expected

weakening of the bridging bonds, causing an increase in their length.

Bridging and terminal bond lengths are similar in both anionic and neutral bridged species.

Both the bridging and terminal lengths in the face-shared bioctahedral complex $[PCl_4][Ti_2Cl_9]$ are shorter than in the edge-sharing bioctahedral anion $[Ti_2Cl_{10}]^{2-}$; this is associated with the shorter metal-metal interionic distances in $[Ti_2Cl_9]^-$ causing a general tightening of all the bonds in the molecule.

Cationic Ti-Cl lengths are not dissimilar from those observed in gaseous and solid $TiCl_4$, but are markedly shorter than those observed in the mononuclear anionic species $[TiCl_5(THF)]^-$ and $[TiCl_6]^{2-}$. Loss of a chloride ion in the cationic $[TiCl_3(MeCN)_3]^+$ species causes a reduction in the electron density around the Ti centre. The stability is maintained by a reduction in the length of the remaining Ti-Cl bonds and coordination of solvent at the vacant sites.

Removal of a further chloride from $[TiCl_3(MeCN)_3]^+$ to form $[TiCl_2(MeCN)_4]^{2+}$ (XI) is likely to cause an even greater decrease in the observed Ti-Cl bond length associated with a more positive charge on the metal centre and a reduction in the number of chlorine atoms bonded to Ti^{IV}. Crystallographic data for (XI) is not available to clarify this.

The anionic species $[TiCl_5(THF)]^-$ has shorter Ti-Cl lengths than those observed in $[TiCl_6]^{2-}$, which is consistent with an increase in the electron density on Ti associated with an increased number of coordinated chlorines.

5.3.Ti(IV) Cations

Evidence for the behaviour of $TiCl_4$ as a chloride ion donor in the literature is scant, therefore its role as a source of cations is unusual; the formation of the cationic species $[TiCl_3(MeCN)_3][SbCl_6]$ [199] and $[TiCl_2(MeCN)_4][SbCl_6]_2$ (XI) (Chapter 2) represents this rather undeveloped area of its chemistry.

Preliminary observations indicate that both are highly reactive species for ligand exchange and chloride replacement reactions; the following results illustrate this. Both neutral and anionic donors were selected in attempts to generate mixed ligand Ti^{IV} cationic complexes. Chloride and bromide anions were used as ligands, and the neutral phosphine, triphenylphosphine (PPh_3).

5.3.1.Discussion of Results: Anionic Ligands

Reaction of $[TiCl_3(MeCN)_3][SbCl_6]$ with Me_4NCl (XXXV)

It is possible to remove chloride ions from $TiCl_4$ to form cations; therefore it must be possible to regenerate $TiCl_4$ by the addition of chloride ions to a cation. Me_4NCl was used as the source of chloride ion and $TiCl_4.2MeCN$ has been regenerated using a 1:1 molar ratio of reactants according to:

$$[TiCl_3(MeCN)_3][SbCl_6] + Me_4N^+Cl^- \xrightarrow[20°C]{MeCN} TiCl_4.2MeCN + [Me_4N][SbCl_6]$$

The bis(acetonitrile) adduct was identified by analytical, IR and UV spectroscopic and m.p. measurements.

The band at 37 313 cm^{-1} in the UV spectrum of the mother liquor (from recrystallization of the solid product initially isolated) is diagnostic of $SbCl_6^-$ in solution. The singlet at δ-0.1123 ppm in the ^{121}Sb nmr spectrum also confirms the presence of $SbCl_6^-$ in solution.

In a similar vein addition of chloride ion to cationic bismuth, $[BiCl_2(MeCN)_4][SbCl_6]$ (XIV), gave $BiCl_3$.

Bromide ligand (from Me_4NBr) was added to $[TiCl_3(MeCN)_3][SbCl_6]$ in an attempt to generate mixed halide titanium species, $[TiCl_3Br.2MeCN]$ in MeCN. Instead this reaction liberated bromine (detected as MeCN-Br-Br-NCMe in the UV spectrum, λ_{max}=38 022 cm^{-1}). Oxidation of Br^- to Br^0 has taken place. The most likely oxidising agent is Sb(V), [$SbCl_6^-$ + $2e \rightarrow SbCl_4^-$, E^0=+0.818 V in 6M HCl (SCE)], [317] which is subsequently reduced to Sb(III) considering the potential of the Sn^{4+}/Sn^{2+} couple. [Sn^{4+} + $2e^- \rightarrow Sn^{2+}$, E^0=+0.154V in aqueous HCl]. The oxidation of Br^- to Br^0 in MeCN proceeds by a two step process: [318]

1st anodic wave: $3Br^- \longrightarrow Br_3^- + 2e^-$ $E_{1/2} = {}^{+}0.42V$ Ag^+/Ag 0.01M MeCl
[$^{+}0.748V$ (SCE)]

2nd anodic wave: $2Br_3^- \longrightarrow 3Br_2 + 2e^-$ $E_{1/2} = {}^{+}0.71V$ as above
[$^{+}1.038V$(SCE)]

The first process is thermodynamically favourable with Sb(V) as oxidant. The 2nd process occurs to give Br_2 due to the formation of Br_3^- as intermediate.

There are precedents for the behaviour of $SbCl_5$ as oxidising agent towards organic molecules [319] and transition metals. [320]

5.3.2.Titanium-Phosphine Systems

5.3.2.1.Introduction

Coordination compounds which contain neutral phosphorus donors are abundant for the majority of the elements in the Periodic Table. Certain elements have relatively little phosphine derivative chemistry, notably the early transition elements of groups 3 and 4 and the lanthanides and actinides. One reason for this lies in their electropositive and oxophilic nature; [321] most complexes of these elements are formed with nitrogen and oxygen based donors. [322]

The comparatively small number of phosphine donor complexes of these elements has also been attributed to the behaviour of P-donors as "soft" ligands, [109] while the metals themselves are "hard" acids. [22] The unsuitability of such interactions in the presence of hard donors may well account for the absence of M-P bonded complexes, but if no preferentially bonding ligands are present in the reaction medium phosphine complexes should form. It is therefore necessary to chose the appropriate ligand and solvent and to ensure that "hard" ligands are not present in excess.

Backbonding is important for the stability of phosphine complexes, the electron deficient nature of the high oxidation states of these metal centres also accounts for the lack of stability of their phosphine complexes. In fact many such complexes are reactive due to the lability of the phosphine ligands.

A number of Ti(IV) phosphine complexes have been reviewed. [323] Phosphine adducts of $TiCl_4$ have received reasonably extensive coverage in the literature; mono $TiCl_4.L$

and bis $TiCl_4.L_2$ species have been made (L=monodentate phosphine); the chelating bidentate phosphine complexes $TiCl_4.L_2$ (L_2=bidentate phosphine, dppe, dmpe etc) are stable adducts. Synthesis is usually effected by mixing the ligand and $TiCl_4$ in benzene in appropriate stoichiometries.

Some cationic Ti(IV) phosphine complexes $[Cp_2TiMe(L)]^+BPh_4^-$ (L=PMe_3, PMe_2Ph, $PMePh_2$, PBu_3) have been prepared. [324]

$$Cp_2TiMeCl + L + NaBPh_4 \xrightarrow[-NaCl]{THF} [Cp_2TiMe(L)]^+BPh_4^-$$

It is noted that even the bulky phosphine PBu_3 forms the above complex, and that these species are formed in the presence of a large excess of THF. This indicates that the phosphines compete effectively with the oxygen donor THF for the vacant site generated on the titanium centre. The above reaction does not take place when L=PPh_3, dppe and dmpe; this is associated with their lower pK_a values compared to those of PMe_3, PMe_2Ph, $PMePh_2$ and PBu_3 (Table 5.2). [5]

Table 5.2. Some pK_a Values of Tertiary Phosphines

Phosphine	pK_a
PBu_3	11.40
PMe_3	8.65
PMe_2Ph	6.49
PPh_3	2.73
$P(4\text{-}ClC_6H_4)_3$	1.03

The species $[(\eta-C_9H_7)_2TiMe(L)]^+BPh_4^-$ have also been prepared as before (L=PMe_3, $PMePh_2$), [324] and the acyl complex $[Cp_2Ti(COMe)PMe_2Ph]^+BPh_4^-$, by phosphine displacement of MeCN. Again this illustrates the ability of Ti(IV) to accept phosphine ligands in preference to hard donor ligands. The cationic species $[Cp_2TiCl(PMe_2Ph)]^+$ is believed to be generated during the electrochemical oxidation of $Cp_2TiCl(PMe_2Ph)$, although it has not been isolated as a salt. [325]

5.3.2.2.Discussion of Results

The following results do not have any accompanying analytical data, the identification of the reaction products is based upon spectroscopic measurements.

Reaction of $[TiCl_3(MeCN)_3][SbCl_6]$ with PPh_3 in MeCN

Reaction of $[TiCl_3(MeCN)_3][SbCl_6]$ with PPh_3 in varying stoichiometries (XXXVI-XXXVIII) gives a mixture of the starting materials and $[TiCl_3(PPh_3)_3][SbCl_6]$.

Reaction of 1:2 and 1:3 stoichiometric quantities of $[TiCl_3(MeCN)_3][SbCl_6]$ with PPh_3 (XXXVII and XXXVIII) respectively causes immediate precipitation of an orange solid of m.p. 209-210°C. Inspection of the IR spectrum reveals the presence of bands associated with the PPh_3 ligand at 1440, 1120, 1060, 1025, 995, 750, 730, 690 and 537 cm^{-1}. (Compare peaks at 1435, 1150, 1090, 1020, 990, 740, 690, 510 and 490 cm^{-1} of PPh_3 itself (Nujol). The bands at 455 and 437 cm^{-1} are assigned to ν(Ti-P). Those at 360 and 340 cm^{-1} are ν(M-Cl); the broad intense band at 340 cm^{-1} may be tentatively assigned to ν(SbCl), while the band at 360 cm^{-1} may be assigned to ν(TiCl). The absence of the characteristic ν(CN) doublet (at *c.a.* 2287-

2325 cm^{-1}) and the δ(CCN) (at 429 cm^{-1}) in the IR spectrum indicates the loss of coordinated acetonitrile from $[TiCl_3(MeCN)_3][SbCl_6]$ and their replacement by three PPh_3 ligands to maintain an octahedral geometry around Ti(IV).

The bands at 45 248, 39 062 and 36 764 cm^{-1} in the UV spectrum can be assigned to $\pi \rightarrow \pi^*$ charge transfer transitions of the phenyl rings of PPh_3, or to $Cl(\pi) \rightarrow Ti$ transitions. Similar bands are observed at 44 200 and 36 100 cm^{-1} in $TiCl_3Me.PPh_3$. [326] The presence of the band expected at 37 037 cm^{-1} for $SbCl_6^-$ is masked by the charge transfer peaks associated with PPh_3.

In the proton nmr spectrum a broad multiplet is found at δ=7.75 ppm (relative to TMS), this is assigned to aromatic protons of the PPh_3 ligands. A similar shift is observed at δ=+7.56 ppm in $TiCl_3Me.PPh_3$. [326]

A singlet is observed at δ=-0.4994 ppm in the ^{31}P nmr spectrum. The chemical shift of free PPh_3 is observed at δ=+5.5 ppm in CH_2Cl_2 at RT (H_3PO_4 as external reference), [327] this upfield shift relative to the free ligand corresponds to coordinated PPh_3. In $(PhO)_2TiCl_2.2PPh_3$ a singlet is observed in the ^{31}P nmr spectrum at δ=+1.8 ppm, relative to H_3PO_4. [328] In the adduct $TiCl_4.PPh_3$ with 1:4 and 1:8 excess of PPh_3 ^{31}P shifts are observed at δ=-20.5 ppm. [327] The presence of a singlet implies a *fac* geometry for the species formed, i.e. all PPh_3 groups are chemically equivalent, this follows the *fac* configuration of $[TiCl_3(MeCN)_3][SbCl_6]$.

The following reaction takes place:

$$[TiCl_3(MeCN)_3][SbCl_6] + 3PPh_3 \xrightarrow[20°C]{MeCN} [TiCl_3(PPh_3)_3][SbCl_6] \quad \text{(XL)}$$

orange product

The complex is thought to have the following structure (Figure 5.10).

Figure 5.10. Proposed Structure for $[TiCl_3(PPh_3)_3][SbCl_6]$

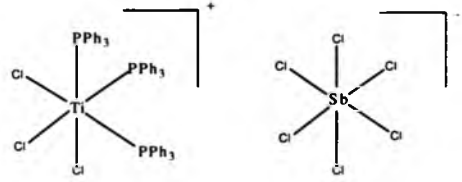

fac

CHAPTER 6

General Experimental

Except where otherwise stated all of the compounds were air or moisture sensitive. All operations were therefore carried out under a N_2 atmosphere using a conventional 'dry box' or under nitrogen on a Schlenk line using standard techniques. Anhydrous metal halides and $SbCl_5$ were used as obtained commercially. $SbCl_3$ was sublimed prior to use on an all glass vacuum-line rig. Phosphine ligands were used directly as supplied. All solvents were dried prior to use. Acetonitrile was freshly distilled and purified following the procedure of Walter and Ramaley. [329] Dichloromethane was freshly distilled from calcium hydride, benzene and hexane from sodium/benzophenone. Dimethylformamide and dimethylsulphoxide were freshly distilled under vacuum. N.m.r solvents were dried over 3Å molecular sieve.

Instrumentation

Infra-red Spectra [4000-200 cm^{-1}] were recorded as nujol mulls located between CsI plates using a Perkin-Elmer 580B spectrometer.

Proton (^1H) Nuclear Magnetic Resonance Spectra (220 MHz) were recorded on a Perkin-Elmer R34 spectrometer, with samples in sealed tubes using TMS as internal reference.

^{31}P [^1H] Nuclear Magnetic Resonance Spectra (162 MHz) were recorded on a Bruker WH400 spectrometer, with samples in sealed tubes as $CDCl_3$ solutions, using 85% H_3PO_4 as external reference.

^{121}Sb Nuclear Magnetic Spectra (95.72 MHz) were recorded on a Bruker WH400 spectrometer. Samples were sealed in tubes

as MeCN solutions doped (10% by volume) with CD_3CN, relative to $[Et_4N][SbCl_6]$ (δ=0, $W_{1/2}$= 190 Hz) as external reference.

^{75} As Nuclear Magnetic Spectra were recorded on a Bruker WH400 spectrometer, with samples as MeCN solutions doped (10% by volume) with CD_3CN, relative to AsO_4^{3-} as external reference.

Visible-Ultraviolet spectroscopic measurements were made with a Shimadzu UV35 spectrophotometer using MeCN solutions sealed in quartz cells with a light path of 1 cm.

Atomic Absorption measurements were made with a Varian Techtron AA6 spectrometer.

Arsenic, antimony and bismuth were determined by Atomic Absorption Spectrometry. Bismuth analyses were carried out on dilute hydrochloric acid solutions (*ca* $5x10^{-4}$ mol dm^{-3}) of the compounds. The wavelength used was 222.8 nm. The spectrometer was calibrated each time of use on standard solutions of bismuth of concentrations in the range 50-200 ppm. These standard solutions were prepared by dissolving a known weight of bismuth metal in a minimum volume of 1:4 hydrochloric acid followed by dilution with distilled water to a known volume in a volumetric flask. A calibration curve was then plotted of concentration against absorption. This plot is slighty curved, however, for the range of concentrations of unknown samples used (typically 75-150 ppm) it is reasonable to approximate this to a straight line. Antimony analyses were carried out on dilute hydrochloric acid solutions of the compounds, using a wavelength of 231.2 nm (concentration of unknown samples 30-80 ppm). Calibration of the spectrometer was effected with standard solutions of antimony of

concentrations in the range 10-150 ppm. These were prepared by dissolving a known mass of potassium antimonyl tartrate in 10% HCl. Arsenic analyses were carried out on dilute sodium hydroxide, nitric acid solutions of the compounds, using a wavelength of 193.7 nm (concentration of unknown samples 75-175 ppm). Calibration of the spectrometer was effected with standard solutions of arsenic of concentrations in the range 50-200 ppm. These were prepared by dissolving a known mass of arsenic(III) oxide in 20% NaOH, which was neutralized with nitric acid and diluted with distilled water to a known volume in a volumetric flask.

Spot tests for arsenic and antimony were carried out by gently warming zinc in dilute sulphuric acid to cause a regular evolution of hydrogen. Approximately 1 cm^3 of the test solution was added and a cotton wool plug moistened with aqueous $AgNO_3$ placed in the top of the test tube. A black spot of metallic Ag confirms the presence of As and Sb, due to the production of AsH_3 and SbH_3.

Elemental analyses of Carbon, Hydrogen and Nitrogen were performed by Butterworth Laboratories Ltd., Teddington, Middlesex, TW11 8LG and Medac Ltd., Department of Chemistry, Brunel University, Uxbridge, Middlesex, UB8 3PH. For this, small samples were sealed in glass tubes under vacuum, to prevent deterioration of the compounds while in transit.

Chloride was determined by the Volhard titration method described in Vogel. [330]

Titanium was determined as the yellow peroxo species $[TiO(SO_4)_2]^{2-}$ obtained from aqueous solutions of Ti^{III} and Ti^{IV}

in 2M sulphuric acid and 10% hydrogen peroxide. The colour intensity was measured at 410 nm and compared with a standard Ti(IV) sulphate calibration curve.

6.1. Experimental Section for Chapter 2

6.1.1: Reaction of $MgCl_2$ with $SbCl_5$ (I)

A solution of $MgCl_2$ (2.20g, 23.10mmol) in MeCN (70cm^3) was obtained by direct Soxhlet extraction. This solution was chilled (0°C) and to it was added dropwise a solution of $SbCl_5$ (6.00cm^3, 46.20mmol) in MeCN (30cm^3). The resulting pale yellow solution was allowed to warm to room temperature and stirred for a further 24h under nitrogen. Removal of solvent *in vacuo* provided a white solid which was collected by filtration and washed with n-hexane (3 x 50cm^3) then pumped dry for 1h (Yield 14.12g, 65.1%). The product was recrystallised from MeCN as colourless air-moisture sensitive crystals of diffraction quality. A structural determination was not performed as neither cation nor anion structures are novel species.

6.6.2: Reaction of $SnCl_2$ with $SbCl_5$ (II)

A solution of $SbCl_5$ (5cm^3, 38.45mmol) in MeCN (50cm^3) was added dropwise to a chilled, stirred solution of $SnCl_2$ (3.64g, 19.2mmol). The resulting colourless solution was stirred for 24h at RT under N_2. Solvent removal *in vacuo* provided a white solid which was collected by filtration, washed with n-hexane (3 x 50cm^3) and pumped dry for 3h (Yield 13.5g, 68%). Recrystallisation from MeCN gave very air-moisture sensitive colourless crystals. Attempts to mount these crystals in 0.25mm diameter Lindemann tubes failed due to their highly air-moisture sensitive nature; hydrolysis

occurred during manipulation of single crystals under sodium-dried nujol prior to their insertion into the Lindemann tube.

6.1.3: Reaction of $SnCl_4$ with $SbCl_5$ (III)

A solution of $SbCl_5$ ($5.54cm^3$, 42.67mmol) in MeCN ($50cm^3$) was added dropwise to a chilled (0^oC) and stirred solution of $SnCl_4$ ($5.00cm^3$, 42.72mmol) in MeCN ($50cm^3$). The resulting pale yellow solution was allowed to warm to room temperature and stirred for a further 24h under nitrogen. Removal of solvent *in vacuo* gave an off-white solid which was collected by filtration. The resultant solid was washed with n-hexane (3 x $50cm^3$) and pumped dry for 2h (Yield 17.92g, 75%). The product was recrystallised from MeCN affording colourless needle crystals of diffraction quality. Attempts to mount a single crystal in a 0.25 mm diameter Lindemann tube under argon for diffraction purposes failed due to the highly air-moisture sensitive nature of the product.

6.1.4: Reaction of $SnCl_4$ with $2SbCl_5$ (IV)

A solution of $SbCl_5$ ($1.73cm^3$, 13.3mmol) in MeCN ($50cm^3$) was added dropwise to a chilled (0^oC) and stirred solution of (III) (9.09g, 13.3mmol) in MeCN ($100cm^3$). The resulting pale yellow solution was allowed to warm to room temperature and stirred for a further 24h under nitrogen. Removal of solvent *in vacuo* gave an off-white solid which was collected by filtration. The resultant solid was washed with n-hexane (3 x $50cm^3$) and pumped dry for 3h (Yield 9.5g, 70%). Recrystallisation from MeCN gave very unstable colourless crystals of diffraction quality. Attempts to mount a single crystal in a 0.25 mm diameter Lindemann tube under argon for

diffraction purposes failed due to their extremely unstable nature.

6.1.5: Reaction of $InCl_3$ with $SbCl_5$ (V)

A solution of $InCl_3$ (1.15g, 5.2mmol) in MeCN($100cm^3$) was obtained by direct Soxhlet extraction under N_2. This solution was allowed to cool to RT and chilled (0°C), to it a solution of $SbCl_5$ ($0.67cm^3$, 5.2mmol) in MeCN ($50cm^3$) was added. The resulting pale yellow solution was allowed to warm to RT and stirred for a further 24h. Solvent removal *in vacuo* gave a white solid which was collected by filtration, washed with n-hexane (3 x $50cm^3$) and pumped dry for 2h (Yield 2.66g, 75%). Recrystallisation from MeCN gave colourless air-moisture sensitive crystals which were not of diffraction quality.

6.1.6: Reaction of $InCl_3$ with $2SbCl_5$

A solution of $InCl_3$ (2.1g, 9.49mmol) in MeCN ($100cm^3$) was obtained by direct Soxhlet extraction under N_2. This solution was allowed to cool to RT and chilled (0°C). To it a solution of $SbCl_5$ ($2.46cm^3$, 18.98mmol) in MeCN ($50cm^3$) was added. The resulting pale yellow solution was allowed to warm to RT and stirred for a further 24h under N_2. Solvent removal *in vacuo* gave a white solid which was collected by filtration, washed with n-hexane(3 x $50cm^3$) and pumped dry for 2h (Yield 6.73g, 52%; based on $[In(MeCN)_6][SbCl_6]_3$). m.p.197-198°C. Recrystallisation from MeCN gave colourless air-moisture sensitive crystals which were not of diffraction quality.

6.1.7: Reaction of $InCl_3$ with $3SbCl_3$ (VI)

A solution of $InCl_3$ (1.9g, 8.59mmol) in MeCN ($100cm^3$) was obtained by direct Soxhlet extraction under N_2. This solution was allowed to cool to RT and chilled(0°C). To it a solution of $SbCl_5$ ($3.35cm^3$, 25.7mmol) in MeCN ($50cm^3$) was added. The resulting pale yellow solution was allowed to warm to RT and stirred for a further 24h. Solvent removal *in vacuo* gave a white solid which was collected by filtration, washed with n-hexane (3 x $50cm^3$) and pumped dry for 2h (Yield 8.4g, 71%). Recrystallisation from MeCN gave colourless air-moisture sensitive crystals which were not of diffraction quality.

6.1.8: Reaction of $ScCl_3$ with $SbCl_5$ (VII)

A solution of $SbCl_5$ ($5cm^3$, 38.45mmol) in MeCN ($100cm^3$) was added dropwise to a chilled (0°C) and stirred solution of $ScCl_3$ (2.72g, 18mmol) in MeCN ($100cm^3$). The resulting pale yellow solution was allowed to warm to room temperature and stirred for a further 24h under nitrogen. Removal of solvent *in vacuo* gave an off-white oily product which was washed with n-hexane (4 x $50cm^3$), left to stand overnight in n-hexane ($100cm^3$) and pumped dry for 3h to give a sticky white solid. Repeated washing with n-hexane and final drying *in vacuo* for 4h gave an extremely air-moisture sensitive product of low yield.

6.1.9: Reaction of YCl_3 with $SbCl_5$ (VIII)

A solution of $SbCl_5$ ($5cm^3$, 38.45mmol) in MeCN($100cm^3$) was added dropwise to a chilled (0°C) cloudy solution of YCl_3 (3.18g, 16.3mmol) in MeCN ($100cm^3$). After approximately 3h the cloudy yellow solution became clear yellow and was allowed to stir for a further 24h under nitrogen at RT. Removal

of solvent *in vacuo* gave a white solid which was collected by filtration, washed with n-hexane (3 x 50cm^3) and pumped dry for 3h (Yield 6.75g, 63%). This air-moisture sensitive solid could not be obtained as crystalline material.

6.1.10: Reaction of $LaCl_3$ with $SbCl_5$ (IX)

A solution of $SbCl_5$ (5cm^3, 38.45mmol) in MeCN (100cm^3) was added dropwise to a chilled (0°C) cloudy solution of $LaCl_3$ (4.36g, 17.8mmol) in MeCN (100cm^3). The resulting cloudy yellow solution was allowed to stir under N_2, full dissolution of $LaCl_3$ occurred to give a clear yellow solution, which was allowed to stir for a further 24h under nitrogen at RT. Removal of solvent *in vacuo* gave a white solid which was collected by filtration, washed with n-hexane (3 x 50cm^3) and pumped dry for 3h (Yield 8.1g, 65%). The resulting air-moisture sensitive solid could not be obtained as crystalline material using standard recrystallisation techniques.

Table 6.1.1 shows the data obtained for the series of complexes I-IX.

Table 6.1.1 Part 1
Microanalytical and Principal Spectroscopic Data for Antimonate(v) Salts

Compound	Colour	M.p.(°C)	Analyses:% found (calc.)				
			C	H	N	Cl	Sb
$[Mg^{II}(MeCN)_6][SbCl_6]_2$	White	-	15.33	1.91	8.92	45.50	25.92
(I)			(15.34)	(1.93)	(8.95)	(45.28)	(26.03)
$[Sn^{II}(MeCN)_6][SbCl_6]_2$	White	115-118	13.07	1.70	7.59	41.83	23.55
(II)			(13.93)	(1.74)	(8.12)	(41.45)	(24.01)
$[Sn^{IV}Cl_3(MeCN)_3][SbCl_6]$	White	74-76	11.8	1.7	6.2	46.7	17.83
(III)			(10.6)	(1.3)	(6.2)	(46.7)	(17.44)
$[SnCl_2(MeCN)_4][SbCl_6]_2 .CH_3CN$	White	96-99	11.18	1.53	6.47	48.2	23.51
(IV)			(11.28)	(1.41)	(6.58)	(48.5)	(23.81)
$[In^{III}Cl_2(MeCN)_4][SbCl_6]$	White	167-168	13.96	1.81	8.19	41.62	17.75
(V)			(14.03)	(1.75)	(8.18)	(41.45)	(17.79)
$[In(MeCN)_6][SbCl_6]_3$	White	196-197	10.68	1.34	6.12	46.16	26.77
(VI)			(10.55)	(1.31)	(6.15)	(46.77)	(26.39)
$[Sc^{III}Cl_2(MeCN)_4][SbCl_6]$	White	180-185	12.89	1.98	7.51	44.09	
(VII)			(15.62)	(1.95)	(9.11)	(46.16)	
$[YCl_2(MeCN)_4][SbCl_6].1.5CH_3CN$	White	229-231	18.19	2.38	10.65	37.0	
(VIII)			(18.33)	(2.29)	(10.69)	(39.4)	
$[LaCl_2(MeCN)_4][SbCl_6]$	White	198-200	17.7	2.0	7.4	39.43	
(IX)			(13.6)	(1.7)	(7.9)	(40.04)	

Table 6.1.1 Part 2

Compound	^{121}SbNMR δ(ppm)	$W_{1/2}$(Hz)	Electronic λ_{max} (cm^{-1})	Infrared (cm^{-1}) ν(M-Cl) [450-200]	ν(CN)
I	-0.12	153	37 037	407 s,sh 346 vs,br	2320 2290
II	-0.16	172	36 630 45 662	406w 340vs,br	2316 2286 2256 2244
III	-0.41	168	37 037 44 843	410sh 373s 342vs,br 310m 265w	2322 2295 2254 2244
IV	-0.22	171	36 900 46 511	410w 382s 342vs,br 308 vw 280w	2312 2280 2248
V	-0.15	162	36 900	396m 342vs,br 297m,br	2318 2292
VI	-0.16	190	37 037	396w 348vs,br 292w,br	2316 2292 2248
VII	-0.54	192	37 037	415s,sh 350vs,br 310(sh)	2320 2290
VIII	-0.55	192	37 037	400m,sh 345vs,br 265m,br	2315 2290 2260
IX	-0.45	287	37 037	400m,sh 350vs,br 290vw 238w	2320 2287

Several attempts were made to isolate $Ti^{(III)}$ and $Ti^{(IV)}$ hexachloroantimonate salts as follows:

6.1.11: Reaction of $TiCl_3$ with $SbCl_5$ (X)

A solution of $TiCl_3$ (2.69g, 17.4 mmol) in MeCN (70cm^3) was obtained by direct Soxhlet extraction. The resultant deep blue solution was allowed to cool to room temperature, then chilled (0°C), a small portion was removed for analytical purposes. $TiCl_3.3MeCN$ m.p.137-138°C Found: Ti, 17.36% $C_6H_9N_9Cl_3Ti$ calc Ti, 17.27; ν_{max} (CN) 2325 and 2292 cm^{-1} (lit., [257] 2305 and 2280 cm^{-1}); λ_{max}. (MeCN) 14 705 and 17 182cm^{-1} (lit., [257] 14 700(sh) and 17 200 cm^{-1}). To the remaining chilled solution a solution of $SbCl_5$ (2.26cm^3, 17.4mmol) in MeCN (30cm^3) was added dropwise. Upon addition of $SbCl_5$ the solution changed from a deep blue to a green colour. The resulting solution was allowed to warm to room temperature and stirred for a further 3h. Removal of solvent *in vacuo* provided a green solid which was collected by filtration. The resultant solid was washed with benzene (3x50cm^3) and then n-hexane (3x50cm^3) and pumped dry for 2h. (Yield 6.44g, 60%). The product was recrystallised from MeCN affording very air-moisture sensitive green crystals, m.p. 85-87°C (Found: C, 15.88; H, 2.34; N, 5.90; Cl, 46.14; Ti, 7.41%. $C_8H_{12}N_4Cl_8TiSb$ requires C, 15.55; H, 1.94; N, 9.07; Cl, 45.94; Ti, 7.75%); ν_{max} (CN) 2320, 2290, and 2250 cm^{-1}; ν_{max} (M-Cl) 422s,sh, 342vs,br, 275w; λ_{max} (MeCN) 36 900, 20 000 and 15 384 cm^{-1}.

6.1.12: Reaction of $TiCl_4$ with excess $SbCl_5$ (XI)

A solution of $SbCl_5$ (3.0cm^3, 23.1mmol) in MeCN (50cm^3) was added dropwise to a chilled, stirred solution of $TiCl_4$ (2.51cm^3, 22.8mmol). The resultant yellow solution was stirred

for 24h at room temperature, solvent removal *in vacuo* provided a bright yellow solid which was collected by filtration and pumped dry for 3h. Recrystallisation from MeCN yielded bright yellow crystals, m.p 96-97°C (lit.,[199] 95-96°C).

A solution of $[TiCl_3(MeCN)_3][SbCl_6]$ (10.2g, 16.6mmol) in MeCN (50cm^3) was added dropwise to a chilled, stirred solution of $SbCl_5$ (3.9cm^3, 30mmol) in MeCN (50cm^3). The resultant orange-yellow solution was allowed to warm to room temperature and stirred for a further 24h. Solvent removal *in vacuo* provided a yellow solid which was collected by filtration. The solid was washed with n-hexane (3x50cm^3) and pumped dry for 3h (Yield 8.7g, 55%). M.p. 88-90°C (Found: C, 10.4; H, 1.5; N, 5.89; Cl, 51.8; Ti, 4.8; Sb, 25.1%. $C_8H_{12}N_4Cl_{14}TiSb_2$ requires C, 10.8; H, 1.3; N, 5.9; Cl, 52.1; Ti, 5.0; Sb, 25.5); ν_{max}. (CN) 2322 and 2295 cm^{-1}; ν_{max}. (M-Cl) 432vs, 412w, 375sh, 352sh, and 344 vs,br; δ_{Sb}(MeCN)-0.48 (s, $SbCl_6^-$)$W_{1/2}$, 177; λ_{max} (MeCN) 37 453 cm^{-1}. Recrystallisation from MeCN afforded yellow crystals, structural determination of which gave $[TiCl_3(MeCN)_3][SbCl_6].CH_3CN$ and a mass of green crystals of poor quality. m.p.84-86°C; ν_{max}(CN) 2320, 2292 and 2252 cm^{-1}; ν_{max} (M-Cl) 424 s,sh, 400w, and 340vs,br cm^{-1}; λ_{max} (MeCN) 37 037 and 14 705 cm^{-1}.

6.2. Experimental Section For Chapter 3

6.2.1. $2MgCl_2.4BiCl_3.12MeCN$ (XII)

An intimate mixture of $BiCl_3$ (19.55g, 61.7mmol) and $MgCl_2$ (3.0g, 31.7mmol) was extracted with hot MeCN (150cm^3) using standard Soxhlet apparatus under nitrogen. The resulting clear colourless solution was concentrated to half its volume and placed in a refrigerator overnight, whereupon colourless needle crystals of the title compound separated. These were filtered and washed with n-hexane (2 x 25cm^3). Yield (19.4g, 64.8%).

6.2.2. $3MgCl_2.4BiCl_3.18MeCN$ (XIII)

An intimate mixture of $BiCl_3$ (3.6g, 11.6mmol) and $MgCl_2$ (0.8g, 8.7mmol) was extracted with hot MeCN (150cm^3) using standard Soxhlet apparatus under nitrogen. Removal of approximately half the solvent *in vacuo* gave a colourless clear solution, which was placed in a refrigerator overnight. This provided a matte of colourless fibrous crystals of the title compound. These were filtered, washed with n-hexane (2 x 25cm^3) and dried by pumping *in vacuo* at room temperature for 2h. Yield (4.1g, 62.2%) Table 6.2.1 shows the spectroscopic and analytical data obtained for these complexes.

Table 6.2.1. Analytical and Principal Spectroscopic Data for (XII) and (XIII)

Complex	(XII)	(XIII)
Colour	White	White
m.p. (°C)	127-128	decomp (>208)
Analyses (%)		
C, H, N, Bi	14.7, 1.9 , 8.6 , 42.1	19.1, 2.8, 10.6, 35.4
found (calc)	(14.8)(1.9)(8.6)(42.9)	(18.9)(2.4)(11.0)(36.5)
Electronic	30 959	48 500 (sh)
λ_{max} (cm^{-1})		43 600 (sh)
		31 055
Infra-red		
ν(CN) cm^{-1}	2322	2320
	2290	2289
[450-200] cm^{-1}	405 vs	401 vs
	340-350 vs, br	335-345 s, br
	276 m	273 (sh)
	250-255 s, br	230-240 s, br
Conductivity	207	251.8
Λ_m (Scm^2mol^{-1})		

6.2.3. Reaction of other Stoichiometric Ratios of $MgCl_2$ with $BiCl_3$

Intimate mixtures of $BiCl_3$ and $MgCl_2$ in varying molar ratios were extracted with hot MeCN ($150cm^3$) using standard Soxhlet apparatus under nitrogen, as before. The following stoichiometric ratios of $MgCl_2$: $BiCl_3$ were used (1:4, 1:3, 2:3, and 1:1) in the Soxhlet filter stick. In reactions where a large excess of $BiCl_3$ was used ie 1:4, and 1:3 unreacted $BiCl_3$ was left on the sides of the Soxhlet flask. The remaining colourless solution was decanted and reduced to approximately half its volume *in vacuo* and placed in a refrigerator overnight, whereupon colourless crystals separated. These were filtered, washed with n-hexane (2 x $25cm^3$) and dried by pumping *in vacuo* at room temperature for 2h. (50-55% yields were obtained).

6.2.4. $BiCl_3.SbCl_5.4MeCN$ (XIV)

$SbCl_5$ ($1.26cm^3$, 9.6mmol) in MeCN ($20cm^3$) was added dropwise to an ice-cold solution of $BiCl_3$ (30g, 9.6mmol) in MeCN ($50cm^3$). The resulting pale yellow solution was stirred at room temperature for 12h. Removal of solvent *in vacuo* provided a white solid which was collected by filtration, washed with n-hexane (2 x $25cm^3$) and pumped dry for 1h. The white solid was recrystallised from $MeCN/CH_2Cl_2$ as colourless crystals of poor definition (Yield 6.11g, 81.3%). See Table 6.2.2.

6.2.5. $BiCl_3.3SbCl_5.8MeCN$ (XV)

$SbCl_5$ ($1.85cm^3$, 14.3 mmol) in MeCN ($30cm^3$) was added dropwise to an ice-cold stirred solution of $BiCl_3$ (1.5g, 4.75mmol) in MeCN ($50cm^3$). The resulting pale yellow solution was stirred at room temperature for 12h. Removal of

solvent *in vacuo* provided a white solid which was collected by filtration, washed with n-hexane (3 x 25cm^3) and pumped dry for 3h. The white solid was recrystallised from MeCN as colourless crystals of poor definition (Yield 5.26g, 72%).

Table 6.2.2 Analytical and Principal Spectroscopic Data For (XIV) and (XV)

Complex	(XIV)	(XV)
Colour	White	White
m.p. (°C)	75-76	134-136
C, H, N, Sb, Bi	12.5, 1.5, 7.4, 16.7, 26.2	12.0, 1.65, 6.93,23.2,13.2
found(calc)	(12.3) (1.5)(7.2)(15.7)(26.8)	(12.4,1.6, 7.2, 23.7, 13.5)
^{121}Sb NMR		
δ(ppm),$W_{1/2}$(Hz)	0.05 182	-0.16 190.5
Electronic	44250, 37037,	44843, 35714
λ_{max} (cm^{-1})	31545 (sh)	
Infra-red	2300	2296
ν(CN) cm^{-1}	2260	2276
		2258
[450-200] cm^{-1}	348 vs, br	340 vs, br
	280 m	280 m, sh
	250-255 m, br	240-245 m, br
Conductivity	142.18	245.6
Λ_o (Scm^{2}mol^{-1})		

6.2.6. Reaction of $TiCl_4$ with $BiCl_3$ in MeCN (XVI)

$TiCl_4$ ($2cm^3$, 18.2 mmol) in MeCN ($50cm^3$) was added dropwise to an ice-cold solution of $BiCl_3$ (5.8g, 18.2mmol) in MeCN ($100cm^3$). The resulting bright yellow solution was stirred at room temperature for 24h under nitrogen. Removal of solvent *in vacuo* provided a bright yellow solid which was collected by filtration, washed with n-hexane (3 x $25cm^3$) and pumped dry for 2h. Yield (7.9g, 62%) (Found: C, 16.41; H, 2.13; N, 9.41; Ti, 7.8; Bi, 29.1%; $C_{10}H_{15}N_5Cl_7BiTi$ requires C, 16.9; H, 2.1; N, 9.85, Ti, 7.62; Bi, 29.43%); ν_{max} 2305, 2300, 2295, 2290 (MeCN), 385vs,br, 320 and 280, m,br cm^{-1} (Nujol); λ_{max} (MeCN), 40 000 and 30 769 cm^{-1}. The yellow solid was recrystallised from MeCN as yellow crystals, m.p. 158-160°C (Found: Ti, 17.2; Cl, 52.8%; calc. for $C_4H_6N_2TiCl_4$; Ti, 17.6; Cl, 52.19); λ_{max} (MeCN), 45 662, 39 682, and 33 557 cm^{-1}; ν_{max} 2310, 2300, 2290, 2280 (MeCN), 380vs, br, 315m, 270m,br cm^{-1} (Nujol).

6.2.7. Reaction of $TiCl_3$ with $BiCl_3$ in acetonitrile (XVII)

A solution of $TiCl_3$ (1.93g, 12.5mmol) in MeCN ($50cm^3$) was obtained by Soxhlet extraction, and added dropwise to an ice-cold solution of $BiCl_3$ (395g, 12.5mmol) in MeCN ($100cm^3$). The resulting purple solution was stirred at room temperature for 24h under nitrogen. Solvent removal *in vacuo* provided a light purple solid which was collected by filtration, washed with n-hexane (3 x $25cm^3$) and pumped dry for 3h. Crystalline material could not be obtained. (Yield 5.1g, 65%) m.p. 99-102°C. (Found: C, 15.9; H, 2.2; N, 9.0; Ti, 7.4; Bi, 32.3%; $C_8H_{12}N_4Cl_6BiTi$ requires C, 15.15; H, 1.90; N, 8.83; Ti, 7.55; Bi, 32.9%). ν_{max} 2305, 2290 (MeCN), 420 s, sh, 390 s, sh, 330 s, sh

and 270m, br cm^{-1} (Nujol); λ_{max} (MeCN) 31 515 and 17 029 cm^{-1}.

6.2.8. Reaction of VCl_3 with $BiCl_3$ in MeCN (XVIII)

A solution of VCl_3 (3g, 19.1mmol) in MeCN (50cm^3) was added dropwise to an ice-cold solution of $BiCl_3$ (6.0g, 19.1mmol) in MeCN (100cm^3). The resulting purple solution was stirred at room temperature for 24h under nitrogen. solvent removal *in vacuo* provided a purple solid which was collected by filtration, washed with n-hexane (3 x 25cm^3) and pumped dry for 3h. The purple solid could not be obtained as crystalline material (Yield 7g, 58%) m.p. 130°C (decomp). (Found: C, 13.9; N, 1.93; N, 8.0; Bi, 32.12%; $C_8H_{12}N_4Cl_6BiV$ requires C, 15.0; H, 1.9; N, 8.7; Bi, 32.8%). ν_{max} 2320, 2290, 2245 (MeCN), 435m, sh, 415w, 378m, sh, 355w, 330w, 285w, 260m, br cm^{-1} (Nujol); λ_{max} (MeCN) 31 017, 20 391 and 17 857 (sh) cm^{-1}.

6.2.9. Reaction of $CrCl_3$ with $BiCl_3$ in MeCN (XIX)

A solution of $CrCl_3$ (2g, 12.62mmol) in MeCN (50cm^3) was added dropwise to an ice-cold solution of $BiCl_3$ (4g, 12.68 mmol) in MeCN (100cm^3). The resulting solution was stirred at room temperature for 24h under nitrogen. Solvent removal *in vacuo* provided a grey-purple coloured solid which was collected by filtration, washed with n-hexane (3 x 25cm^3) and pumped dry for 3h. Crystalline material could not be obtained. (Yield 5.6g, 65.4%) m.p. 90-92°C. (Found: C, 17.4; H, 2.29; N, 95; Bi, 31.5%; $C_{10}H_{15}N_5Cl_6BiCr$ requires C, 17.6; H, 2.21; N, 10.3; Bi, 30.8%). ν_{max} 2315, 2300, 2260 (MeCN) 440 m, sh, 420 m, sh,

390 s, sh, 370 s, sh, 265 m, br cm^{-1} (Nujol); λ_{max} (MeCN) 35 112, 31 585, 22 222, 16 356 cm^{-1}.

6.2.10. Reaction of $FeCl_3$ with $BiCl_3$ in MeCN (XX)

A red-orange solution of $FeCl_3$ (3.35g, 20.6mmol) in MeCN ($50cm^3$) was obtained by Soxhlet extraction under nitrogen and added dropwise to an ice-cold solution of $BiCl_3$ (6.51g, 20.6mmol) in MeCN ($100cm^3$). This became a red-brown colour which was stirred at room temperature for 24h under nitrogen. Solvent removal *in vacuo* provided an orange coloured solid, which was collected by filtration, washed with n-hexane (3 x $25cm^3$) and pumped dry for 3h. Crystalline material could not be obtained. (Yield 8.9g, 67.3%) m.p. 54-56°C. (Found: C, 10.61; H, 1.49; N, 6.02, Bi, 33.1%; $C_8H_{12}N_4Cl_6BiFe$ requires C, 14.9; H, 1.87; N, 8.72; Bi, 32.5%). ν_{max} 2305, 2290, 2260 (MeCN) 385vs, br, 280m, br, 250 m, br cm^{-1} (Nujol); λ_{max} (MeCN) 47 778, 41 946, 35 087(sh), 32 154 and 28 011 cm^{-1}.

6.2.11. Reaction of $SnCl_4$ with $BiCl_3$ in MeCN (XXI)

A solution of $SnCl_4$ ($2cm^3$, 17.1mmol) in MeCN ($50cm^3$) was added dropwise to an ice-cold solution of $BiCl_3$ (5.4g, 17.1mmol) in MeCN ($100cm^3$). The resulting colourless solution was stirred at room temperature for 24h under nitrogen. Solvent removal *in vacuo* provided a white solid, which was collected by filtration, washed with n-hexane (3 x $25cm^3$) and pumped dry for 3h (Yield 8.6g, 68%). (Found: C, 12.52; H, 1.6; N, 7.25; Bi, 28.4%; $C_8H_{12}N_4Cl_7BiSn$ requires C, 12.97; H, 1.62; N, 7.56; Bi, 28.27%); ν_{max}, 2310, 2280 (MeCN) 410w, 400w, 395w, 365m, 340s, br, 305m, 250m cm^{-1} (Nujol); λ_{max} (MeCN) 34 722, 31 347 cm^{-1}. The white solid was recrystallised from MeCN affording colourless crystals, m.p. 95-97°C; ν_{max} 2310, 2285

(MeCN), 410w, 395w, 365m, 340 s, br, 305m cm^{-1} (Lit [259] ν_{max} 397w, 393w, 367s, 333-345vs, 305m cm^{-1}).

6.3. Experimental Section for Chapter 4

6.3.1: Oxidation of As(III) to As(V)

6.3.1.1: Me_4NCl Reaction (XXII)

Me_4NCl (5.28g, 48.23mmol) and $AsCl_3$ (4.1cm^3, 48.9mmol) were dissolved in MeCN (300cm^3) and the solution chilled to 0°C. Chlorine gas was passed into the colourless solution until it became saturated with the gas and turned orange. The Me_4NCl dissolved fully in MeCN to give an orange solution. Cl_2 was periodically passed into the solution to maintain a saturated environment, which was then stirred for 24h under N_2 at RT. Removal of solvent and excess Cl_2 *in vacuo* gave a yellow coloured solid which was collected by filtration, washed with n-hexane (3 x 50cm^3) and pumped dry rapidly. Recrystallization from MeCN gave a semi-crystalline yellow solid (Yield 12g, 69%) m.p. 230-233°C with decomposition. (Found: Cl, 59.12; As, 20.42%; $C_4H_{12}NCl_6As$ requires Cl, 58.82; As, 20.71%); ν_{max} 387m,sh and 350vs, br cm^{-1} (Nujol); λ_{max} (MeCN) 38 759, 37 453(sh) and 36 900 cm^{-1}; Λ_m=99.14 Scm^2mol^{-1} at 25.0 ± 0.1°C in DMF solution.

6.3.1.2: $MgCl_2$ Reaction (XXIII)

Chlorine gas was passed into a chilled (0°C) solution of $AsCl_3$ (11.45cm^3, 136.7mmol) in MeCN (200cm^3) until the solution became saturated with gas. A solution of $MgCl_2$ (6.51g, 68.36mmol) in MeCN (100cm^3) was obtained by direct Soxhlet extraction, then added dropwise under N_2 to the chlorine saturated solution of $AsCl_3$ in MeCN. Immediate precipitation of

a yellow-orange coloured solid occurred. Chlorine gas was periodically passed into the orange solution, which was allowed to warm to RT and stirred for a further 24h under N_2. Removal of solvent and excess Cl_2 *in vacuo* gave a pale yellow coloured solid, which was collected by filtration, washed with n-hexane (3 x 50cm^3) and pumped dry rapidly. Recrystallization from MeCN gave a semi-crystalline material (Yield 40g, 69%) m.p. 66-68°C. (Found: Cl, 51.1; As, 17.93%; $C_{12}H_{18}N_6Cl_{12}As_2$ requires Cl, 50.312; As, 17.72%); ν_{max} 2316, 2286 (MeCN), 406m (CCN), 385s,sh and 345vs,br cm^{-1} (MCl) Nujol; λ_{max} 36 764, 37 453(sh) and 38 759cm^{-1}; Λ_m=157.67 Scm^{2}mol^{-1} at 25 ± 0.1°C in DMF solution.

6.3.1.3: $ZnCl_2$ Reaction (XXIV)

Chlorine gas was passed into a chilled (0°C) solution of $AsCl_3$ (10.12cm^3, 120.7mmol) in MeCN (200cm^3) until the solution became saturated with gas. To this a solution of $ZnCl_2$ (8.23g, 60.3mmol) in MeCN (50cm^3) was added dropwise under N_2. Chlorine gas was periodically passed into the resulting yellow solution to maintain a level of saturation, which was then allowed to warm to room temperature and stirred for a further 24h under N_2. Solvent removal *in vacuo* afforded a white solid which was collected by filtration, washed with n-hexane (3 x 50cm^3) and pumped dry rapidly. The white solid was not obtained as crystalline material. (Yield 9.21g, 70%). m.p. 95-98°C. (Found: Cl, 32.51%; $C_4H_6N_2Cl_2Zn$ requires Cl, 32.48%); ν_{max} 2316, 2284 (MeCN), 402m,sh (CCN), 383m, 347s,br, 310s, br and 245m,br cm^{-1} (MCl).

6.3.1.4: $TiCl_4$ Reaction (XXV)

Chlorine gas was passed into a chilled (0°C) solution of $AsCl_3$ (3.82cm^3, 45.6mmol) in MeCN (200cm^3) until the solution became saturated with gas. To this a solution of $TiCl_4$ (5.0cm^3, 45.6mmol) in MeCN (100cm^3) was added dropwise under N_2. Chlorine gas was periodically passed into the resulting bright orange solution to maintain a level of saturation, which was then allowed to warm to room temperature and stirred for a further 24h under N_2. Solvent removal *in vacuo* afforded a bright yellow solid which was collected by filtration, washed with n-hexane (3 x 50cm^3) and pumped dry rapidly. Recrystallization from MeCN afforded bright yellow crystals (Yield 7.4g, 60%). m.p. 150-152°C. (Found: Cl, 52.61; Ti, 17.81%; $C_4H_6N_2Cl_4Ti$ requires Cl, 52.19; Ti 17.62%); ν_{max} 2310, 2300, 2280 and 2270 cm^{-1}(MeCN), 410m, 380vs, br, and 315m,sh cm^{-1} (Nujol); λ_{max}(MeCN) 44 444, 37 037 and 32 679 cm^{-1}.

6.3.1.5: $SnCl_4$ Reaction (XXVI)

Chlorine gas was passed into a chilled (0°C) solution of $AsCl_3$ (3.6cm^3, 42.9mmol) in MeCN (200cm^3) until the solution became saturated with gas. To this a solution of $SnCl_4$ (5.0cm^3, 42.7mmol) in MeCN (50cm^3) was added dropwise under N_2. The resulting colourless solution was periodically saturated with Cl_2 to give an orange coloured solution, which was then allowed to warm to room temperature and stirred for a further 24h under N_2. Solvent removal *in vacuo* afforded a white solid which was collected by filtration, washed with n-hexane (3 x 50cm^3) and pumped dry rapidly. Recrystallization from MeCN afforded colourless crystals (Yield 8g, 55%). m.p. 110-112°C.(Lit,[291] 112-114°C). (Found: Cl, 41.7%; $C_4H_6N_2Cl_4Sn$

requires Cl, 41.4%); ν_{max} 2312, 2280 (MeCN), 410m, sh, 392w 366s, 334vs, br and 303s cm^{-1} (Nujol).

6.3.2: Sb(III) as a Lewis Acid

6.3.2.1: Reaction of $TiCl_4$ with $SbCl_3$ (XXVII)

A solution of sublimed $SbCl_3$ (5.6g, 24.6mmol) in MeCN ($100cm^3$) was added dropwise to an ice-cold solution of $TiCl_4$ ($1.35cm^3$, 12.3mmol) in MeCN ($100cm^3$). The resultant bright yellow solution was allowed to warm to room temperature and stirred for a further 24h under N_2. Solvent removal in vacuo afforded a bright yellow solid which was collected by filtration, washed with n-hexane (3 x $50cm^3$) and pumped dry for 2h. (Yield 11.03g, 72%; based on $TiCl_4.SbCl_3.5MeCN$). (Found: Ti, 7.62; Sb, 19.77; Cl, 39.2%; $C_{10}H_{15}N_5Cl_7TiSb$ requires Ti, 7.68; Sb, 19.55; Cl, 39.84%); ν_{max} 2310, 2300, 2280 and 2270 (MeCN), 420vw, 402vw, 378vs,br, 352m,br, 316vs,br cm^{-1} (Nujol); λ_{max}(MeCN) 45 871 and 38 610 cm^{-1}. Recrystallization from MeCN gave bright yellow crystals m.p. 158-160°C.(Found: Ti, 17.51; Cl, 51.95%; $C_4H_6N_2Cl_4Ti$ requires Ti, 17.62; Cl, 52.19%); ν_{max} 2310, 2300, 2280, 2280 (MeCN), 378vs,br, 316s,br cm^{-1} (Nujol); λ_{max}(MeCN) 45 871 and 38 610 cm^{-1}.

6.3.2.2: Reaction of $TiCl_3$ with $SbCl_3$ (XXVIII)

A solution of $TiCl_3$ (4.76g, 30.85mmol) in MeCN ($100cm^3$) was obtained by direct Soxhlet extraction. The resulting deep blue solution was filtered and allowed to cool to RT. This solution was chilled (0°C) and to it was added a solution of sublimed $SbCl_3$ (14.07g, 61.6mmol) in MeCN ($100cm^3$). The resulting purple coloured solution was allowed to warm to RT and stirred for a further 24h under N_2. Solvent removal *in vacuo* afforded a purple solid which was collected by filtration,

washed with n-hexane (3 x 50cm^3) and pumped dry for 2h. (Yield 13.56g, 70%; based on $TiCl_3.SbCl_3.6MeCN$), m.p. 52-54°C. Crystalline material could not be obtained. (Found: Ti, 7.03; Sb, 19.51; Cl, 33.29%; $C_{12}H_{18}N_6Cl_6TiSb$ requires Ti, 7.61; Sb 19.37; Cl, 33.85%); ν_{max} 2310, 2282 (MeCN), 409s,sh, 375s,br, 344w, 323s,br and 308w cm^{-1} (Nujol); λ_{max}(MeCN) 46 728, 40 485, 30 959, 20 080(sh) and 17 182 cm^{-1}.

6.3.2.3: Reaction of $FeCl_3$ with $SbCl_3$ (XXIX)

A solution of $FeCl_3$ (3.25g, 20.05mmol) in MeCN (100cm^3) was obtained by direct Soxhlet extraction. The resulting deep red solution was filtered and allowed to cool to RT. This solution was chilled (0°C) and to it was added a solution of sublimed $SbCl_3$ (4.87g, 21.3mmol) in MeCN (50cm^3). The resulting orange-red coloured solution became bright orange within minutes, continued stirring at RT under N_2 allowed observation of a further colour change to that of bright yellow. Solvent removal *in vacuo* afforded a yellow-orange coloured solid which was collected by filtration, washed with n-hexane (3 x 50cm^3) and pumped dry for 2h. The solid was washed with benzene (3 x 50cm^3) to remove further impurities, n-hexane (3 x 50cm^3) and pumped dry for 3h.(Yield 7.22g, 65%; based on $FeCl_3.SbCl_3.4MeCN$) m.p. 90-92°C. (Found: C, 17.12; H, 2.55; N, 10.75; Cl, 38.57; Sb, 21.25%; $C_8H_{12}N_4Cl_6SbFe$ requires C, 17.31; H, 2.16; N, 10.10; Cl, 38.37; Sb, 21.96%); ν_{max} 2320, 2295 (MeCN), 378vs,br, 350m and 250m,br cm^{-1} (Nujol); λ_{max}(MeCN) 41 841, 37 313(sh), 32 051 and 27 700 cm^{-1}.

6.3.2.4: Reaction of $InCl_3$ with $SbCl_3$ (XXX)

A solution of $InCl_3$ (1.54g, 6.94mmol) in MeCN (100cm^3) was obtained by direct Soxhlet extraction. The solution was

filtered and allowed to cool to RT and was chilled (0°C). To it a solution of sublimed $SbCl_3$ (4.2g, 18.4mmol) in MeCN (50cm^3) was added dropwise. The resulting cloudy white solution was allowed to warm to RT and stirred for a further 24h under N_2. Solvent removal *in vacuo* afforded a white oily product which was pumped dry for 3h, washed with n-hexane (5 x 50cm^3) and pumped dry for a further 3h to give a sticky white solid.(Yield 2.46g, 51%; based on $InCl_3.SbCl_3.6MeCN$). (Found: Cl, 30.45; Sb, 17.39%; $C_{12}H_{18}N_6Cl_6SbIn$ requires Cl, 30.59; Sb, 17.51%); ν_{max} 2312, 2284 (MeCN), 389m,sh, 312s,br, 290s, and 258s cm-1; λ_{max} (MeCN) 39 682 cm^{-1}.

6.3.2.5: Reaction of $SnCl_4$ with $SbCl_3$ (XXXI)

A solution of sublimed $SbCl_3$ (7.83g, 34.3mmol) in MeCN (50cm^3) was added dropwise to an ice-cold solution of $SnCl_4$ (2.0cm^3, 17.1mmol) in MeCN (100cm^3). The resultant colourless solution was allowed to warm to room temperature and stirred for a further 24h under N_2. Solvent removal in vacuo afforded a white solid which was collected by filtration, washed with n-hexane (3 x 50cm^3) and pumped dry for 2h. (Yield 15.46g, 65%; based on $SnCl_4.SbCl_3.5MeCN$). (Found: Sb, 17.5; Cl, 35.61%; $C_{10}H_{15}N_5Cl_7SnSb$ requires Sb, 17.55; Cl, 35.77%); ν_{max} 2304, 2276 (MeCN), 408w, 392w, 360m, 334vs,br, 304m cm^{-1} (Nujol). Recrystallization from MeCN gave colourless crystals, m.p. 92-94°C; (Found: Cl, 41.6%, $C_4H_6N_2Cl_4Sn$ requires Cl, 41.40%); ν_{max} 2304, 2276 (MeCN); 392w, 360m, 334vs,br, 304m cm^{-1} (Nujol). (Lit [259] ν_{max} 397w, 393w, 367s, 333-345vs, 305m cm^{-1}).

6.3.2.6: Reaction of $SbCl_5$ with $SbCl_3$ (XXXII)

A solution of sublimed $SbCl_3$ (11.72g, 51.37mmol) in MeCN (50cm^3) was added dropwise to an ice-cold solution of

$SbCl_5$ (6.7cm^3, 51.5mmol) in MeCN (100cm^3). The resultant pale yellow solution was allowed to warm to room temperature and stirred for a further 24h under N_2. Solvent removal in vacuo afforded a white solid which was collected by filtration, washed with n-hexane (3 x 50cm^3) and pumped dry for 2h. (Yield 24.85g, 70%; based on $SbCl_5.SbCl_3.4MeCN$). Extremely moisture sensitive colourless crystals were obtained from MeCN, but were not of diffraction quality, m.p. 140-142°C; (Found: Cl, 40.67; Sb, 34.76%; $C_8H_{12}N_4Sb_2Cl_8$ requires Cl, 41.03; Sb 35.23%); ν_{max} 2310, 2280 (MeCN), 346vs,br, 290w and 260s,br cm^{-1} (Nujol); λ_{max}(MeCN) 37 313 and 46 082(sh) cm^{-1}; $\delta(^{121}Sb)$(MeCN)-0.17 (1 Sb, s, $SbCl_6^-$), $W_{1/2}$=175 Hz.

6.3.2.7: Reaction of $BiCl_3$ with $SbCl_3$ (XXXIII)

A solution of $BiCl_3$ (6.58g, 20.86mmol) in MeCN (100cm^3) was obtained by direct Soxhlet extraction. The solution was allowed to cool to RT and was chilled (0°C). To this a solution of purified $SbCl_3$ (4.70g, 20.60mmol) in MeCN (50cm^3) was added dropwise, the resulting colourless solution solution was allowed to warm to RT and stirred for a further 24h under N_2. Solvent removal *in vacuo* afforded a white solid, which was collected by filtration, washed with n-hexane (3 x 50cm^3) and pumped dry for 2h. (Yield 9.88g, 60%; based on $BiCl_3.SbCl_3.6MeCN$) m.p. 67-69°C. This product could not be obtained as crystalline material. (Found: Cl, 26.5; Sb, 14.91; Bi, 26.32%; $C_{12}H_{18}N_6Cl_6BiSb$ requires Cl, 26.94; Sb, 15.4; Bi, 26.47%); ν_{max} 2300, 2260 (MeCN), 385m,sh, 350m,sh, 310s,br, 280s,br and 240s,br; λ_{max}(MeCN) 45 045(sh), 24 965 and 31 847(sh) cm^{-1}.

6.4.1. Experimental Section for Chapter 5.

6.4.1.1.$TiCl_4$ as a Lewis Acid.

Reaction of $TiCl_4$ with $MgCl_2$ in MeCN (XXXIV).

A solution of $MgCl_2$ (4.1g, 43.1mmol) in MeCN (150 cm^3) was obtained by direct Soxhlet extraction under N_2, this was added dropwise to a chilled (0°C) stirred solution of $TiCl_4$ (4.8cm^3, 43.7mmol) in MeCN. Immediate precipitation of a bright yellow solid occurred. The solution was allowed to warm to room temperature and stirred for a further 3h. Solvent removal *in vacuo* gave more yellow solid which was collected by filtration, washed with n-hexane (3 x 50cm^3) and pumped dry for 2h. Recrystallisation from MeCN gave a mass of air-moisture sensitive bright yellow needle crystals (structural determination pending). (Yield 16g, 70%). m.p. 145-146°C. (Found: C, 28.79; H, 3.85; N, 15.93; Ti, 9.21%; $C_{12}H_{18}N_6Cl_6TiMg$ requires C, 27.13; H, 3.42; N, 15.82; Ti, 9.02%). Flame test and Titan yellow test provide evidence for the presence of Mg. ν_{max} 2304, 2276 (MeCN), 412 m, sh, 402 w and 330 vs, br cm^{-1} (Nujol); λ_{max} (MeCN) 43 668 and 38 461 (sh) cm^{-1}. $\Lambda_m = 73$ Scm^2mol^{-1} at $10^{-2}M$ at 25.0 ± 0.1°C (Λ_o=110.76 Scm^2mol^{-1}).

6.4.2. Ti(IV) Cations

6.4.2.1. Reaction of $[TiCl_3(MeCN)_3][SbCl_6]$ with Me_4NCl (XXXV)

A solution of $[TiCl_3(MeCN)_3][SbCl_6]$ m.p.95-96°C (6.14g, 10mmol) in MeCN (100cm^3) was added dropwise to a chilled (0°C), stirred suspension of vacuum dried Me_4NCl (1.05g, 9.82mmol) in MeCN (100cm^3). The bright yellow suspension was allowed to warm to RT and left to stir for 24h under N_2. Full dissolution of Me_4NCl had occurred to give a clear bright yellow solution. Solvent removal *in vacuo* gave a bright yellow

solid which was collected by filtration, washed with n-hexane (3 x 50cm^3) and pumped dry for 2h. Recrystallization from MeCN gave bright yellow air-sensitive crystals, m.p. 158-160°C; (Found: Ti, 17.45; Cl, 52.6%; $C_4H_6N_2TiCl_4$ requires Ti, 17.62; Cl, 52.19%); ν_{max} 2310, 2300, 2290, 2285 (MeCN), 385 vs, br and 315 w cm^{-1} ν(TiCl); λ_{max} (MeCN) 45 248, 38 610 and 32 679 cm^{-1}. The mother liquor from this recrystallisation has λ_{max} 37 313 cm^{-1}; δ_{Sb} (CD_3CN) -0.1123 (1Sb, s, $SbCl_6^-$) $W_{1/2}$, 172 Hz.

6.4.2.2. Reaction of $[TiCl_3(MeCN)_3][SbCl_6]$ with PPh_3 (XXXVI)

A solution of PPh_3 (1.53g, 5.83mmol) in MeCN (100cm^3) was added dropwise to a chilled (0°C) solution of $[TiCl_3(MeCN)_3][SbCl_6]$ (3.6g, 5.83mmol) in MeCN (70cm^3). The resulting yellow solution was allowed to warm to RT and stirred for 24h under N_2. Solvent removal *in vacuo* gave a yellow solid which was collected by filtration, washed with n-hexane (3 x 50cm^3) and pumped dry for 2h.

6.4.2.3. Reaction of $[TiCl_3(MeCN)_3][SbCl_6]$ with PPh_3 (XXXVII)

A solution of PPh_3 (3.2g, 12.19mmol) in MeCN (100cm^3) was added dropwise to a chilled (0°C) solution of $[TiCl_3(MeCN)_3][SbCl_6]$ (3.73g, 6.1mmol) in MeCN (100cm^3). An orange coloured precipitate formed within minutes of addition of the phosphine. This suspension was allowed to warm to RT and stirred for 24h under N_2. Solvent removal *in vacuo* gave more orange solid which was collected by filtration, washed with n-hexane (3 x 50cm^3) and pumped dry for 3h. Yield 62%. This air-sensitive solid was not obtained as crystalline material, its solubility in common organic solvents (and concentrated mineral acids) was extremely low. m.p. 209-210°C. (Found: Ti, 3.9%; $C_{54}H_{45}Cl_9P_3TiSb$ requires Ti, 3.75%) spot test positive for

Sb; ν_{max} 1440 s, 1120 s, 1060 s, 1025 m, 995 m, sh, 750 m, sh, 730 s, sh, 690 m, sh, 537 s, sh, 455 w, sh, 437 m, sh, 360 w, 340 s, br and 280 m, br cm^{-1} (Nujol); λ_{max} (MeCN) 45 248, 39 062 and 36 764 cm-1; δ_H ($(CD_3)_2SO$) 7.75 (45H, m, Ph); Λ_m=171.59 Scm^2mol^{-1} at 10^{-3}M in DMSO solution.

6.4.2.4. Reaction of $[TiCl_3(MeCN)_3][SbCl_6]$ with PPh_3 (XXXVIII)

A solution of PPh_3 (3.44g, 13.14mmol) in MeCN ($100cm^3$) was added dropwise to a chilled (0°C) solution of $[TiCl_3(MeCN)_3][SbCl_6]$ (2.68g, 4.38mmol) in MeCN ($100cm^3$). An orange coloured precipitate formed within minutes of addition of the phosphine. This suspension was allowed to warm to RT and stirred for 24h under N_2. Solvent removal *in vacuo* gave more orange solid which was collected by filtration, washed with n-hexane (3 x $50cm^3$) and pumped dry for 3h. (Yield 65%) m.p. 208-210°C. This air-sensitive solid was not obtained as crystalline material, its solubility in common organic solvents and concentrated acids was very low. (Found: Ti, 4.2%; $C_{54}H_{45}Cl_9P_3TiSb$ requires Ti, 3.75%) spot test positive for Sb; ν_{max} 1435 s, 1120 s, 1050 s, 1020 m, 990 m, sh, 740 m, sh, 720 s, sh, 690 m, sh, 535 s, sh, 455 w, 435 m, sh, 360 w, 340 s, br and 280 m, br cm^{-1} (Nujol); λ_{max} (MeCN) 44 642 , 38 314 and 36 764 cm^{-1}; δ_H ($(CD_3)_2SO$) 7.75 (45H, m, Ph); $^{31}P\{^1H\}$ ($(CD_3)_2SO$) -0.4994 (3P, S *P* Ph_3); Λ_m=160.52 Scm^2mol^{-1} at 10^{-3}M in DMSO solution.

APPENDIX 1

Appendix 1

Conductivity Measurements

Conductivity measurements were carried using a Philips PW 9527 digital conductivity meter with solutions contained in a glass apparatus having a side-arm attachment incorporating the Pt electrodes. The sample, from a previously accurately weighed ampoule, was placed into the vessel under N_2. The ampoule was then reweighed, and the accurate mass of the sample determined by difference. The whole cell was weighed. Dry MeCN was introduced from the distillation unit. In cases where DMF and DMSO were used previously purified dried solvent was placed into the vessel under N_2. The weight of solvent was determined by difference. Full dissolution of the sample was ensured, which was then thermostatted at 25.0 ± 0.1°C for 30 minutes before the conductivity was measured. Series of conductivity readings were taken at increasing concentrations by removal of the solvent in vacuo and repeating the above procedure. This allowed application of the Onsager Law.

Prior calibration of the cell was effected with aqueous 0.1 and 0.2M potassium chloride solutions. The cell constant was measured as 0.254 cm^{-1} at 25.0 ± 0.1°C.

The most widely used expressions for comparison of electrolyte types are the equivalent and molar conductivity, Λ_e and Λ_m respectively. They are related to κ, the specific conductivity of a solution by the following expressions:

$$\Lambda_e = \kappa V_e \qquad \text{and} \qquad \Lambda_m = \kappa V_m$$

$$\Lambda_e = \kappa / c_e \qquad \text{and} \qquad \Lambda_m = \kappa / c_m$$

V_e and V_m are the volumes (cm^3) containing one equivalent or mole of solute respectively. c_e and c_m are solute concentrations in equiv.cm^{-3} or mol.dm^{-3} respectively.

Rather than using a single value for calculation of Λ_m to determine the electrolyte type the Onsager Law was used by measuring the conductivity over a concentration range. For strong electrolytes the molar conductivity, Λ_m varies with concentration according to the Onsager equation: (This illustrates only a weak dependence on concentration)

$$\Lambda_o - \Lambda_m = (A + \omega B \Lambda_o) c^{1/2}$$

The molar conductance, Λ_m was initially plotted against $c^{1/2}$, the linear portion was extrapolated to zero concentration to obtain Λ_o as intercept. $(\Lambda_o - \Lambda_m)$ was plotted against $c^{1/2}$ to obtain a straight line of slope $(A + \omega B \Lambda_o)$. This term necessarily directly reflects the electrolyte type of the complex as it depends upon the charges of the ions concerned, amongst other factors (for example, the dielectric constant of the solvent).

The use of equivalent concentration, c_e and equivalent conductance Λ_e has been common in conductivity studies. This is explained by Feltham and Hayter, [331] who suggest that the equivalent weights of the complexes $[ML_4]X_2$ and $[M_2L_8]X_4$ are half the monomer weight. For complexes where the cations or anion does not enter into the coordination sphere of the complex the equivalent weight is independent of the molecular complexity z in solution. A single Λ_e determination cannot determine z in complexes $[ML_n]_z X_{yz}$, or the charge type, but use of the Onsager Law by measurement of conductivity at

different concentrations differentiates between electrolyte types of ionized complexes.

In the complexes studied the molar weight has been used rather than the equivalent weight. Using the same example; the equivalent weight of $[ML_n]^{2+}[ClO_4]_2^-$ is 1/2 the formula weight, and the equivalent weight of $[M_2L_{2n}]^{4+}[ClO_4]_4^-$ is (2 x formula weight)/4 or 1/2 the formula weight, assumptions are still made regarding the molecular complexity of the complexes in the use of equivalent weights. The use of the molar weight in these conductivity studies is appropriate. Further evidence for such molecular weight assumptions is based upon analytical figures obtained for the complexes, which reflects their electrolyte type.

Tabulated Data for Conductivity Measurements

Table A.1.1. $[Mg(MeCN)_6][SbCl_6]_2$ (I)

c ($moldm^{-3}$)	$c^{1/2}$ ($moldm^{-3}$)	κ ($mS\ cm^{-1}$)	Λ_m (Scm^2mol^{-1})	Λ_o-Λ_m (Scm^2mol^{-1})
2.58×10^{-3}	0.0507	0.7188	278.9	60.11
2.79×10^{-3}	0.0528	0.7636	273.1	65.91
3.16×10^{-3}	0.056	0.854	270.23	68.78
3.65×10^{-3}	0.0603	0.964	264.32	74.69
4.24×10^{-3}	0.06509	1.097	258.9	80.11
5.03×10^{-3}	0.0709	1.266	251.68	87.33
6.13×10^{-3}	0.0782	1.497	244.2	94.81

Table A.1.2. $[Sn(MeCN)_6][SbCl_6]_2$ (II)

c ($moldm^{-3}$)	$c^{1/2}$ ($moldm^{-3}$)	κ ($mS\ cm^{-1}$)	Λ_m (Scm^2mol^{-1})	Λ_o-Λ_m (Scm^2mol^{-1})
2.77×10^{-3}	0.0526	0.469	169.38	15.54
3.07×10^{-3}	0.0554	0.520	169.3	15.62
3.52×10^{-3}	0.0593	0.591	167.84	17.08
4.84×10^{-3}	0.0695	0.810	166.77	18.15
5.71×10^{-3}	0.0755	0.948	165.88	19.04
6.93×10^{-3}	0.0832	1.104	159.28	25.64

Table A.1.3. $[SnCl_3(MeCN)_3][SbCl_6]$ (III)

c ($moldm^{-3}$)	$c^{1/2}$ ($moldm^{-3}$)	κ ($mS\ cm^{-1}$)	Λ_m (Scm^2mol^{-1})	Λ_o-Λ_m (Scm^2mol^{-1})
0.016	0.1264	1.129	70.56	16.736
0.0183	0.1352	1.271	69.45	17.846
0.02114	0.1453	1.443	68.25	19.046
0.0248	0.1574	1.673	67.45	19.846
0.031	0.176	2.016	65.03	22.266
0.0411	0.2027	2.476	60.25	27.046

Table A.1.4. $[SnCl_2(MeCN)_4][SbCl_6]_2$ (IV)

c ($moldm^{-3}$)	$c^{1/2}$ ($moldm^{-3}$)	κ ($mS\ cm^{-1}$)	Λ_m (Scm^2mol^{-1})	$\Lambda_o-\Lambda_m$ (Scm^2mol^{-1})
1.602×10^{-3}	0.04	0.3211	200.4	18.65
1.805×10^{-3}	0.0424	0.3601	199.5	19.55
2.08×10^{-3}	0.0456	0.4105	197.35	21.7
2.41×10^{-3}	0.049	0.4722	195.93	23.12
2.826×10^{-3}	0.0531	0.5468	193.48	25.57
3.39×10^{-3}	0.0582	0.651	192.03	27.02
3.856×10^{-3}	0.062	0.7311	190.11	28.94

Table A.1.5. $[InCl_2(MeCN)_4][SbCl_6]$ (V)

c ($moldm^{-3}$)	$c^{1/2}$ ($moldm^{-3}$)	κ ($mS\ cm^{-1}$)	Λ_m (Scm^2mol^{-1})	Λ_o-Λ_m (Scm^2mol^{-1})
5.39×10^{-4}	0.0232	0.0864	160.3	21.66
6.61×10^{-4}	0.026	0.1034	156.4	25.56
7.56×10^{-4}	0.0275	0.1174	155.22	26.74
8.75×10^{-4}	0.0295	0.1339	152.97	28.99
1.012×10^{-3}	0.0318	0.1523	150.49	31.47
1.223×10^{-3}	0.0349	0.1817	148.56	33.4
1.487×10^{-3}	0.03856	0.2152	144.72	37.24

Table A.1.6. $[In(MeCN)_6][SbCl_6]_3$ (VI)

c ($moldm^{-3}$)	$c^{1/2}$ ($moldm^{-3}$)	κ ($mS\ cm^{-1}$)	Λ_m (Scm^2mol^{-1})	$\Lambda_o-\Lambda_m$ (Scm^2mol^{-1})
1.844×10^{-3}	0.0429	0.5969	323.7	59.42
2.047×10^{-3}	0.0452	0.6581	321.5	61.62
2.17×10^{-3}	0.0466	0.697	320.96	62.16
2.47×10^{-3}	0.0497	0.7818	316.39	66.73
2.79×10^{-3}	0.0528	0.8578	306.68	76.44
3.25×10^{-3}	0.0569	0.9868	304.13	78.99
3.55×10^{-3}	0.0596	1.081	304.16	78.96
4.00×10^{-3}	0.0632	1.186	296.20	86.92

Table A.1.7. $[BiCl_2(MeCN)_4][SbCl_6]$ (XIV)

c ($moldm^{-3}$)	$c^{1/2}$ ($moldm^{-3}$)	κ ($mS\ cm^{-1}$)	Λ_m (Scm^2mol^{-1})	$\Lambda_o-\Lambda_m$ (Scm^2mol^{-1})
0.01647	0.1283	1.900	115.36	26.82
0.01951	0.1396	2.129	109.12	33.06
0.02291	0.1513	2.394	104.49	37.69
0.02706	0.1644	2.637	97.45	44.73

Table A.1.8. $[Bi(MeCN)_6][SbCl_6]_3$ (XV)

c ($moldm^{-3}$)	$c^{1/2}$ ($moldm^{-3}$)	κ ($mS\ cm^{-1}$)	Λ_m (Scm^2mol^{-1})	$\Lambda_o-\Lambda_m$ (Scm^2mol^{-1})
2.89×10^{-3}	0.0537	0.5744	198.75	46.85
3.211×10^{-3}	0.0566	0.6295	196.04	49.59
4.235×10^{-3}	0.065	0.7933	187.32	58.28
7.021×10^{-3}	0.0837	1.269	180.75	64.85
8.576×10^{-3}	0.0926	1.369	159.6	86.0

Table A.1.9. $[Mg(MeCN)_6]_3[Bi_4Cl_{16}]$ (XIII)

c ($moldm^{-3}$)	$c^{1/2}$ ($moldm^{-3}$)	κ ($mS\ cm^{-1}$)	Λ_m (Scm^2mol^{-1})	$\Lambda_o-\Lambda_m$ (Scm^2mol^{-1})
3.81×10^{-3}	0.0617	0.768	201.57	124.6
3.93×10^{-3}	0.0626	0.7876	200.4	125.77
4.017×10^{-3}	0.0633	0.7917	197.08	129.09
4.12×10^{-3}	0.0641	0.8105	196.7	129.47
4.34×10^{-3}	0.0658	0.8371	192.88	133.29
4.49×10^{-3}	0.067	0.851	189.62	136.55
4.66×10^{-3}	0.068	0.8841	189.72	136.45

Table A.1.10. $SbCl_3.SbCl_5.4MeCN.$(XXXII)

c ($moldm^{-3}$)	$c^{1/2}$ ($moldm^{-3}$)	κ ($mS\ cm^{-1}$)	Λ_m (Scm^2mol^{-1})	Λ_o-Λ_m (Scm^2mol^{-1})
8.40×10^{-3}	0.092	1.191	141.75	35.75
9.37×10^{-3}	0.097	1.271	135.64	41.86
0.010	0.10	1.366	130.96	46.54
0.012	0.108	1.530	131.105	46.395
0.013	0.114	1.667	128.32	49.18
0.037	0.19	3.536	95.67	81.83

Table A.1.11. $TiCl_4.MeCl_2.6MeCN$ (XXXIV)

c ($moldm^{-3}$)	$c^{1/2}$ ($moldm^{-3}$)	κ ($mS\ cm^{-1}$)	Λ_m (Scm^2mol^{-1})	Λ_o-Λ_m (Scm^2mol^{-1})
0.017	0.13	1.224	72.85	37.91
0.18	0.13	1.302	72.98	37.78
0.02	0.14	1.358	68.93	41.83
0.023	0.15	1.446	64.26	46.5
0.024	0.15	1.508	63.09	47.67
0.028	0.17	1.695	59.73	51.03
0.03	0.18	1.839	57.11	53.65
0.038	0.19	2.074	54.01	56.75

APPENDIX 2

Appendix 2

Crystal Structure Determination of $[Mg(MeCN)_6]_2[Bi_4Cl_{16}]$ (XII)

The crystals were prepared as described previously. A crystal of approximate size 0.35 x 0.25 x 0.20mm was set up to rotate about the *a* axis on a Stoe Stadi2 diffractometer and data were collected via variable width ω scan. Background counts were for 20s and a scan rate of $0.0333^{o}s^{-1}$ was applied to a width of $(1.5 + \sin\mu/\tan\theta)$. 5200 independent reflections were measured of which 1635 with $I > 3\sigma(I)$ were used in subsequent refinement. No deterioration in the crystal was observed during the data collection. An empirical absorption correction was made. [332] The structure was determined by direct methods. Hydrogen atoms on the methyl groups of several of the MeCN ligands could not be located either from a difference Fourier map or via refinement as a rigid group, and were therefore not included in the refinement. The Bi, Cl and Mg atoms were refined anisotropically and the N, C atoms isotropically. Data was given a weighting scheme in the form $w = 1/[\sigma^2(F) + 0.003 F^2]$. The final R value was 0.067 (R_w = 0.065). Calculations were carried out using Shelx76 [333] and some programs on the Amdahl 5870 at the University of Reading. In the final cycles of refinement, no shift/error ratio was greater than 0.1σ. In the final difference Fourier maps, the maximum and minimum peaks were $1.65eÅ^{-1}$ (located close to bismuth atoms), and $^{-}1.35e/Å^3$.

Crystal data and refinement details are given in Table A.2.1. Positional parameters are given in Table A.2.2, bond lengths and angles in Tables A.2.3 and A.2.4.

Table A.2.1. Crystal data and refinement details for $[Mg(MeCN)_6]_2[Bi_4Cl_6]$

Compound	$[Mg(MeCN)_6]_2[Bi_4Cl_{16}]$
Formula	$N_{12}C_{24}H_{36}Mg_2Bi_4Cl_{16}$
M	972.0
Space group	$P2_{1/a}$
a(Å)	16.022(11)
b(Å)	21.513(22)
c(Å)	9.217(10)
β(°)	96.5(1)
U(Å)	3156.6
F(000)	1784
Z	2
D_{calc} (gcm^{-3})	2.04
D_{obs} (gcm^{-3})	2.10
μ(cm^{-1})	112.9
λ(Å)	0.7107

Table A.2.2. Atomic co-ordinates ($x10^4$), with estimated standard deviations in parentheses

Atom	*x*	*y*	*z*
Bi (1)	4821 (1)	6036 (1)	5376 (2)
Bi (2)	2680 (1)	4750 (1)	4532 (3)
Cl (1)	4244 (8)	4816 (7)	6508 (18)
Cl (2)	3699 (9)	3922 (7)	2840 (18)
Cl (3)	2223 (8)	3837 (5)	5978 (17)
Cl (4)	1940 (10)	5447 (8)	6013 (19)
Cl (5)	1436 (9)	4635 (8)	2562 (21)
Cl (6)	3504 (7)	5852 (6)	3359 (16)
Cl (7)	5123 (11)	7020 (8)	4199 (22)
Cl (8)	3992 (11)	6534 (10)	7227 (21)
Mg	1205 (9)	6753 (7)	5 (17)
N (11)	1802 (21)	6899 (17)	2274 (33)
C (12)	2010 (22)	7120 (18)	3414 (33)
C (13)	2237 (17)	7193 (16)	4989 (30)
N (21)	2290 (18)	7268 (17)	-643 (43)
C (22)	2727 (21)	7645 (17)	-1042 (48)
C (23)	3279 (31)	8104 (25)	-1662 (69)
N (31)	220 (18)	6212 (15)	975 (40)
C (32)	-121 (21)	5792 (17)	1431 (47)
C (33)	-803 (28)	5325 (23)	1564 (63)
N (41)	648 (24)	6504 (21)	-2259 (36)
C (42)	347 (4)	6507 (34)	-3464 (44)
C (43)	34 (19)	6303 (17)	-4947 (33)
N (51)	430 (23)	7625 (15)	55 (49)
C (52)	320 (29)	8139 (17)	400 (64)
C (53)	139 (40)	8789 (19)	791 (85)
N (61)	2093 (23)	5953 (17)	-192 (52)
C (62)	2563 (22)	5564 (16)	-215 (49)
C (63)	3083 (23)	5032 (16)	-282 (53)

Table A.2.3. Dimensions in the Anion Coordination Sphere
(Distances, Å; angles, degrees)

Bi (1)	Cl (1)	3.009 (16)	
Bi (1)	Cl (6)	2.678 (13)	
Bi (1)	Cl (7)	2.453 (18)	
Bi (1)	Cl (8)	2.516 (20)	
Bi (1)	Cl (2i)	2.730 (14)	
Bi (1)	Cl (1i)	3.034 (16)	
Bi (2)	Cl (1)	2.930 (14)	
Bi (2)	Cl (2)	2.974 (17)	
Bi (2)	Cl (3)	2.528 (14)	
Bi (2)	Cl (4)	2.426 (16)	
Bi (2)	Cl (5)	2.552 (16)	
Bi (2)	Cl (6)	2.976 (13)	
Cl (1)	Bi (1)	Cl (6)	82.1 (4)
Cl (1)	Bi (1)	Cl (7)	172.1 (5)
Cl (6)	Bi (1)	Cl (7)	90.0 (5)
Cl (1)	Bi (1)	Cl (8)	86.0 (5)
Cl (6)	Bi (1)	Cl (8)	95.7 (5)
Cl (7)	Bi (1)	Cl (8)	94.5 (6)
Cl (1i)	Bi (1)	Cl (1)	82.1 (4)
Cl (1i)	Bi (1)	Cl (6)	170.1 (4)

Cl (2i)	Bi (1)	Cl (6)	170.1 (4)
Cl (2i)	Bi (1)	Cl (7)	92.1 (5)
Cl (2i)	Bi (1)	Cl (8)	93.8 (5)
Cl (2i)	Bi (1)	Cl (1)	85.0 (4)
Cl (7)	Bi (1)	Cl (1i)	97.7 (5)
Cl (8)	Bi (1)	Cl (1i)	167.8 (6)
Cl (1)	Bi (2)	Cl (2)	82.7 (4)
Cl (1)	Bi (2)	Cl (3)	89.3 (4)
Cl (2)	Bi (2)	Cl (3)	91.1 (4)
Cl (1)	Bi (2)	Cl (4)	93.4 (5)
Cl (2)	Bi (2)	Cl (4)	176.0 (5)
Cl (3)	Bi (2)	Cl (4)	89.7 (5)
Cl (1)	Bi (2)	Cl (5)	172.4 (5)
Cl (2)	Bi (2)	Cl (5)	90.0 (5)
Cl (3)	Bi (2)	Cl (5)	92.9 (5)
Cl (4)	Bi (2)	Cl (5)	93.9 (5)
Cl (1)	Bi (2)	Cl (6)	78.7 (4)
Cl (2)	Bi (2)	Cl (6)	89.6 (4)
Cl (3)	Bi (2)	Cl (6)	167.8 (4)
Cl (4)	Bi (2)	Cl (6)	88.7 (5)
Cl (5)	Bi (2)	Cl (6)	99.3 (5)
Bi (1)	Cl (1)	Bi (2)	95.8 (5)
Bi (1)	Cl (6)	Bi (2)	102.3 (4)

Table A.2.4. Dimensions in the Cation

Mg	N (11)	2.221 (26)	
Mg	N (21)	2.202 (25)	
Mg	N (31)	2.227 (25)	
Mg	N (41)	2.239 (27)	
Mg	N (51)	2.254 (26)	
Mg	N (61)	2.252 (26)	
N (11)	Mg	N (21)	85.1 (15)
N (11)	Mg	N (31)	86.9 (14)
N (21)	Mg	N (31)	171.6 (15)
N (11)	Mg	N (41)	174.2 (16)
N (21)	Mg	N (41)	96.3 (15)
N (31)	Mg	N (41)	91.4 (15)
N (11)	Mg	N (51)	92.4 (15)
N (21)	Mg	N (51)	92.2 (15)
N (31)	Mg	N (51)	90.6 (14)
N (41)	Mg	N (51)	93.2 (16)
N (11)	Mg	N (61)	88.6 (15)
N (21)	Mg	N (61)	80.6 (15)
N (31)	Mg	N (61)	96.7 (15)
N (41)	Mg	N (61)	86.1 (16)
N (51)	Mg	N (61)	172.7 (18)
N (11)	C (12)	1.167 (30)	
C (12)	C (13)	1.465 (32)	
N (21)	C (22)	1.159 (30)	
C (22)	C (23)	1.481 (34)	
N (31)	C (32)	1.176 (30)	
C (32)	C (33)	1.486 (34)	

N (41)	C (42)	1.160 (32)	
C (42)	C (43)	1.469 (34)	
N (51)	C (52)	1.170 (31)	
C (52)	C (53)	1.481 (35)	
N (61)	C (62)	1.127 (29)	
C (62)	C (63)	1.422 (32)	
Mg	N (11)	C (12)	163 (3)
N (11)	C (12)	C (13)	162. (4)
Mg	N (21)	C (22)	164 (3)
N (21)	C (22)	C (23)	176 (5)
Mg	N (31)	C (32)	159 (3)
N (31)	C (32)	C (33)	158 (4)
Mg	N (41)	C (42)	166 (5)
N (41)	C (42)	C (43)	162 (7)
Mg	N (51)	C (52)	153 (4)
N (51)	C (52)	C (53)	177 (5)
Mg	N (61)	C (62)	176 (4)
N (61)	C (62)	C (63)	174 (4)

REFERENCES

1) J.D.Smith, *Comprehensive Inorganic Chemistry*, Pergamon Press, Oxford, 1973, Vol 2.

2) F.A.Cotton, G.Wilkinson, *Advanced Inorganic Chemistry*, Wiley Interscience, 5th Edition, 1988, Chapter 11.

3) N.N.Greenwood, A.Earnshaw, *Chemistry of the Elements*, Pergamon Press, 1st Edition, 1984, Chapter 13.

4) K.Kwart, K.King, *D-Orbitals in the Chemistry of Silicon, Phosphorus and Sulphur*, Springer-Verlag, 1977.

5) C.A.McAuliffe, *Comprehensive Coordination Chemistry*, Ed's. G.Wilkinson, R.D.Gillard, J.A.McCleverty, Pergamon Press, Oxford, 1987, Vol 2, Chapter 14 and references therein.

6) R.Bhula, P.Osvath and D.C.Weatherburn, *Coord. Chem. Rev.*, 1988, **91**, 134.

7) E.P.Kyba and S.-S.P.Chou, *J. Chem. Soc., Chem. Commun.*, 1980, 449; E. P. Kyba and S.-S.P.Chou, *J. Org. Chem.*, 1981, **46**, 860.

8) O.J.Scherer, *Angew. Chem., Int. Edn. Engl.*, 1985, **24**, 924 and references therein.

9) F.Mathey, J.Fischer and J.H.Nelson, *Structure and Bonding*, Berlin, 1983, **55**, 153 and references therein.

10) A.J.Dimaio and A.L.Rheingold, *Chem. Rev.*, 1990, **90**, 169 and references therein.

11) M.A.Petrie, S.C.Shoner, H.V.Rasika-Dias and P.P.Power, *Angew. Chem., Int. Edn. Engl.*, 1990, **29**, 1033.

12) G.Huttner, B.Sigworth, O.Scheidsteger, L.Zsolnai and O.Orama, *Organometallics.*, 1985, **4**, 326; G.Huttner and H.Jungman, *Angew. Chem., Int. Edn. Engl.*, 1979, **18**, 953; G.Huttner, *Pure Appl. Chem.*, 1986, **58**, 585;

H. Schafer, D.Binder and D.Fenske, *Angew. Chem. Int. Edn. Engl.*, 1985, **24**, 522; M.H.Chisholm, K.Folting, J.C.Huffman and J.J.Koh, *Polyhedron*, 1985, **4**, 893.

13) T.T.Derencsengi, *Inorg. Chem.*, 1981, **20**, 665.

14) D.C.Mente, J.L.Mills and R.E.Mitchell, *Inorg. Chem.*, 1975, **14**, 123; D.C.Mente, J.L.Mills, *ibid.*, 1862.

15) T.P.Debies, J.W.Rabalais, *Inorg. Chem.*, 1974, **13**, 308.

16) W.P.Giering, M.N.Golovin, M.Rahman and J.E.Belmonte, *Organometallics*, 1985, **4**, 1981; R.V.Honeychuck and W.H.Hersch, *Inorg. Chem.*, 1987, **26**, 1826.

17) D.E.Ellis, W.C.Trogler, S.-X. Xiao and Z.Berkovitch-Yellin, *J. Amer. Chem. Soc.*, 1983, **105**, 7033.

18) D.S.Marynick, *J. Amer. Chem. Soc.*, 1984, **106**, 4064; D.S.Marynick, S.Askari and D.F.Nickerson, *Inorg. Chem.*, 1985, **24**, 868; M.Braga, *ibid.*, 2702.

19) J.C.Glordan, J.A.Tossell and J.H.Moore, *ibid.*, 1100.

20) A.G.Orpen, N.G.Connelly, *J. Chem. Soc., Chem. Commun.*, 1985, 1310.

21) G.M.Bodner, M.P.May, L.E.McKinney, *Inorg. Chem.*, 1980, **19**, 1951; T.Bartik, T.Himmler, H.G.Schulte and K.Seevogel, *J. Organomet. Chem.*, 1984, **272**, 29.

22) J.E.Huheey, *Inorganic Chemistry, Principles of Structure and Reactivity*, Harper and Row, New York, 2nd Edn, 1978.

23) C.A.Tolman, *J. Amer. Chem. Soc.*, 1970, **92**, 2956; C.A.Tolman, *Chem. Rev.*, 1977, **77**, 313.

24) M.C.Baird and R.T.Smith, *Inorg. Chim. Acta*, 1982, **62**, 135.

25) I.S.Butler and A.A.Ismail, *Inorg. Chem.*, 1986, **25**, 3910.

26) C.A.McAuliffe and W.Levanson, *Phophine, Arsine and Stibine Complexes of Transition Elements*, Elsevier, Amsterdam, Vol 1, 1979.

27) L.Pazsitka, R.Bertram, *J. Electroanalyt. Chem.* 1970, **28**, 119.

28) G.P.Smith et al, *J. Amer. Chem. Soc.*, 1986, **108**, 654.

29) E.C.Baughan, *The Chemistry of Non Aqueous Solvents*, Ed. J.J.Lagowski, Academic Press, New York. 1976, Vol4, p129.

30) E.G.Braine, R.C.Ferguson and G.J.Thomas, *Anal. Chem.*, 1967, **39**, 517.

31) R.J.Gillespie and R.S.Nyholm, *Quarterly Rev.*, 1957, **11**, 368.

32) H.Hartl, J.Schoner, J.Jeneler and H.Schulz, *Z. Anorg. Allgm. Chem.*, 1975, **413**, 61.

33) R.Enjalbert and J.Galy, *C. R. Acad. Sci., Ser.C*, 1978, **287**, 259.

34) R.Enjalbert, J.M.Savariault, J.P.Legros, *C. R. Acad. Sci., Ser. C*, 1980, **290**, 239.

35) H.Hartl, M.Rama, A.Simon and H.J.Diesroth, *Z. Naturforsch, B*, 1979, **34**, 1035.

36) R.Enjalbert and J.Galy, *C.R.Acad. Sci., Ser. C*, 1979, **289**, 441.

37) P.Kisluik and C.H.Townes, *J. Chem. Phys.*, 1950, **18**, 1109.

38) J.Trotter, *Z. Krist.*, 1965, **122**, 230.

39) R.Enjalbert and J.Galy, *Acta Crystallogr., Sect. B*, 1980, **36**, 914.

40) A.J.Edwards, *J. Chem. Soc. A*, 1970, 2751.

41) A.Lipka, *Acta Crystallogr., Sect B*, 1979, **35**, 3020.

42) E.Johnson, A.H.Narten, W.E.Thiessen and R.Triolo, *Chem. Soc. (London) Faraday Disc.*, 1978, **66**, 287.

43) J.Trotter and T.Zobel, *Z. Krist.*, 1966, **123**, 67.

44) O.Gries and M.Martinez-Ripoll, *Z. Anorg. Allgm. Chem.*, 1977, **436**, 105.

45) A.K.Cheetham and N.Norma, *Acta Chem. Scand., Ser. A.*, 1974, **28**, 55.

46) S.C.Nyberg, G.A.Ozin and J.T.Szymanski, *Acta Crystallogr., Sect. B*, 1971, **27**, 2298.

47) H.Benda, *Z. Krist.*, 1980, **151**, 271.

48) N.W.Alcock, *Adv. Inorg. Chem. Radiochem.*, 1972, **15**, 1.

49) J.F.Sawyer and R.J.Gillespie, *Prog. Inorg. Chem.*, 1986, **34**, 65.

50) R.J.Gillespie, *Molecular Geometry*, Van Nostrand, Reinhold, London 1972; *J. Chem. Ed.*, 1974, **51**, 367.

51) R.Hillel, J.Bouix and R.Avre, *Bull. Soc. Chim. Fr.*, 1975, 2458.

52) P.Kisluik and C.H.Townes, *J. Chem. Phys.*, 1950, **18**, 1109.

53) A.G.Robiette, *J. Mol. Struct.*, 1976, **35**, 81.

54) Y.Morino, T.Ukaji and T.Ito, *Bull. Chem. Soc. Japan.*, 1966, **39**, 71.

55) S.Konaka and M.Kimura, *ibid.*, 1973, **46**, 404.

56) S.Konaka and M.Kimura, *ibid.*, 1973, **46**, 413.

57) H.A.Skinner and L.E.Sutton, *Trans. Faraday Soc.*, 1940, **36**, 681.

58) I.Lindqvist and A.Niggli, *J. Inorg. Nucl. Chem.* 1956, **2**, 345.

59) B.Kruss and M.L.Ziegler, *Z. Anorg. Allgm. Chem.*, 1972, **388**, 158.

60) H.A.Abdel-Rehim and E.A.Meyers, *Crystal Struct. Commun.*, 1973, **2**, 121.

61) R.Enjalbert and J.Galy, *Acta Crystallogr., Sect. B*, 1979, **35**, 546.

62) A.Lipka, *Z. Anorg. Allgm. Chem.*, 1980, **469**, 218.

63) D.R.Schroeder and R.A.Jacobson, *Inorg. Chem.*, 1973, **12**, 210.

64) J.I.Musher, *Angew. Chem., Int. Edn. Engl.*, 1969, **8**, 54.

65) T.Birchall, B.Della Valle, E.Martineau and J.B.Milne, *J. Chem. Soc., A*, 1971, 1855.

66) C.R.Hubbard and R.A.Jacobson, *Inorg. Chem.*, 1972, **11**, 2247.

67) K.Seppelt, *Angew. Chem., Int. Edn. Engl.*, 1976, **15**, 377.

68) F.Claus, M.Glaser, V.Wolfel and R.Minkwitz, *Z. Anorg. Allgm. Chem.*, 1984, **517**, 207.

69) F.Claus, M.Glaser and R.Minkwitz, *Z. Anorg. Allgm. Chem.*, 1983, **506**, 178.

70) R.Minkwitz and H.Prenzel, *Z. Anorg. Allgm. Chem.*, 1987, **548**, 103.

71) F.Claus and R.Minkwitz, *Z. Anorg. Allgm. Chem.*, 1983, **501**, 19.

72) R.Minkwitz and H.Prenzel, Z. *Anorg. Allgm. Chem.*, 1987, **534**, 150.

73) K.Kolditz, Z. *Anorg. Allgm. Chem.*, 1955, **280**, 313.

74) H.Priess, Z. *Anorg. Allgm. Chem.*, 1971, **388**, 45; J.Weidlein and K.Dehnicke, Z. *Anorg. Allgm. Chem.*, 1965, **337**, 113.

75) R.Minkwitz, H.Prenzel, A.Schardey and H.Oberhammer, *Inorg. Chem.*, 1987, **26**, 2730.

76) K.Seppelt, Z. *Anorg. Allgm. Chem.*, 1977, **434**, 5.

77) R.R.Holmes, *Prog. Inorg. Chem.*, 1984, **32**, 119.

78) R.R.Holmes, *Acc. Chem. Res.*, 1979, **12**, 257.

79) K.W.Hansen, L.S.Bartell, *Inorg. Chem.*, 1965, **4**, 1775.

80) H.S.Gutowsky, D.W.McCall and G.P.Slichter, *J. Chem. Phys.*, 1953, **21**, 279.

81) R.S.Berry, *J. Chem. Phys.*, 1960, **32**, 933.

82) C.J.Marsden, *J. Chem. Soc. Chem. Commun.*, 1984, 401.

83) R.Hillel, J.Bouix and R.Avre, *Bull. Soc. Chim. Fr.*, 1975, 2458.

84) J.Brunvoll, A.A.Ischenko, I.N.Miakshin, G.V.Romanov, V.P.Spiridonov, T.G.Strand and V.F.Sukhoverkhov, *Acta Chem. Scand., Ser. A.*, 1980, **34**, 733.

85) T.K.Davies and K.C.Moss, *J. Chem. Soc., A*, 1970, 1054.

86) A.J.Edwards and P.Taylor, *J. Chem. Soc., Chem. Commun.*, 1971, 1376.

87) C.Hebecker, Z. *Anorg. Allgm. Chem.*, 1971, **384**, 111.

88) D.Clark, H.M.Powell and A.F.Wells, *J. Chem. Soc.*, 1942, 642.

89) H.D.B.Jenkins, K.P.Thakur, A.Finch and P.N.Gates, *Inorg. Chem.*, 1982, **21**, 423 and references cited therein.

90) D.S.Payne, *J. Chem. Soc.*, 1953, 1052.

91) S.M.Ohlberg, *J. Amer. Chem. Soc.*, 1959, **81**, 811.

92) W.Bues, F.Demiray and W.Brockner, *Spectrochim. Acta.*, 1974, **30A**, 1709; W.Brockner, S.J.Cyvin and H.Hovalan., *Inorg. Nucl. Chem. Lett.*, 1975, **11**, 171.

93) G.S.Harris and D.S.Payne, *J. Chem. Soc.*, 1956, 4617.

94) W.Gabes and K.Olie, *Acta Crystallogr., Sect. B*, 1970, **26**, 443.

95) A.Finch, P.N.Gates and A.S.Muir, *Polyhedron.*, 1986, **5**, 1537.

96) N.G.Feshchenko, V.G.Kostina and A.V.Kirsanov, *J. Gen. Chem.*, 1978, **48**, 195.

97) I.Tornieporth-Oetting and T.Klapotke, *J. Chem. Soc., Chem. Commun.*, 1990, 132.

98) S.Pohl, *Z. Anorg. Allgm. Chem.*, 1983, 498, 15.

99) J.Zemann, *Z. Anorg. Allgm. Chem.*, 1963, 324, 241.

100) W.R.Scheidt and C.A.Reed, *Inorg. Chem.*, 1985, 24, 4325.

101) A.J.Edwards and K.I.Khallow, *J. Chem. Soc., Chem. Commun.*, 1984, 50; J.Fawcett, J.H.Holloway, D.Laycock and D.R.Russell, *J. Chem. Soc., Dalton Trans.*, 1982, 1355.

102) P.Boldrini, R.J.Gillespie, R.P.Ireland and G.J.Schrobilgen, *Inorg. Chem.*, 1974, **13**, 1690.

103) R.J.Gillespie, D.Martin, G.J.Schrobilgen and D.R.Slim, *J. Chem. Soc., Dalton Trans.*, 1977, 2234.

104) G.A.Olah, G.K.S.Prakash and J.Sommer, *Superacids*, Wiley, New York, 1985.

105) G.Yakobson, G.G.Furin, *Synthesis*, 1980, 345 and references therein.

106) R.D.Chambers, M.Salisbury, G.Apsey, T.F.Holmes and S.Modena, *J. Chem. Soc., Chem. Commun.*, 1988, 10, 679.

107) V.Gutmann, *Monatsh*, 1951, 82, 473; A.W.Cronander, *Bull. Soc. Chim. de Paris*, 1873, **19**, 499.

108) D.S.Payne, *Topics in Phosphorus Chemistry*, 1967, **4**, 85.

109) R.G.Pearson, *J. Amer. Chem. Soc.*, 1963, **85**, 3533; R.G.Pearson, *J. Chem. Educ.*, 1965, **45**, 581; 643.

110) R.G.Pearson, *Coord. Chem. Rev.*, 1990, **100**, 403 and references therein.

111) R.Hulme and J.C.Scrutton, *J. Chem. Soc., A*, 1968, 2448.

112) M.Webster and S.Keats, *J. Chem. Soc., A*, 1971, 836.

113) B.Rubin, F.J.Heldrich, W.K.Dean, D.J.Williams and A.Viebeck, *Inorg. Chem.*, 1981, **20**, 4434.

114) I.Lindquist, *Inorganic Adduct Molecules Molecules of Oxo Compounds*, Springer, Berlin, 1963.

115) R.Hulme,D.Mullen and J.C.Scrutton, *Acta Crystallogr., Sect. A*, 1969, **25**, S171.

116) J.M.Kisyeni, Ph.D. Thesis, Warwick University, 1983.

117) P.P.K.Claire, G.R.Willey and M.G.B.Drew, *J. Chem. Soc., Dalton Trans.*, 1987, 263.

118) M.G.B.Drew, J.M.Kisyeni and G.R.Willey, *J. Chem. Soc., Dalton Trans.*, 1982, 1729.

119) C.L.Raston and A.H.White, *J. Chem. Soc. Dalton Trans.*, 1976, 791.

120)

121) N.W.Alcock, M.Ravindran and G.R.Willey, *J. Chem. Soc., Chem. Commun.*, 1989, 1063.

122) M.Schafer, J.Pebler, B.Borgsen, F.Weller and K.Dehnicke, *Z. Naturforsch*, 1990, 1243.

123) E.Hough, D.G.Nicholson and A.K.Vasudevan, *J. Chem. Soc. Dalton Trans.*, 1987, 427.

124) N.W.Alcock, M.Ravindran, S.M.Roe and G.R.Willey, *Inorg. Chim. Acta*, 1990, **167**, 115.

125) W.Smith, *J. Chem. Soc. London*, 1879, **35**, 309; W.Smith and G.W.Davis, *J. Chem. Soc*, 1882, **41**, 411.

126) B.N.Menshutkin, *Chem. Zentr.*, 1912, 1436; B.N.Menshutkin, *J. Russ. Phys. Chem. Soc.*, 1912, **43**, 1805; 1329.

127) H.Schmidbaur, W.Bublak, B.Huber and G.Muller, *Angew. Chem., Int. Edn. Engl.*, 1987, **26**, 234.

128) H.Schmidbaur, R.Nowak, O.Steigelmann and G.Muller, *Chem. Ber.*, 1990, **123**, 1221.

129) H.Schmidbaur, J.M.Wallis, R.Nowak, B.Huber and G.Muller, *Chem. Ber.*, 1987, **120**, 1837.

130) H.Schmidbaur, J.M.Wallis, R.Nowak, B.Huber, A.Schier and G.Muller, *Chem. Ber.*, 1987, **120**, 1829.

131) A.Schier, J.M.Wallis, G.Muller and H.Schmidbaur, *Angew. Chem. Int. Edn. Engl.*, 1986, **25**, 757.

132) R.Hulme and J.T.Szymanski, *Acta Crystallogr., Sect. B*, 1969, **25**, 753.

133) H.Schmidbaur, R.Nowak, B.Huber and G.Muller, *Organometallics*, 1987, **6**, 2266.

134) L.Pauling, *General Chemistry*, W.H.Freeman and Co., San Francisco, 3rd.Edn.,1970.

135) K.S.Pitzer, *Acc. Chem. Res.*, 1979, **12**, 271; P.Pyykko and J.P.Desclaux, *ibid.*, 1979, **12**, 277.

136) S.Pohl, W.Saak and D.Haase, *Angew. Chem., Int. Edn. Engl.*, 1987, **26**, 467.

137) A.Lipka, *Z. Anorg. Allgm. Chem.*, 1980, **469**, 218.

138) M.Edstrand, M.Inge, N.Ingri, *Acta Chem. Scand.*, 1955, **9**, 122.

139) L.R.Morss and W.R.Robinson, *Acta Crystallogr., Sect. B*, 1972, **28**, 653.

140) J.Kaub and W.S.Sheldrick, *Z. Naturforsch., B*, 1984, **39**, 1252, 1257.

141) A.Kalell and J.W.Bats, *Acta Crystallogr., Sect. C*, 1985, **41**, 1022.

142) W.Willing, U.Muller, J.Eicher and K.Dehnicke, *Z. Anorg. Allgm. Chem.*, 1986, **537**, 145.

143) B.Aurivillius and C.Stalhandske, *Acta Chem. Scand., Ser. A*, 1978, **32**, 715.

144) J.W.George, *Prog. Inorg. Chem.*, 1960, **2**, 33.

145) N.Habibi, B.Bonnet and B.Ducourant, *J. Fluorine. Chem.*, 1978, **12**, 237.

146) N.Habibi, B.Bonnet, B.Ducourant and R.Fourcade, *J. Fluorine. Chem.*, 1978, **12**, 63.

147) R.R.Ryan and D.T.Cromer, *Inorg. Chem.*, 1972, **11**, 2322.

148) S.H.Mastin and R.R.Ryan, *Inorg. Chem.*, 1971, **10**, 1757.

149) R.R.Ryan, S.H.Mastin and A.C.Larson, *Inorg. Chem.*, 1971, **10**, 2793.

150) D.Tichit, B.Ducourant, G.Mascherpa and R.Fourcade, *J. Fluorine. Chem.*, 1979, **13**, 45.

151) B.Ducourant, G.Mascherpa and R.Fourcade, *Rev. Chim. Miner.*, 1983, **20**, 314.

152) G.Mascherpa, E.Philippot and R.Fourcade, *Acta Crystallogr.*, 1975, **B31**, 2322.

153) B.Ducourant, G.Mascherpa, E.Philippot and R.Fourcade, *Rev. Chim. Miner.*, 1975, **12**, 553.

154) D.R.Schroeder and R.A.Jabobson, *Inorg. Chem.*, 1973, **12**, 515.

155) R.J.Gillespie, J.P.Kent, J.F.Sawyer, D.R.Slim and J.D.Tyrer, *Inorg. Chem.*, 1981, **20**, 3799.

156) M.J.Collins, R.J.Gillespie, J.F.Sawyer and J.E.Vekris, unpublished results.

157) R.J.Gillespie, R.Kapoor, R.Faggiani, C.L.Lock, M.Murchie and J.Passmore, *J. Chem. Soc., Chem. Commun.*, 1983, 8.

158) R.C.Burns, M.J.Collins, S.M.Eicher, R.J.Gillespie and J.F.Sawyer, *Inorg. Chem.*, 1988, **27**, 1807.

159) M.J.Collins, R.J.Gillespie, G.J.Schrobilgen and J.F.Sawyer, *Inorg. Chem.*., in the press.

160) G.Cardinal, R.J.Gillespie, J.F.Sawyer and J.E.Vekris, *J. Chem. Soc., Dalton Trans.*, 1982, 765.

161) U.Muller, *Z. Anorg. Allgm. Chem.*, 1978, 447, 171.

162) A.J.Edwards and D.R.Slim, *J. Chem. Soc., Chem. Commun.*, 1974, 178.

163) R.J.Gillespie, D.R.Slim and J.E.Vekris, *J. Chem. Soc., Dalton Trans.*, 1977, 971.

164) W.A.S.Nandana, J.Passmore, D.C.N.Swindells, P.Taylor, P.S.White and J.E.Vekris, *J. Chem. Soc., Dalton Trans.*, 1983, 619.

165) J.Passmore and P.S.White, unpublished results.

166) W.A.S.Nandana, J.Passmore, P.S.White and C.M.Wong, *J. Chem. Soc. Dalton Trans.*, 1987, 1989.

167) A.J.Edwards, personal communication.

168) R.D.W.Kemmit, D.R.Russell and D.W.A.Sharp, *J. Chem. Soc.*, 1963, 4408 and references therein.

169) B.Frlec, D.Gantar, and J.H.Holloway, *J. Fluorine. Chem.*, 1982, 20, 385.

170) M.J.Collins, R.J.Gillespie and J.F.Sawyer, *Inorg. Chem.*., 1987, 26, 1476, and references therein.

171) F.Pauer, M.Erhart, R.Mews and D.Stalke, *Z. Naturforsch*, 1990, 45b, 271 and references therein.

172) R.Minkwitz, H.Preut and R.Lekies, *Z. Naturforsch*, 1987, 42b, 1227.

173) I.Tornieporth-Oetting and T.Klapotke, *Chem. Ber.*, 1990, 123, 1343.

174) S.Bellard, A.V.Rivera and G.M.Sheldrick, *Acta Crystallogr., Sect. B*, 1978, 34, 1034.

175) J.Fawcett, J.H.Holloway, D.Laycock and D.R.Russell, *J. Chem. Soc., Dalton Trans.*, 1982, 1355; D.Gantar, B.Frlec and B.Volavsek, *J. Chem. Soc., Dalton Trans.*, 1984, 93.

176) J.H.Holloway, D.Laycock and R.Bougon, *J. Chem. Soc., Dalton Trans.*, 1983, 2303 and references therein.

177) W.A.S.Nandana, J.Passmore, P.S.White and C.M.Wong, *Inorg. Chem...*, 1990, **29**, 3529; A.J.Edwards and P.Taylor, *J. Chem. Soc., Dalton Trans.*, 1975, 2174; M.D.Lind and K.O.Christie, *Inorg. Chem.*, 1972, **11**, 608.

178) J.Bacon, P.A.W.Dean and R.J.Gillespie, *Can. J. Chem.*, 1970, **48**, 3413.

179) R.J.Gillespie, D.Martin, G.J.Schrobilgen, *J. Chem. Soc., Dalton Trans.*, 1980, 1898.

180) R.Bougon, T.Bui Huy, A.Cadet, P.Charpin and R.Rousson, *Inorg. Chem...*, 1974, **13**, 690.

181) A.J.Edwards and R.J.C.Sills, *J. Chem. Soc. A*, 1971, 942.

182) T.Klapotke and U.Thewalt, *J. Organomet. Chem.*, 1988, **356**, 173.

183) P.Gowik, T.Klapotke and U.Thewalt, *J. Organomet. Chem.*, 1990, **385**, 345.

184) P.Gowik and T.Klapotke, *J. Organomet. Chem.*, 1990, **387**, C27.

185) I.Leban, D.Gantar, B.Frlec and J.H.Holloway, *J. Chem. Soc. Dalton Trans.*, 1987, 2379.

186) R Bougon, P.Charpin, K.O.Christie, J.Isabey, M.Lance, M.Nierlich, J.Vigner and W.W.Wilson, *Inorg. Chem.*, 1988, **27**, 1389.

187) I.Leban, D.Gantar, B.Frlec, D.R.Russell and J.H.Holloway, *Acta Crystallogr., Sect. C., Cryst. Struct. Commun.*, 1987, **43**, 1888.

188) G.S.H.Chen, J.Passmore, P.Taylor, T.K.Whidden and P.S.White, *J. Chem. Soc. Dalton Trans.*, 1985, 9.

189) R.J.Gillespie, K.Ouchi, G P Pez, *Inorg. Chem...*, 1969, **8**, 63.

190) M.Webster, *Chem. Rev.*, 1966, 66, 87.

191) D.Neubauer, J.Weiss, *Z. Anorg. Allgm. Chem.*, 1960, **303**, 28.

192) R.Weber, *Pogg. Ann. Phys.*, 1865, **125**, 325.

193) Y.Hermudsson, *Acta. Chem. Scand.*, 1967, **21**, 1313.

194) R.Stendel, T.Sandow and J.Steidel, *J. Chem. Soc., Chem. Commun.*, 1980, 180.

195) D.S. Payne, *Halides and Oxyhalides of Group V Elements as Solvents in Nonaqueous Solvent Systems* , Ed. T.C. Waddington, Academic Press, London, 1965, Chapter 8.

196) A.P. Zuur and W.L. Groeneveld, *Rec. Trav. Chim*, 1967, **86**, 1089; W.L. Dressen, L.M. Van Geldrop, and W.L. Groeneveld, *Rec. Trav. Chim.*, 1970, **89**, 1271 and references therein.

197) M.H.B.Stiddard and R.E. Townsend, *J. Chem.Soc., A.*, 1968, 2355.

198) J.K. Ruff, *Inorg. Chem.*, 1963, **2**, 813.

199) P.P.K.Claire, G.R.Willey and M.G.B.Drew, *J. Chem. Soc., Chem. Commun.*, 1987, 1100.

200) P.N.Billinger, P.P.K.Claire, H.Collins and G.R.Willey, *Inorg. Chim. Acta*, 1988, **149**, 63.

201) R.G. Kidd and R.W. Matthews, *J. Inorg. Nucl. Chem..*, 1975, **37**, 661.

202) P. Stilbs and G. Olofsson, *Acta Chem .Scand., Sect .A.*, 1974, **28**, 647.

203)W. Gerrard, M.F. Lappert, H. Pyszora and J.W. Wallis, *J. Chem. Soc.*, 1960, 2182.

204) Nightingale, *Proc. 7th Internat. Conf. Coordination Chemistry, Stockholm*, 1962, p.217.

205) J. Venkateswarlu, *J. Chem. Phys.*, 1951, **19**, 293.

206) G. Herzberg, *Infra-red and Raman Spectra* , Van Nostrand, New York, 1960.

207) M. Burgard, and J. MacCordick, *Inorg. Nucl. Chem. Lett.*, 1970, **6**, 599.

208) M Webster, I.R. Beattie, *J. Chem. Soc.*, 1963, 38.

209) K. Nakamoto *Infra red and Raman Spectra of Inorganic and Coordination Compounds* , Wiley-Interscience, New York, 1986.

210) R.J.H. Clark, *Spectrochim. Acta*, 1965, **21**, 955.

211) I.R. Beattie, G.P. McQuillan, L. Rule and M. Webster, *J. Chem. Soc.*, 1963, 1514.

212) J. Reedijk, A.P. Zuur, and W.L. Groeneveld, *Rec. Trav. Chim.*, 1967, **86**, 1127.

213) P.P.K. Claire, M.G.B. Drew and G.R. Willey *J. Chem. Soc., Dalton Trans.*, 1988, 215.

214) J. Reedijk and W.L. Groenveld, *Rec. Trav. Chim.*, 1968, **87**, 513.

215) B.A. Stork-Blaisse, G.C. Verschoor, and C. Romers, *Acta Crystallogr., Sect. B*, 1972, **28**, 2445.

216) P. Sobota, T. Pluzinski, and T. Lis, *Z. Anorg. Allgm. Chem.*, 1986, 533, 215.

217) P.Sobota, J.Utko and Z.Janas, *J. Organometallic Chem.*, 1986, **316**, 19.

218) H.J. Haupt, F. Huber and H. Preut, *Z. Anorg. Allgm. Chem.*, 1976, 422, **97**, 255.

219) P.G. Harrison, B.J. Haylett and T.J. King, *Inorg. Chim. Acta.*, 1983, **75**, 265.

220) R.H. Andrews, S.J. Clark, J.D. Donaldson, J.C. Dewan and J. Silver, *J. Chem. Soc., Dalton Trans.*, 1983, 767.

221) C.C. Hsu and R.A. Geanangel, *Inorg. Chem.*, 1980, **19**, 110.

222) A.J. Edwards and K.I. Khallow, *J. Chem. Soc., Chem Commun.*, 1984, 50.

223) F.W.B. Einstein, and B.R. Penfold, *J. Chem. Soc. A.*, 1968, 3019.

224) G. Van Koten, J.T.B.H. Jastrzebskii, J.G. Nortes, A.L. Spek and J.C. Schoone, *J. Organomet. Chem.*, 1978, **148**, 233.

225) P. Gans and J.B. Gill, *J. Chem. Soc., Dalton Trans.*, 1976, 779.

226) A.J. Carty and D.G. Tuck, *J. Chem. Soc.*, 1964, 6012.

227) P. Carty, D.G. Tuck and E.J. Woodhouse, *J. Chem. Soc.*, A, 1966, 1077.

228) J.J. Habeeb, F.F. Said, and D.G. Tuck, *J. Chem. Soc., Dalton Trans.*, 1981, 118.

229) F.J. Brinkmann, and H. Gerding, *Inorg. Nucl. Chem. Lett.*, 1969, **5**, 119.

230) R.C. Vickery, *J. Chem. Soc.*, 1955, 251.

231) A.I. Grigorev, N.K. Evseeva, and V.A. Sipachev, *J. Struct. Chem. (Engl.Transl.)*, 1969, **10**, 387.

232) T. Moeller, and G. Vicentini, *J. Inorg. Nucl. Chem.*, 1965, **27**, 1477.

233) J.L. Martin, L.C. Thompson, L.S. Radonovich, and M.D. Glick, *J. Am. Chem. Soc.*, 1968, **90**, 4493.

234) H Hartmann, H.L. Schlafer, and K.H. Hansen, *Z. Anorg. Allgm. Chem.*, 1956, **284**, 153.

235) P.J. McCarthy, and M.F. Richardson, *Inorg. Chem*, 1983, **22**, 2979.

236) K. Folting, J.C. Huffman, R.L. Bansemer, and K.G. Caulton, *Inorg. Chem.*, 1984, **23**, 3289.

237) A Flamini, and A.M. Giuliani, *Inorg. Chim. Acta*, 1986, **112**, L7 and references therein.

238) P. Sobota, J. Utko, T. Lis, *J. Chem. Soc. Dalton Trans.*, 1984, 2077.

239) J. Shamir, S. Schneider, A. Bino, and S. Cohen, *Inorg. Chim. Acta.*, 1986, **111**, 141.

240) T.J. Kistenmacher, and G.D. Stucky, *Inorg. Chem.*, 1971, **10**, 122.

241) M.S.Elder, G.M.Prinz, P.Thornton and D.R.Busch, *Inorg. Chem.*, 1968, **7**, 2426.

242) W.J.Geary, *Coord. Chem. Rev.*, 1971, **7**, 81.

243) A. Herschaft, and J.D. Corbett, *Inorg. Chem.*, 1963, **2**, 979.

244) K. Kihara, and T. Sudo, *Acta Crystallogr., Sect. B*, 1974, **30**, 1088.

245) N.W. Alcock, M. Ravindran, and G.R. Willey, *J. Chem. Soc., Chem Commun.*, 1989, 1063.

246) J.D. Corbett, *Prog. Inorg. Chem.*, 1976, **21**, 129.

247) B. Krebs, M. Hucke and C.J. Brendel, *Angew. Chem., Int. Ed. Engl.*, 1982, **21**, 455.

248) L. P. Battaglia, A. Bonamartini Corradi, G.Pelizzi and M. E.Vidoni-Tani, *Cryst. Struct. Comm.*, 1975, **4**, 399.

249) L. P. Battaglia, A. Bonamartini Corradi, M. Nardelli, and M. E.Vidoni-Tani, *J. Chem. Soc. Dalton Trans.*, 1978, 583.

250) W.Frank, J.Weber and E.Fuchs, *Angew. Chem., Int. Edn. Engl.*, 1987, **26**, 74.

251) G.Valle, G.Baruzzi, G.Paganetto, G.Depaoli, R.Zannetti and A.Marigo, *Inorg. Chim. Acta*, 1989, **156**, 157.

252) B.Cole and E.M.Holt, *J. Chem. Soc., Perkin 2*, 1986, 1997.

253) L.Newman and D.N.Hume, *J. Am. Chem. Soc.*, 1957, **79**, 4576.

254) J.Laane and P.W.Jagodzinski, *Inorg. Chem.*, 1980, **19**, 44.

255) H.Remy and L.Pellens, *Chem. Ber.*, 1928, **61**, 862.

256) V.Plyushchev, E.Stepina and I.V.Viasova, *Dokl. Akad. Nauk, SSSR.*, 1968, **126**, 180.

257) M.W.Duckworth, G.W.A.Fowles and R.A.Hoodless, *J. Chem. Soc.*, 1963, 5665.

258) B.J.Hathaway and D.G.Holah, *J. Chem. Soc.*, 1964, 2408.

259) T.L. Brown, and M. Kubota, *J. Am. Chem. Soc.*, 1961, 4175.

260) U.Ensinger, W.Schwarz and A.Schmidt, *Z. Naturforsch., B*, 1982, **37**, 1584.

261) B.Buss and B.Krebs, *Inorg. Chem.*, 1971, **10**, 2795.

262) P.Born, R.Kniep and D.Mootz, *Z. Anorg. Allgm. Chem.*, 1979, **451**, 12.

263) R.N.Hargreaves and M.R.Truter, *J. Chem. Soc., A*, 1971, 90.

264) A.J.Edwards, R.D.Peacock and R.W.H.Small, *J. Chem. Soc.*, 1962, 4486; A.J.Edwards, *J. Chem. Soc.*, 1964, 3714.

265) D.A.Wright and D.A.Williams, *Acta Crystallogr., Sect. B*, 1968, **24**, 1107.

266) L.Antolini, A.Benedetti, A.C.Fabretti and A.Guisti, *J. Chem. Soc., Dalton Trans.*, 1988, 2501.

267) A.L.Rheingold, A.D.Uhler and A.G.Landers, *Inorg. Chem.*, 1983, **22**, 3255.

268) F.Lazarini, *Acta Crystallogr., Sect. B*, 1977, **33**, 1954; *Acta Crystallogr., Sect. C*, 1985, **41**, 1617 and references therein.

269) S.S.Nagapetyan, A.R.Arakelova, E.A.Ziger, V.M.Koshkin, Yu.T.Struchkov and V.E.S.Schklover, *Russian J. Inorg. Chem.*, 1989, **34**, 1276.

270) B.K.Robertson, W.G.McPherson and E.A.Meyers, *J. Phys. Chem.*, 1967, **71**, 3531.

271) N.J.Mammano, A.Zalkin, A.Landers and A.L.Rheingold, *Inorg. Chem.*, 1977, **16**, 297.

272) W.G.McPherson and E.A.Meyers, *J. Phys. Chem.*, 1968, **72**, 532.

273) F.Lazarini and I.Leban, *Acta Crystallogr., Sect. B*, 1980, **36**, 2745; F.Lazarini, *Acta Crystallogr., Sect. B*, 1980, **36**, 2748.

274) S.K.Porter and R.A.Jacobson, *J. Chem. Soc., A*, 1970, 1356.

275) U.Ensinger, W.Schwarz and A.Schmidt, *Z. Naturforsch., B*, 1983, **38**, 149

276) A.Lipka and D.Mootz, *Z. Anorg. Allgm. Chem.*, 1978, **440**, 231.

277) M.Webster and S.Keats, *J. Chem. Soc., A*, 1971, 298.

278) R.K.Wiamer and R.A.Jacobson, *Inorg. Chem.*, 1974, **13**, 1678.

279) A.Lipka, *Z. Anorg. Allgm. Chem.*, 1980, **469**, 229.

280) A.Lipka, *Z. Naturforsch., B*, 1983, **38**, 1615.

281) D.R.Schroeder and R.A.Jacobson, *Inorg. Chem.*, 1973, **12**, 210.

282) S.L.Lawton, R.A.Jacobson and R.S.Frye, *Inorg. Chem.*, 1971, **10**, 701, 2813.

283) J.I.Musher, *Angew. Chem., Int. Edn. Engl.*, 1969, **54**, 8.

284) A.T.Mohammed and U.Muller, *Z. Naturforsch., B*, 1985, **40**, 562.

285) S.Pohl, W.Saak, P.Mayer and A.Schmidpeter, *Angew. Chem., Int. Edn. Engl.*, 1986, **25**, 825.

286) T.Toan and L.F.Dahl, *Inorg. Chem.*, 1976, **15**, 2953.

287) P.P.K.Claire, M.G.B.Drew and G.R.Willey, *J. Chem. Soc., Dalton Trans.*, 1989, 57.

288 a) C.D.Schmulbach, *Inorg. Chem.*, 1965, **4**, 1232; b) I.Lindqvist and G.Oloffson, *Acta Chem. Scand.*, 1959, **13**, 1753.

289) J.Bebendorf and U.Muller, *Z. Naturforsch., B*, 1990, **45**, 927.

290) I.R.Beattie, T.Gilson, K.Livingston, V.Fawcett and G.A.Ozin, *J. Chem. Soc., A*, 1967, 712.

291) H.J.Coerver and C.Curran, *J. Amer. Chem. Soc.*, 1958, **80**, 3522.

292) C.Balimann and P.S.Pregosin, *J. Mag. Reson.*, 1977, **26**, 283.

293) M.F.A.Dove, J.C.P.Sanders, E.L.Jones and M.J.Parkin., *J. Chem. Soc., Chem Commun.*, 1984, 1578.

294) L.Kolditz and W.Schmidt, *Z. Anorg. Allgm. Chem.*, 1958, **296**, 188.

295) V.Gutmann, *Monatsh. Chem.*, 1951, **82**, 473.

296) A.F.Demiray and W.Brockner, *Monatsh. Chem.*, 1979, **110**, 799.

297) K.Seppelt, D.Lentz, H.-H.Eysel, *Z. Anorg. Allgm. Chem.*, 1978, **439**, 5.

298) M.Hall and D.B.Sowerby, *J. Chem. Soc., Dalton Trans.*, 1983, 1095.

299) G.Wilkinson, *J. Amer. Chem. Soc.*, 1951, **73**, 5502.

300) C.Peylhard, P.Teulon and A.Potier, *Z. Anorg. Allgm. Chem.*, 1981, 483, 236.

301) C.A.McAuliffe and D,S,Barrett, in *Comprehensive Coordination Chemistry*, Ed's G.Wilkinson, R.D.Gillard and J.A.McCleverty, Pergamon Press, Oxford, 1987, Vol 3.

302) G.Wilkinson and J.M.Birmingham, *J. Amer. Chem. Soc.*, 1954, **76**, 4281.

303) R.Guilard and C.Lecomte, *Coord. Chem. Rev.*, 1985, **65**, 87.

304) R.J.H.Clark, J,Lewis, R.S.Nyholm, P.Pauling and G.B.Robertson, *Nature (London)*, 1961, **192**, 222.

305) J.A.Creighton and J.H.S.Green, *J. Chem. Soc., A*, 1968, 808.

306) D.M.Adams and D.C.Newton, *J. Chem. Soc., A*, 1968, 2262.

307) J.Eicher, P.Klingelhoffer, U.Muller and K.Dehnicke, *Z. Anorg. Allgm. Chem.*, 1984, **514**, 79.

308) P.D.Gavens, M.Bottrill, J.W.Kelland and J.McMeeking in *Comprehensive Organometallic Chemistry*, Ed's G.Wilkinson, F.G.A.Stone and E.W.Abel, Pergamon Press, Oxford, 1982, Vol 3.

309) P.Sobota, T.Plusinski, J.Utko and T.Lis, *Inorg. Chem.*, 1989, **28**, 2217.

310) J.C.J.Bart, M.Calcaterra, E.Albizzati, U.Giannini and S.Parodi, *Z. Anorg. Allgm. Chem.*, 1981, **482**, 121.

311) J.C.J.Bart, I.W.Bassi, M.Calcaterra, U.Giannini and E.Albizzati, *Z. Anorg. Allgm. Chem.*, 1983, **496**, 205.

312) G.Giunchi, E.Albizzati, L.Malpezzi and E.Giannetti, *Inorg. Chim. Acta.*, 1988, **147**, 159.

313) P.Sobota, T.Pluzinski and T.Lis, *Polyhedron.*, 1984, **3**, 45.

314) C.K.Jorgensen, *Absorption Spectra and Chemical Bonding in Complexes, Pergamon Press*, Oxford, 1962.

315) M.W.Lister and E.L.Sutton, *Trans. Faraday Soc.*, 1941, **37**, 393; P.Brand and H.Sackmann, *Z. Anorg. Allgm. Chem.*, 1963, **321**, 262; P.Brand and H.Sackmann, *Acta Crystallogr.*, 1963, **16**, 446.

316) G.Del. Piero and M.Cesari, unpublished results, see Z. *Anorg. Allgm. Chem.*, 1981, **482**, 121.

317) R.A.Brown and E.H.Swift, *J. Amer. Chem. Soc.*, 1949, **71**, 2719.

318) A.J.Bard, *Encyclopedia of the Electrochemistry of the Elements*, Marcel Dekker Inc., New York, 1973, Vol 1.

319) J.Holmes and R.Pettit, *J. Org. Chem.*, 1963, **28**, 1695; P.Day, *Inorg. Chem.*, 1963, **2**, 452; I.C.Lewis, L.S.Singer, *J. Chem. Phys.*, 1965, **43**, 2712; O.W.Howarth and G.K.Fraenkel, *J. Amer. Chem. Soc.*, 1966, **88**, 4514; G.W.Cowell, A.Ledwith, A.C.White and H.J.Woods, *J. Chem. Soc., B*, 1970, 227.

320) M.R.Snow, M.H.B.Stiddard, *Chem Commun.*, 1965, 580; T.V.Howell and L.M.Venanzi, *J. Chem. Soc., A*, 1967, 1007; M.H.B.Stiddard and R.E.Townsend, *J. Chem. Soc., A*, 1969, 2355.

321) P.J.Fagan, J.M.Manriquez, E.A.Maata, A.M.Seyam and T.J.Marks, *J. Amer. Chem. Soc.*, 1981, **103**, 6650 and references therein.

322) T.Moeller, *Chem. Rev.*, 1965, **1**, 65.

323) M.D.Fryzuk, T.S.Haddad and D.J.Berg, *Coord. Chem. Rev.*, 1990, **99**, 137 and references therein.

324) M.Bochman, L.M.Wilson, M.B.Hursthouse and R.L.Short, *Organometallics.*, 1987, **6**, 2556.

325) Y.Mugnier, C.Moise and E.Laviron, *J. Organomet. Chem.*, 1981, **210**, 69.

326) G.W.A.Fowles, D.A.Rice and J.D.Wilkins, *J. Chem. Soc., A*, 1971, 1920.

327) F.Calderazzo, S.A.Losi and B.P.Susz, *Helv. Chim. Acta.*, 1971, **54**, 1156.

328) D.Gordon and M.G.H.Wallbridge, *Inorg. Chim. Acta.*, 1986, **111**, 77.

329) M.Walter and L.Ramaley, *Anal. Chem.*, 1973, **45**, 165.

330) A.I.Vogel, *Textbook of Quantitative Inorganic Analysis*, Longman, London, 4th Edition, 1978, page 342.

331) R.D.Feltam and R.G.Hayter, *J. Chem. Soc.*, 1964, 4587.

332) N. Walker, and D. Stuart, *Acta Crystallogr., Sect. A*, 1983, **39**, 158.

333) SHELX76 Package for Crystal Structure Determination, G.M. Sheldrick, University of Cambridge, 1976.

TITLE Halide Transfer Reactions of Arsenic, Antimony and Bismuth

AUTHOR Helen Collins

INSTITUTION and DATE University of Warwick, 1991